TEXAS Geosciences
The University of Texas at Austin
Jackson School of Geosciences

5th Annual Jackson School of Geosciences Student Research Symposium

February 6, 2016

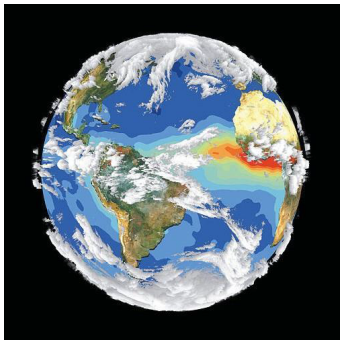

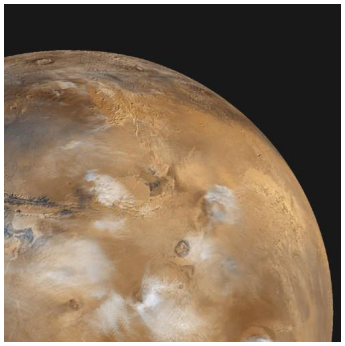

ConocoPhillips

Jackson School of Geosciences
GSEC
Graduate Student Executive Committee

Welcome to the 5th Annual Jackson School Research Symposium

It is with great pleasure we welcome you all to the 5th Annual Jackson School Research Symposium at UT-Austin! This symposium would not have been possible without the hard work of student volunteers, the support of faculty/research scientists, and generous support from ConocoPhillips. Thank you for taking part in supporting our students and growing research program within the Jackson School. Enjoy the posters!

Schedule of Presentations and Events

Breakfast, A.M. session poster set-up.....8:30 a.m.

Early Career Graduate (ECG) posters.....9:00-11:30 a.m.

Late Career Masters (LCM) posters.....9:00-11:30 a.m.

Lunch, A.M. session poster take-down.....11:30 a.m.

P.M. session poster set-up.....12:30 p.m.

Undergraduate (U) posters….....1:00-3:30 p.m.

Late Career PhD (LCPhD) posters.....1:00-3:30 p.m.

Happy hour/judging.....3:30 p.m.

Awards/closing.....4:00 p.m.

Table of Contents

Program Schedule ii
Poster/abstract list .....iii-xi
AM Poster Layout Map.....xii
PM Poster Layout Map.....xiii
Student abstracts.....1-131
(*Ordered by judging category, then theme, then last name. See below.)*

Poster ID	Last Name	First Name	Title	Page
Early Career Graduate Student (ECG)				
Climate, Carbon & Geobiology (CCG)				
ECG-1	Chung	Seungwon	A framework for modelng of riverine nitrogen transport by using the Noah-MP model	1
ECG-2	Cooperdock	Sol	Soil ecosystem regeneration following a stand-replacing wildfire	2
ECG-3	Hattori	Kelly	Validation of Taxon-Specific Sampling for Studying Drilling Predation on Fossil Bivalves	3
ECG-4	Li	Lingcheng	What factors control forest ecosystem water use efficiency?	4
ECG-5	Scarpetta	Simon	Cranial osteology of extant and extinct gerrhonotine lizards	5
ECG-6	Sun	Tianyi	Identifying the Role of Extratropical Air-Sea Interactions in North Pacific Climate Variability with a Hierarchy of CESM Simulations	6
ECG-7	Wallace	Rachel	New Description and Phylogenetic Analysis of a Mammalian Relative from Late Triassic Argentina, and the Importance of CT Imagery for Ambiguous Taxa	7
ECG-8	Weiss	Anna	Importance of the Association Between Crustose Coralline Algae and Corals to Reef Building in the Fossil Record	8
Energy Geosciences (EG)				
ECG-9	Alulaiw	Badr	PRESTACK SEISMIC INVERSION BY QUANTUM ANNEALING: APPLICATION TO CANA FIELD	9
ECG-10	Alzayer	Yaser	Mechanical Stratigraphy and Fracturing of Icehouse Carbonate Mound Complexes	10
ECG-11	Barone	Anthony	Anisotropic Analysis and Fracture Characterization of the Haynesville Shale, Panola County, Texas	11
ECG-12	Darnell	Kristopher	Mixed hydrate thermodynamics for the CH4/N2/CO2 system	12
ECG-13	Datta	Debanjan	Global Full Waveform Inversion using Particle Swarm Optimization	13
ECG-14	Haegele	Tess	An Analysis of the Evolution of the Austin Water Network *withdrawn*	14
ECG-15	Li	John	Quantifying Natural Fracture Spatial Organization in Horizontal Image Logs: Application in Unconventional Reservoirs	15

Poster ID	Last Name	First Name	Title	Page
ECG-16	Meazell	Patrick	The Depositional Evolution of the Terrebonne Basin, Northern Gulf of Mexico.	16
ECG-17	Phillips	Mason	Structure-oriented Sobel filter for edge enhancement in seismic images	17
ECG-18	Pinkston	Francis W.	Pore Pressure and Stress Regime at the Macondo Prospect, Gulf of Mexico	18
ECG-19	Shi	Yunzhi	Velocity-Independent Localization of Passive Seismic Events Using Local Slopes	19
ECG-20	Smith	Benjamin	Integrated Stratigraphic and Structural Evolution of the Guadalupian Seven Rivers Formation, McKittrick Canyon, NM	20
ECG-21	Soto-Kerans	Peter	Reservoir Characterization of an Intrashelf Basin Hybrid Play: Integration of a predictive reservoir model for the Upper Glen Rose, East Texas Basin	21
ECG-22	Verma	Rahul	PROSPECTIVITY MODELING FOR CAMBRIAN–ORDOVICIAN HYDRAULIC FRACTURING SAND RESOURCES AROUND THE LLANO UPLIFT, CENTRAL TEXAS	22
Marine Geosciences (MG)				
ECG-23	Harding	Jennifer	Wide-Angle Refraction Tomographic Inversion of Mid Cayman Spreading Center and its Ocean Core Complex, CaySEIS Experiment	23
ECG-24	Kunpitaktakun	Takonporn	Architecture of Basin Scale Clinoforms Using Well Logs and Seismic Data in Dacian Basin, Romania	24
ECG-25	Lockhart	Landon	Velocity-Effective Stress Relationships at Mad Dog, GoM	25
ECG-26	West	Logan	Deepwater Architecture of the Pliocene Lycium Turbidite Deposits, Fish Creek-Vallecito Mountains Basin, California: Large-Scale Supercritical Bedforms?	26
Planetary Sciences (PS)				
ECG-27	Cardenas	Benjamin	River meander traverse asymmetry as a paleoflow direction indicator for Martian channel belts	27
Solid Earth & Tectonic Processes (SETP)				
ECG-28	Boyd	Patrick	Defining the Thermal Evolution of Magma-Poor, Hyperextended Rift Margins, the Err and Tasna Nappes, Eastern Switzerland	28
ECG-29	Capaldi	Tomas	U-Pb geochronology of modern river sands from wedge-top foreland depo-centers; when sinks becomes the source	29
ECG-30	Clow	Travis	Pleistocene to recent incision rates for the Rio Grande Gorge, northern New Mexico	30
ECG-31	George	Sarah	Basin evolution in northern Peru: Implications for the growth of topographic barriers linking the Central and Northern Andes	31

Poster ID	Last Name	First Name	Title	Page
ECG-32	Jackson	Lily	Early Cenozoic shortening and foreland basin sedimentation in the Marañon fold-thrust belt, central Peruvian Andes	32
ECG-33	Mackaman-Lofland	Chelsea	Depositional and provenance records of Mesozoic basin evolution and Cenozoic shortening in the High Andes, La Ramada fold-thrust belt, southern-central Andes (32-33°S)	33
ECG-34	Munoz	Juan	Holocene Geologic Slip Rate for the Mission Creek Strand of the southern San Andreas Fault, Indio Hills, California	34
ECG-35	Nelson	Peter	Deep mantle S-wave velocity model under Yellowstone	35
ECG-36	Odlum	Margaret	Studying tectonic inversion in the eastern Pyrenees using (U-Th)/He and U-Pb bedrock thermochronology	36
ECG-37	Speciale	Pamela	Longevity of Strain Localization Associated with Dynamic Recrystallization of Olivine in Mantle Rocks	37
ECG-38	Tong	Xinyue	Seismiccycle at Sumatra	38
Surface & Hydrologic Processes (SHP)				
ECG-39	Clayton	Clarke	Multiple Cut and Fill Episodes During the Evolution of the Wilcox Yoakum Canyon	39
ECG-40	Ferencz	Stephen	Seasonal Distribution of Mean Temperature and Diurnal Variation for Streams Across the Contiguous United States: A Case Study for Dec. 2012 to Nov. 2013	40
ECG-41	Hassenruck-Gudipati	Hima	Diurnal Water Characteristics in the Annapurna Himals	41
ECG-42	Koo	Woong Mo	VARIABILITY of TRANSITIONAL FLOWS on SUBMARINE FAN FRINGES	42
Late Career Masters Student (LCMS)				
CCG				
LCMS-1	Marroquin	Selva	Taxonomy of Plesioteuthididae and the first Loligosepiina coleoids from North America spanning the Pliensbachian and Toarcian Stages (Early Jurassic), Alberta, Canada	43
LCMS-2	Sekhon	Natasha	Investigating multidecadal rainfall variability in the South Pacific Convergence Zone using the geochemistry of stalagmites from the Solomon Islands *withdrawn*	44
LCMS-3	Tornabene	Chiara	Testing Proxies to Determine Whether There is Evidence for Photosymbiosis in Fossil Corals	45
EG				

Poster ID	Last Name	First Name	Title	Page
LCMS-4	Ayhan	Oguzhan	Depositional Environment Distribution, Diagenesis and Reservoir Quality of the Middle Bakken Member in the Williston Basin, North Dakota	46
LCMS-5	Danger	Nick	Formation and Evolution of Strandplain Grainstones and Facies Variability Along the Leeward Margin of West Caicos, British West Indies	47
LCMS-6	De La Rocha	Luciana	Southern Gulf of Mexico Paleocene through Miocene Paleogeography: Investigating siliciclastic sedimentation in Mexico Deepwater	48
LCMS-7	Doungkaew	Natchanan	An integrated structural and geochemical study of fracture aperture growth in the Campito Formation of eastern California	49
LCMS-8	Hu	Ningjie	Sedimentology and Sedimentary Dynamics of the Desmoinesian Cherokee Group, Deep Anadarko Basin, Texas Panhandle *withdrawn*	50
LCMS-9	Jones	Rebecca	Paleoenvironments of Anchor Mine Tongue and Upper Sego Equivalent Strata in the Rangely Area of Colorado: Tidally-influenced Deposits and Variable Ichnology Along a Complex Coastline	51
LCMS-10	McKenzie	Kyle	Facies and Cycle Architecture of the Upper Artesia Group in the Gulf PDB-04 Core, New Mexico: Integration of Outcrop Derived Models Into the Subsurface	52
LCMS-11	Obrien	Casey	Coupled Mechanical and Chemical Diagenetic Processes in Deformation Bands: Microstructure and Field Observations from the Entrada Sandstone at the San Rafael Swell, Utah	53
LCMS-12	Redmond	Lauren	Tying Core Descriptions and Optical Petrography with XRF Geochemical Data for a Detailed Characterization of the Mississippian Barnett Formation in the Southern Fort Worth Basin of North-Central Texas	54
LCMS-13	Regimbal	Kelly	Optimizing CMP Stacking Using the Seislet Transform	55
LCMS-14	Tinker	Nathan	Analysis of Fracture Style and Development Associated with Differential Compaction Around Carbonate Mounds, Sacramento Mountains, New Mexico	56
LCMS-15	Voorhees	Kristopher	Anatomy, Dimensions, and Significance of the Penultimate Yates Tepee-Shelf Crest Complex, G25 Hairpin HFS, Guadalupe Mountains, New Mexico and Texas *withdrawn*	57
LCMS-16	Wang	Qiqi	Characterizing Bedding-Parallel Fractures in Shale: Aperture-Size Distributions and Spatial Organization	58

Poster ID	Last Name	First Name	Title	Page
LCMS-17	Wright	Erick	Potentially Conductive Channels in Fracture Cements of Low Permeability Rocks	59
LCMS-18	Zheng	Hanyue	Stratigraphic Cyclicity and Reservoir Potential of Upper Pennsylvanian Cline Shale, Midland Basin, Texas	60
PS				
LCMS-19	Shover	Katherine	Unraveling Ancient Martian Hydrological Conditions Through Erosional/Depositional Mass Balance Studies of Sedimentary Fans	61
SETP				
LCMS-20	Colleps	Cody	Himalayan thrust belt dynamics, weathering, and Cenozoic seawater chemistry	62
LCMS-21	Hinds	Dorothy	Initial results of research on gold mineralization in the Surselva district, Switzerland	63
LCMS-22	Ledvina	Matthew	Investigating the Pathways and P-T-X Conditions of Hydrothermal Fluid Flow Responsible for Cu-Au Mineralization in the Ertsberg East Skarn System, Papua, Indonesia	64
LCMS-23	Thomson	Kelly	Detrital Zircon Geo- and Thermochronometry of the Eocene Ainsa Basin, South Central Pyrenees, Spain: Insights into Paleodrainage Evolution During Orogenesis	65
LCMS-24	Williams	Nathan	An Evaluation of Predictive Indicators of Mississippi Valley Type Mineralization in Southeast Missouri Using Weights of Evidence	66
SHP				
LCMS-25	Jung	Eunsil	Physical Modeling of a Prograding Delta on a Mobile Substrate	67
LCMS-26	Vamaraju	Janaki	Comparative Assessment of FWI (Full Waveform Inversion),MASW(Multichannel Analysis of Spectral Waves) and SASW (Spectral Analysis of Surface Waves) method for near surface characterization	68
LCMS-27	Watson	Jeffery	DOWNSTREAM CHANGES IN THE THERMAL REGIME OF THE HYPORHEIC ZONE OF THE HYDROPEAKED COLORADO RIVER, AUSTIN, TEXAS	69
Late Career PhD Student (LCPHD)				
CCG				
LCPHD-1	Carlson	Peter	Clumped-isotope Thermometry and Oxygen Isotope Systematics in Speleothem Calcite from a Near Cave Entrance Environment	70
LCPHD-2	Chakraborty	Sudip	Scale up the influence of aerosols on deep convection derived from GoAmazon/CHUVA measurement to Amazon basin.	71

Poster ID	Last Name	First Name	Title	Page
LCPHD-3	Gelnaw	William	DisintegratoR: an upcoming package for evaluating phylogenetic trees while accounting for correlation between character states	72
LCPHD-4	Guiltinan	Eric	The Wettability of Caprock by CO2 and Its Impact on Geologic CO2 Sequestration	73
LCPHD-5	Halubok	Maryia	Using solar-induced fluorescence measurements from the space to estimate global and time-resolved land photosynthesis and to monitor droughts in the United States	74
LCPHD-6	Kwon	Yonghwan	Improving the Radiance Assimilation Performance in Estimating Snow Water Storage Across Snow and Land Cover Types in North America	75
LCPHD-7	Lin	Peirong	The role of Northern Hemisphere snow data assimilation in seasonal predictions of surface air temperature	76
LCPHD-8	Parajuli	Sagar	Development of an empirical model for predicting dust aerosol optical depth using satellite and reanalysis data	77
LCPHD-9	Zhang	Xiangxiang	Evaluating and Improving the Performance of Common Land Model Using FLUXNET Data	78
EG				
LCPHD-10	Biswas	Reetam	Trans-dimensional Seismic Inversion	79
LCPHD-11	He	Yawen	INFLUENCE OF SPATIAL VELOCITY DISTRIBUTION ON SEISMIC IMAGING OF MIXED CARBONATE-SILICICLASTIC CLINOFORMS, THE PERMIAN SAN ANDRES FORMATION, LAST CHANCE CANYON, NM	80
LCPHD-12	Liu	Han	3D simulation of seismic wave propagation in fractured medium using an integral method accommodating irregular geometries	81
LCPHD-13	Major	Jonathan	Effect of Chemical Environment and Rock Composition on Fracture Mechanics Properties of Reservoir Lithologies in Context of CO2 Sequestration	82
LCPHD-14	Merzlikin	Dmitrii	Path-Integral Diffraction Imaging	83
LCPHD-15	Meyer	Dylan	Methane hydrate formation in a saturated, coarse-grained sample through the induction of a propagating gas front	84
LCPHD-16	Nolting	Andrea	Spatial and Temporal Characterization of Mechnical Rock Properties From West Caicos, BWI	85
LCPHD-17	Ren	Qi	Greedy Annealing Importance Sampling Inversion Method, an application on Eagle Ford Formation	86
LCPHD-18	Sripanich	Yanadet	Muir-Dellinger parameters for anisotropic signatures analysis in shales	87

Poster ID	Last Name	First Name	Title	Page
LCPHD-19	Sun	Junzhe	Imaging microseismic and diffraction events with cross-correlation imaging condition	88
LCPHD-20	Xue	Zhiguang	Simultaneous Inversion of Velocity and Attenuation Models with Adaptive Matching Filter	89
LCPHD-21	Zhao	Zeyu	Reciprocity and Double Plane Wave Migration	90
MG				
LCPHD-22	Davis	Joshua	New Somali Basin Magnetic Anomalies and a Plate Model for the Early Indian Ocean	91
LCPHD-23	Frederik	Marina	Seafloor Changes Offshore Northern Sumatra from 1997-2008 Bathymetric Data	92
LCPHD-24	Gao	Baiyuan	Geomechanical Modeling in Fold-and-Thrust Belts Systems	93
LCPHD-25	Walton	Maureen	Revisiting the 1899 Earthquakes of Yakutat Bay, Alaska Using New and Existing Geophysical Data	94
LCPHD-26	Xu	Jie	Point-bar scaling and application to the Lower Miocene drainage system of the Gulf of Mexico basin	95
PS				
LCPHD-27	Hanna	Romy	3D measurement of fine-grained rims in CM Murchison using XCT	96
SETP				
LCPHD-28	Barber	Douglas	Thermokinematic modeling of fold-thrust belts: Bitlis-Zagros orogen, Kurdistan, Iraq	97
LCPHD-29	Bernard	Rachel	Constraints from Xenoliths on the Rheology of the Mojave Lower Crust and Lithospheric Mantle	98
LCPHD-30	Callahan	Owen	The effects of chemical alteration on fracture mechanical properties in hydrothermal systems	99
LCPHD-31	Calle	Amanda	LATE CRETACEOUS-CENOZOIC EVOLUTION of the CENTRAL ANDEAN FORELAND BASIN SYSTEM in the EASTERN CORDILLERA to SUBANDEAN ZONE, SOUTHERN BOLIVIA	100
LCPHD-32	Gevedon	Michelle	Direct U-Pb dating of skarn garnets: A case study from Black Rock Mine skarn, eastern California	101
LCPHD-33	Gold	Peter	New Geologic Slip Rates for the Agua Blanca Fault, Northern Baja California, Mexico	102
LCPHD-34	Goldsmith	Adam	Zircon (U-Th)/He: Effects of Radiation Damage on 4He diffusion and Age	103
LCPHD-35	Hernandez Goldstein (Cooperdock)	Emily	A New Approach to Date Serpentinites with Magnetite (U-Th)/He Thermochronology	104
LCPHD-36	Kotowski	Alissa	Rheological Heterogeneity Along the Deep Subduction Interface: Insights From Exhumed HP Metamorphic Rocks Exposed on Syros Island, Greece	105

Poster ID	Last Name	First Name	Title	Page
LCPHD-37	Lima	Rodrigo	Extensional Evolution of the Lower Crust with Orogenic Inheritance: Observations from the Basin-and-Range and the Pyrenees	106
LCPHD-38	Lu	Chang	The Effect of Subducting Slabs in Global Shear Wave Tomography	107
LCPHD-39	McCormack	Kimberly	Numerical Modeling of Initial Slip and Poroelastic Effects of the 2012 Costa Rica Earthquake	108
LCPHD-40	Mohammed Koshnaw	Renas	Kinematic Linkages Among Fold-thrust Belt Advance, Drainage Network Evolution, and Foreland Basin Development in the Zagros Fold-thrust Belt and Foreland Basin, Northern Iraq, Kurdistan	109
LCPHD-41	Prior	Michael	Miocene extensional development of the Harquahala Mountains core complex, west-central Arizona: Magnitude and rates of slip along the Eagle Eye Detachment	110
LCPHD-42	Pujols	Edgardo	(U-Th)/He and U-Pb double dating constraints on the interplay between thrust deformation and basin development, Sevier foreland basin, Utah	111
LCPHD-43	Seman	Spencer	The km-scale structure of the Cycladic Blueschist Unit on Syros Island, Greece	112
LCPHD-44	Wafforn	Stephanie	Duration of Ore Formation and Rate of Deep-seated Cooling in the Ertsberg-Grasberg Mining District, Papua, Indonesia	113
SHP				
LCPHD-45	Fong-Ngern	Rattanaporn	Toe-of-Slope: Definition, Trajectory and Significance to Basin Margin Architecture	114
LCPHD-46	Fried	Mason	Mass Loss Down Under: Distributed Subglacial Discharge Drives Significant Submarine Melt at a Tidewater Glacier	115
LCPHD-47	Goodwin	Kealie	A Numerical Model of Armor Development in Flash Flood-Dominated Channels: Sensitivity to Sediment Supply, Hydrograph Shape, and Base Flow	116
LCPHD-48	Hurd	Gregory	Large-Scale Inflections in Slope Angle Below the Shelf Break: A First Order Control on the Stratigraphic Architecture of Carbonate Slopes; Delaware Basin	117
LCPHD-49	Kaufman	Matthew	The Dynamic Response of Hyporheic Redox Zonation After Surface Flow Perturbation	118
LCPHD-50	Mason	Jasmine	Spatio-temporal variation in bed-material load using dune topography collected during a severe flood on the coastal Trinity River, east TX, USA	119
LCPHD-51	O'Connor	Michael	Controls on Arctic groundwater flow and its impacts on carbon processing	120

Poster ID	Last Name	First Name	Title	Page
LCPHD-52	Rossi	Valentina	The Effect of Tides on Deltaic Morphology and Stratigraphy in River-Dominated Conditions	121
Undergraduate (U)				
CCG				
U-1	Heitmann	Emma	Obliquity (41kyr) paced SE Asian Monsoon variability following the MCT	122
EG				
U-2	Hill	John	PETROGRAPHIC AND ISOTOPIC EVIDENCE FOR MICROBIAL INFLUENCE IN THE ORIGIN OF THE BOLING SALT DOME CALCITE CAP ROCK, HOUSTON DIAPIR PROVINCE, TEXAS	123
MG				
U-3	Morey	Susannah	The Evolution of the Surveyor Fan and Channel System, Gulf of Alaska Based on Core-Log-Seismic Integration at IODP Site U1417	124
SETP				
U-4	Fryer	Rosemarie	Holocene geologic slip rate for Mission Creek strand of the southern San Andreas Fault	125
U-5	Hart	Dylan	Sediment dispersal during rift to drift transition in the central North Atlantic – Insights from U-Pb- He provenance data from the Lusitania Basin, Portugal	126
U-6	Raia	Natalie	Petrogenesis of Cycladic Serpentinites: Understanding the Tectonic History Preserved in Metamorphic Rocks in Syros, Greece	127
U-7	Ruthven	Rachel	Testing Mechanisms and Scales of Equilibrium Using Textural and Compositional Analysis of Porphyroblasts in Rocks with Heterogeneous Garnet Distributions	128
SHP				
U-8	Dafov	Laura	Using Detrital Zircon U-Pb Geochronology to Quantify the Disrupted Flow of Sediment Down the Colorado River by Texas Hill Country Dams	129
U-9	Palermo	Rose	Rates and Mechanisms of Erosion Generating a Wave-Cut Platform at Sargent Beach, Texas, USA	130
U-10	Pease	Emily	Depositional Environment and Provenance of a Boulder-Rich Diamictite, Witmarsum, Paraná State, Brazil	131

A.M. POSTER LAYOUT

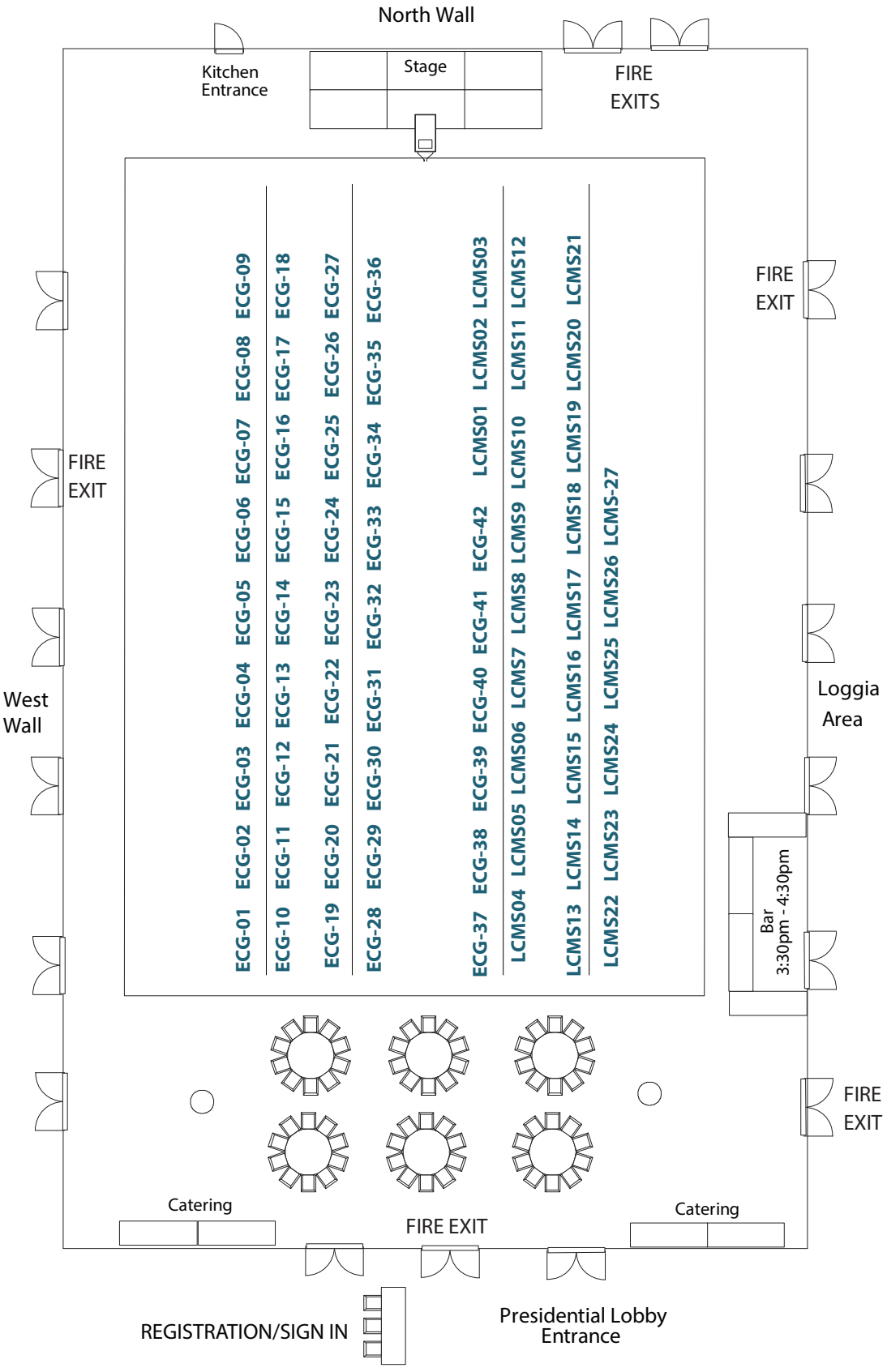

P.M. POSTER LAYOUT

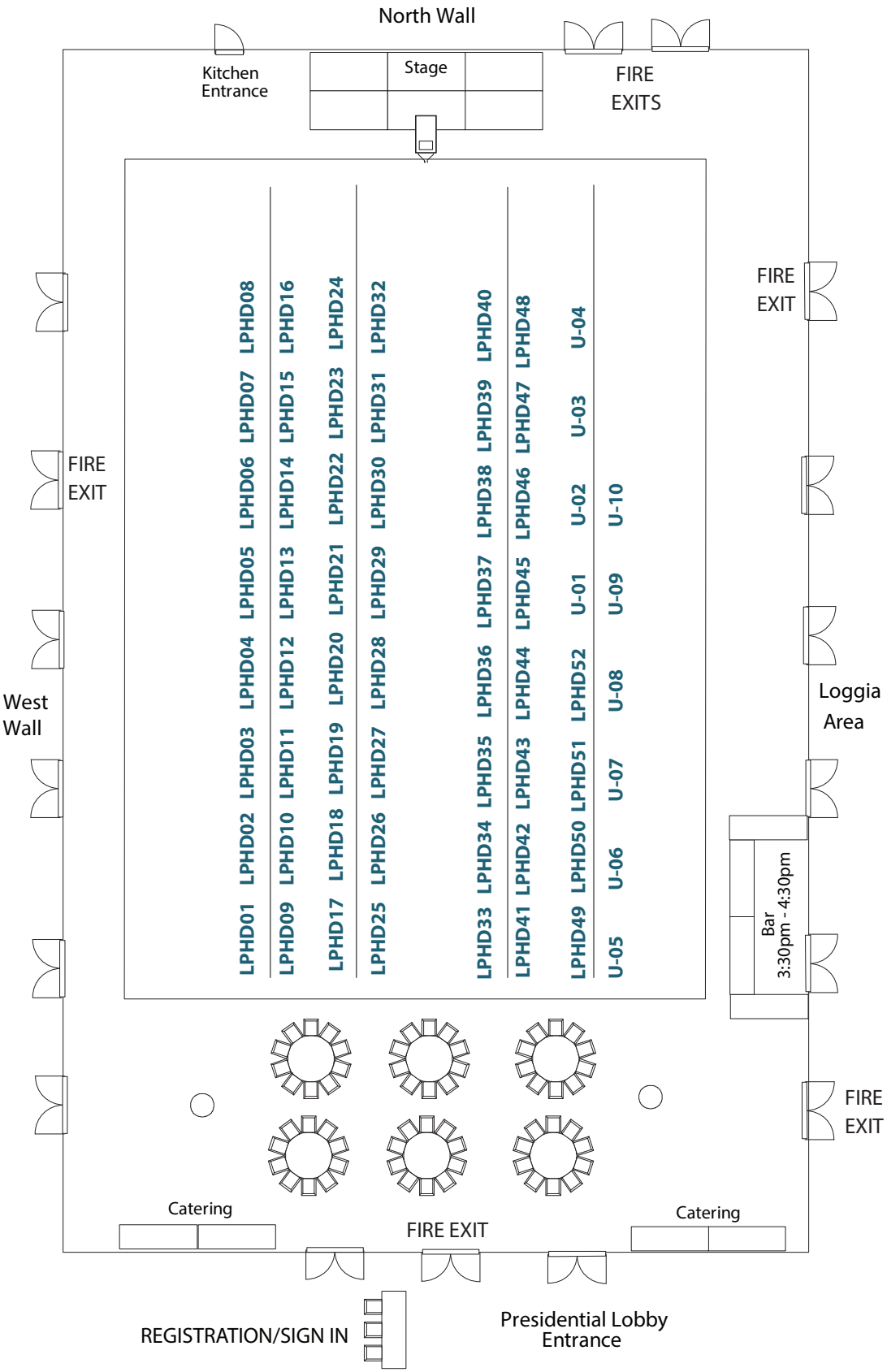

CCG
ECG

A framework for modelng of riverine nitrogen transport by using the Noah-MP model

Seungwon Chung
Chung, S., The University of Texas at Austin, Austin, TX
Yang, Z., The University of Texas at Austin, Austin, TX

Nitrogen transport from the atmosphere, across the land, and to the coast is tightly coupled to climatologic and physiographic characteristics of a watershed. Human modications of the nitrogen transport also have a large impact effect on this coupled process through extensive use of fertilizers and land cover/use changes. Excessive nutrients loaded by this human activities lead to eutrophication, and the amplitude, frequency and duration of eutrophication can be altered by interactions between land use and climate change. The consequences of overabundant nitrogen export emphasize the necessity to improve our understanding of nitrogen transport in large coastal watersheds and how terrestrial ecosystems respond to combined changes in the hydrological and biogeochemical cycles. We integrated the Fixation & Uptake of Nitrogen (FUN) plant model, based on carbon cost theory, and the Soil and Water Assessment Tool (SWAT) soil nitrogen dynamics, representing the impacts of agricultural management on the nitrogen cycle, into Noah land surface model with multi-physics (Noah-MP). As a result, we present how the addition of nitrogen dynamics effects the modeling of the carbon and water cycles and how land use and climate impact on nitrogen transport in a watershed.

Keywords: nitrogen, land surface model, surface water hydrology

ECG-2

CCG
ECG

Soil ecosystem regeneration following a stand-replacing wildfire

Sol Cooperdock
Cooperdock, S., Department of Geological Sciences, The University of Texas at Austin, Austin, TX
Breecker, D., Department of Geological Sciences, The University of Texas at Austin, Austin, TX

Fire is potentially the most transforming natural disturbance that an ecosystem can undergo. It can affect not only the physical dimensions of the ecosystem, but also the chemical ones. Following a fire, many nutrients may have been volatilized or mobilized and leached out of the soil because of excessive heat or the death of nutrient-immobilizing microbes. If the nutrient ratios have been disturbed too much and the microbial community has been hindered or removed from the ecosystem, nutrient availability will likely be much lower and it will take much longer for it to return to normal levels. Therefore, primary regeneration following a fire is extremely important for the overall regeneration of the ecosystem and microbial communities are important to speed up that process. Carbon and nutrient dynamics in the soil will shift during primary regeneration, following specific patterns depending on what biotic and abiotic factors are driving the regeneration. The recent fires in Smithville, TX along with the 2011 fires in Bastrop, TX have created a unique opportunity to study the nutrient and community regeneration pattern in order to understand what factors limit regrowth and when they are overcome. Four areas will be chosen for soil measurements: an unaffected forest stand, a stand which was burned in the 2015 fires, a stand which was burned in the 2011 fires and a stand which was burned in both fires. All sites will be in the “Lost Pines” ecosystem, a disconnected stand of Loblolly pine[i] [/i]located inside the Post Oak Savannah of eastern Texas. This ecosystem is considered to be the westernmost stand of Loblolly pines and also includes post oak and ashe juniper. All sites are chosen for their pre-burn characteristics, with similar plant community distributions. The soil of the entire ecosystem is considered to be “edge gravelly fine sandy loam” or “Padina fine sand” depending on the slope of the microsite. Unburned sites have a very thin organic and duff layer and burned sites have less organic and duff layers depending on fire severity and regeneration time. As soils regenerate, measurements will be taken in order to compare chemical characteristics between sampling sites. Soil respiration, total organic carbon, total nitrogen, soil organic matter, pH and temperature measurements will be taken at monthly intervals as the ecosystem regenerates and coupled with field observations of plant recolonization. The data will be used to further understand microbial communities’ roles in the reestablishment of ecosystems and how the carbon and nutrient dynamics are disrupted following fire.

Keywords: carbon, fire, soil, forest, succession

CCG
ECG

Validation of Taxon-Specific Sampling for Studying Drilling Predation on Fossil Bivalves

Kelly Hattori
Hattori, K., University of North Carolina Wilmington
Moore, N., University of North Carolina Wilmington
Simpson, S., University of North Carolina Wilmington
Zappulla, A., University of North Carolina Wilmington
Kelley, P., University of North Carolina Wilmington
Dietl, G., Paleontological Research Institution
Visaggi, C., Georgia State University

Although taxon-specific (targeted) sampling has been considered biased compared to bulk sampling for studying predation in the fossil record, previous studies have demonstrated that targeted sampling, even by a trained novice, can yield results comparable to bulk sampling. The present study examines whether the previous novice was atypical or if other trained novices could produce results comparable to those of experienced collectors and to those from bulk samples. It compares drilling predation metrics for samples made by five novice collectors and three veteran collectors to determine whether trained novices could produce results comparable to those of experienced collectors, and whether targeted sampling produced results comparable to bulk sampling.Targeted sampling was used in the lower Waccamaw Formation (Lower Pleistocene) at Register Quarry near Old Dock, NC. Five replicate taxon-specific samples were made by each collector, retrieving every specimen visible within ~ 1 – 4 m2 areas for the bivalves [i]Astarte concentrica[/i], [i]Cyclocardia granulata[/i],and [i]Lirophora latilirata[/i]. Shell length and thickness were measured and position and size of drillholes determined. Frequency of left valves, drilling frequency (number of valves with a complete drillhole divided by half the number of valves), prey effectiveness (% of drillholes that were incomplete), and size selectivity (correlation of drillhole size and prey size) were determined for each taxon replicate.For each variable, we compared the results for the novice collectors to results from bulk samples and to those for all veteran collectors. Comparisons were made before and after size standardizing data. Of 298 comparisons between unstandardized data from bulk samples and replicates collected by the five novices and three veterans, 89% showed no significant difference between targeted and bulk samples. Less than 3% of 142 comparisons of standardized data for the same samples showed a significant difference between targeted and bulk samples. Of 245 unstandardized comparisons between the novices and veterans, 95% showed no significant difference. None of the 114 size-standardized comparisons between the novices and veterans showed a significant difference. Previous results were not anomalous; use of targeted sampling as well as trained novice collectors in studying drilling predation is again validated.

Keywords: taxon-specific sampling, paleoecology, bivalves, pleistocene, targeted sampling

ECG-4

CCG
ECG

What factors control forest ecosystem water use efficiency?

Lingcheng Li
Li, L., Jackson School of Geosciences, University of Texas at Austin, Austin, TX
Lin, P., Jackson School of Geosciences, University of Texas at Austin, Austin, TX
Zheng, H., Institute of Atmospheric Physics, Chinese Academy of Sciences, Beijing, China
Yang, Z., Jackson School of Geosciences, University of Texas at Austin, Austin, TX
Zhang, K., Jackson School of Geosciences, University of Texas at Austin, Austin, TX

Water use efficiency (WUE), defined as ratio between net/gross primary production and evapotranspiration loss, represents how efficient ecosystem can translate water into carbon. It is an important term describing the coupling between carbon and hydrological cycle. However, relationships between WUE and other meteorological or ecological factors are still largely unknown. Here we use satellite observations or climate reanalysis datasets to investigate the relationships between WUE and a variety of factors, including aridity index (AI), leaf area index (LAI), normalized difference vegetation index (NDVI), solar-induced chlorophyll fluorescence (SIF), forest canopy height, forest age, and tree density. Our analyses focused on the North American (20°– 85°N, -170°– -45°W) forest ecosystem during growing season (June, July, August). We found that 1) WUE have a positive relationship with LAI, NDVI and SIF, and WUE increase rates become larger as latitudes increase. 2) WUE is more sensitive to SIF and NDVI than LAI. 3) As AI increases under other specific factors, WUE exhibits double peak. This study deeps our understanding of the general relationships between WUE and meteorological or ecological factors, and provides a universal guide for future related study.

Keywords: Water use efficiency, Forest ecosystem, Carbon cycle, Water cycle

ECG-5

CCG
ECG

Cranial osteology of extant and extinct gerrhonotine lizards

Simon Scarpetta
Scarpetta, S., The University of Texas at Austin, Austin, TX
Ledesma, D., The University of Texas at Austin, Austin, TX

Gerrhonotines are an extant clade of anguid lizards with a rich Cenozoic fossil record in the Americas. Species belonging to the genera *Elgaria* and *Gerrhonotus* are currently found in western and central North America, often in mesic habitats. Despite the relative familiarity to biologists and paleontologists of some species, comprehensive studies of the cranial anatomy of *Elgaria* and *Gerrhonotus* currently are lacking. Description of the bones in the skull supplies useful data for examining morphological variation and phylogeny, and thus is an excellent tool for any morphological study. Here, we aim to describe the anatomy of the skulls of all species of *Elgaria* and *Gerrhonotus* as well as representativess of other gerrhonotine taxa, particularly species of *Mesaspis* and *Barisia*. This will provide novel anatomical information for modern species, but also the framework for diagnosing phylogenetic placement of fossil specimens. We employ traditionally prepared skeletons as well as x-ray computer tomography (CT) scans; the latter offer previously impossible insights into the anatomy of lizard skulls for which no skeletal material currently exists. We partially described the cranial osteology of *Elgaria panamintina,* a somewhat poorly known species inhabiting a small area in California and whose skeletal anatomy was never before analyzed. Synapomorphies previously utilized to diagnose *Elgaria*, such as the presence of a distinct surangular foramen and the absence of a notch on the coronoid and surangular processes of the dentary, were observed. Morphology of a previously known but unidentified Pliocene lizard from the Anza Borrego desert in California demonstrates it to be a gerrhonotine, but more specific taxonomic assignation has yet to be determined and provides the main objective of this study.

Keywords: Morphology, osteology, gerrhonotines, phylogenetics, fossils

ECG-6

CCG
ECG

Identifying the Role of Extratropical Air-Sea Interactions in North Pacific Climate Variability with a Hierarchy of CESM Simulations

Tianyi Sun
Sun, T., Institute for Geophysics, The University of Texas at Austin, TX
Okumura, Y., Institute for Geophysics, The University of Texas at Austin, TX

Large-scale patterns of extratropical sea surface temperature (SST) variability are primarily driven by intrinsic modes of atmospheric circulation variability through changes in surface heat fluxes and ocean currents. While these changes in extratropical SSTs in turn affect the atmospheric circulation, it remains unclear to what extent the oceanic feedback modifies the overall climate variability. The present study focuses on North Pacific variability and revisits this long-standing problem by analyzing multi-century-millennium control simulations of an atmospheric model (CAM4) coupled to the ocean with varying degrees: a 300-yr run of standalone CAM4, 500-year run of CAM4 coupled to a slab ocean (CAM4SOM), and 1300-yr run of fully coupled model (CCSM4). The leading mode of North Pacific atmospheric variability is very similar among three models and resembles the observed Pacific-North American (PNA) pattern, in support of the stochastic climate model. In CAM4SOM, the associated surface heat flux anomalies induce SST changes during boreal winter, which tend to persist into the following winter through positive cloud feedback. These SST changes leave weak, but distinct imprints on the atmosphere. The atmospheric response is highly seasonally dependent and projects onto the original PNA pattern in the upper troposphere during boreal winter while a direct baroclinic response becomes prevalent in the other seasons. The thermodynamic air-sea interactions only marginally increase the persistency of PNA variability in CAM4SOM compared to the standalone CAM4 simulation. In CCSM4, a similar influence of extratropical SSTs is suggested but difficult to isolate due to the dominant impact of El Nino-Southern Oscillation and associated atmospheric teleconnections. Nevertheless, dynamically-induced SST variability in the oceanic frontal region appears to add more persistency to atmospheric variability because of its low-frequency nature.

Keywords: extratropical air-sea interaction, model hierarchy

ECG-7

CCG
ECG

New Description and Phylogenetic Analysis of a Mammalian Relative from Late Triassic Argentina, and the Importance of CT Imagery for Ambiguous Taxa

Rachel Wallace
Wallace, R., The University of Texas at Austin, Austin, TX

The closest relative to Mammaliaformes (most recent common ancestor of the extinct [i]Morganucodon[/i] and mammals, and all of its descendents) is hotly debated among paleontologists. Historically, tritylodontids and tritheledontids (of which the monophyly is ambiguous) have contended for the sister-taxon position to Mammaliaformes. A decade ago, a new group of non-mammalian cynodonts, brasilodontids, were introduced to the debate, affecting the conversation of the evolution of mammalian characteristics. Reasonably, brasilodontids have not been unanimously accepted, and have been challenged everywhere from genus identification, to its validity as a natural group, to its sister-taxon relationship with Mammaliaformes. Here, we report on a new putative brasilodontid specimen, PVSJ 882, from the Ischigualasto Formation of Late Triassic Argentina. A slender zygomatic arch is shared with other eucynodonts closely related to Mammaliaformes, while the post-canine anatomy and presence of an interpterygoid vacuity further unite PVSJ 882 with other brasilodontids. However, primitive anatomical characteristics including a prefrontal, postorbital and postorbital bar, and a high orbitosphenoid suggest that it is more basal than the brasilodontids and other derived eucynodonts. Autapomorphies including a low orbital process of the palatine; large, slender canines; small, simple post-canines behind a moderate diastema; and a strongly posteriorly reaching lambdoidal crest beyond the occipital condyles support generic distinction. A preliminary parsimony analysis suggests that PVSJ 882 is a new genus of non-mammalian eucynodont more closely related to tritylodonts than to tritheledonts, brasilodontids, and Mammaliaformes. A monophyletic relationship of the brasilodontids, [i]Brasilodon[/i] and [i]Brasilitherium[/i], is also unsupported. The recovered relationships among derived, non-mammaliaform eucynodonts differ from the results of previous analyses, and are likely to change upon further observation and inclusion of new cranial characters. But such ambiguity of results suggests rapid diversification of cynodonts before the evolution of true mammals, and highlights the importance for thorough, detailed observation of these taxa. Some cranial features of PVSJ 882 that are crucial for determining the relationship of non-mammalian eucynodonts have been overlooked in previous analyses, stressing the importance of x-ray computed tomography (CT) technology in paleontology. Those features may also be present in other taxa including [i]Brasilodon[/i] and [i]Brasilitherium[/i], though such elements are likely hard to see unless examined in high-resolution cross-sectional scans. Further, CT data shows that PVSJ 882 does not have replacement teeth and therefore is likely not a juvenile as has been previously suspected. Because these taxa are important for understanding how mammals evolved, and because they each possess a unique mosaic of primitive and derived characteristics, it is encouraged that more specimens be CT scanned to facilitate careful, thorough observation.

Keywords: Eucynodontia, phylogenetic systematics, Brasilodontidae, Brasilodon, Brasilitherium, Mammaliaformes, CT, Computed Tomography, paleontology, vertebrate paleontology

ECG-8

CCG
ECG

Importance of the Association Between Crustose Coralline Algae and Corals to Reef Building in the Fossil Record

Anna Weiss
Weiss, A., Department of Geosciences, The University of Texas at Austin, Austin, TX
Martindale, R., Department of Geosciences, The University of Texas at Austin, Austin, TX

In modern oceans, crustose coralline algae (CCA) play a vital role in coral reef health by providing structural stability and inducing the settlement of reef building coral larvae. It has been suggested that CCA played a similar role in ancient reefs as far back as the Cretaceous. However, there has been no definitive analysis of their importance in deep time. The goal of this project is to quantitatively assess the importance of CCA on ancient coral reefs (Jurassic through Pleistocene) using the Paleobiology Database and the PaleoReefs database. If the relationship between corals and CCA in fossil reefs was similar to the modern association, coral reefs with higher abundances of CCA are expected to have greater relief and overall carbonate production. It is also predicted that coral reefs with greater amounts of CCA will have greater taxonomic diversity. The parameters used in this project are reef thickness and volume as well as reef diversity to assess carbonate production and ecological health, respectively. Additional factors taken into consideration are paleolatitude, reef type, and percent of CCA on the reef. The parameters are either listed or can be calculated from the aforementioned databases. As calcifying organisms, modern CCA are particularly sensitive to changes in ocean chemistry (e.g. acidification and anoxia). It is important to understand the relationship between CCA and reef-building corals in order to better preserve this relationship in currently changing oceans.

Keywords: Coralline Algae, Reefs, Paleobiology, Database

ECG-9

EG
ECG

PRESTACK SEISMIC INVERSION BY QUANTUM ANNEALING: APPLICATION TO CANA FIELD

Badr Alulaiw
Alulaiw, B., The University of Texas at Austin, Austin, TX
Sen, M., Institute for Geophysics, The University of Texas at Austin, Austin, TX

The aim of seismic inversion is to estimate the subsurface elastic properties. This is accomplished by finding the minimum of a suitably defined error function. Deterministic inversion can be used to find a single solution of this minimization problem; this solution is the closest to the initial model. Seismic inversion is a highly non-linear problem that has multiple minima of different heights. Although deterministic inversion is computationally cheap, it fails in finding the global minimum when the initial model is far from it. Moreover, deterministic inversion is band limited. Thus, global minimization methods are preferred in such problems. Because the model space in a typical geophysical inversion problem is very large, the grid search algorithm is not a practical approach. Pure Monte Carlo method, which randomly evaluates the error function at many points, is still very expensive. Simulated Annealing (SA) is another global optimization method that randomly samples the proposal distribution but also utilizes Metropolis criterion to accept or reject the next trial solution. Hence, SA converges to the global minimum faster than pure Monte Carlo method. Unfortunately, SA could be trapped in a local minimum if the annealing scheduled is not properly designed. Moreover, it is still a very expensive method in geophysical inversion where we invert for a large number of parameters. Quantum Annealing (QA) is relatively a new global optimization method that is inspired from quantum mechanics. Several applications have demonstrated that QA converges faster than SA and escapes from being trapped in a local minimum. Here, we apply QA algorithm in a seismic prestack inversion to resolve Woodford formation in the Cana field, Oklahoma. The results are compared with those obtained by a deterministic inversion. Our results clearly demonstrate superior performance of our stochastic QA inversion over standard SA and deterministic inversion of field data.

Keywords: Seismic, Prestack, Inversion, Global Optimization, Reservoir Characterization

EG
ECG

Mechanical Stratigraphy and Fracturing of Icehouse Carbonate Mound Complexes

Yaser Alzayer
Alzayer, Y., Department of Geological Sciences, The University of Texas at Austin
Zahm, C., Bureau of Economic Geology, The University of Texas at Austin
Janson, X., Bureau of Economic Geology, The University of Texas at Austin
Kerans, C., Department of Geological Sciences, The University of Texas at Austin

Phylloid algal mound complexes of the Pennsylvanian Holder Formation in the Sacramento Mountains, NM, were examined for fracture distribution, mechanical stratigraphy, and current rock strength. Early cementation of mound facies can create brittleness contrast with younger rocks that may fracture when strain is exacerbated by differential compaction. Finite-discrete element 2D Elfen models under the realistic constraints of gravity, evolving mechanical properties, pore pressure, and mechanical stratigraphy can be utilized to quantify the effect of differential compaction, mound geometry, and mechanical unit thickness on fracture attributes and distribution. The validity of such models can then be tested by comparison to field observations.
Fracture density maps of Yucca Canyon northern wall show high fracture density values located on beds overlying the steep side of a phylloid mound (up to 0.36 frac/ft2) as well as in the middle of the mounds (up to 0.24 frac/ft2). However, beds that are indirectly above the mound and do not exhibit depositional draping have low fracture density. Fractures are bounded or encompassed by 4 types of mechanical units. Each mechanical unit is associated with specific depositional facies: (1) massive phylloid algal boundstones; (2) massive grainstones and grain-dominated packstones; (3) thinly bedded recessive fusilinid-phylloid algae wackestones and packestones; and (4) recessive shale/mudstone. Unconfined compressive strength (UCS) of all facies was estimated from a total of 285 Schmidt hammer hardness measurements. There is no discernable difference in the UCS values between facies (Median UCS = ~50 MPa) except for the significantly stronger boundstones located in phylloid mounds core (Median UCS = ~ 70 MPa). UCS values are consistent with previous cement stratigraphy work indicating that mounds were lithified by early meteoric water cementation and the remaining facies underwent compaction and late cementation in episodes that predate and postdate fracturing. The highest mechanical contrast is expected to be present soon after deposition of rocks younger than phylloid mounds. This highlights the utility of geomechanical modeling to unravel the evolution of fractures as mechanical properties evolve temporally. Thus, we present 2D Elfen models that accounts for the deposition and compaction of strata above the cemented rigid phylloid mounds.

Keywords: Fractures, Numerical Modeling, Carbonate Mounds, Differential Compaction

EG
ECG

Anisotropic Analysis and Fracture Characterization of the Haynesville Shale, Panola County, Texas

Anthony Barone
Barone, A., The University of Texas at Austin, Institute for Geophysics (UTIG) and Jackson School of Geosciences
Sen, M., The University of Texas at Austin, Institute for Geophysics (UTIG) and Jackson School of Geosciences

In unconventional resources such as the Haynesville Shale, a proper understanding of natural fracture patterns is essential to enhancing the economic success of petroleum extraction. The spatial density of naturally occurring fracture sets affects drainage area and optimal drilling location(s), and the azimuth of the strike of the predominant fracture set affects the ideal orientation of wells. In the absence of data to directly determine these fracture characteristics, such as Formation Microimaging (FMI) logs, these natural fracture patterns can be analyzed by examining the seismic anisotropy present in the reservoir. Anisotropy introduced from aligned fracture sets creates predictable azimuthal variations in the seismic wavefield. This allows the reservoir anisotropy, and thus the fracturing present in the reservoir, to be studied indirectly through the azimuthal analysis of industry standard 3D seismic data. The work presented here outlines three distinct methodologies, which utilize azimuthal amplitude variations (AVAZ) present in 3D seismic data, to infer fracture characteristics without the need for substantial well log information. Two of these methods have been previously established and assume the reservoir to be characteristic of Horizontally Transverse Isotropic (HTI). The last method is novel and assumes orthorhombic anisotropy when inverting for fracture density and is able to unambiguously invert for fracture azimuth. All methodologies used in this work produced similar results, increasing confidence in the accuracy of these results through statistical repeatability. Fracture density inversion results indicate spatially varying fracture density throughout the area, with a distinct area of higher fracture density present in the Northwestern corner of the area analyzed. Spatially varying fracture density and localized pockets of fracturing is consistent with expectation from analyzing production data and FMI logs from other areas of the Haynesville. Fracture azimuth inversion results showed some variability; however, the novel method presented in this thesis indicates that the azimuth of the predominant fracture set is oriented at a compass bearing of approximately 82 degrees – rotated slightly counterclockwise from an east-west orientation. Fracture azimuth results agree well with expectations from a regional stress analysis and from examining comparable formations with known fracture patterns in the surrounding area.

Keywords: Fracture Characterization, Haynesville Shale

ECG-12

EG
ECG

Mixed hydrate thermodynamics for the CH4/N2/CO2 system

Kristopher Darnell
Darnell, K., Jackson School of Geosciences
Flemings, P., Jackson School of Geosciences

We investigate guest molecule exchange of hydrates as a method for simultaneous carbon dioxide storage and methane production. We simulate N2/CO2 binary gas mixture injection into marine and terrestrial methane hydrate bearing sediments. Different compositions of the injected gas can lead to four possible outcomes: 1) Injected gas flows downstream past methane hydrate and does not alter the methane hydrate, 2) Injected gas causes complete dissociation of methane hydrate, which creates a gas mixture of methane and injected gas that flows downstream, 3) Injected gas causes complete dissociation of methane hydrate with flow of methane gas downstream and all injected gas replaces methane in the hydrate cage, 4) Injected gas causes partial dissociation of methane hydrate with some replacement of methane in the hydrate cage and downstream flow of a methane and injected gas mixture. We focus on how composition of injected gas affects the outcome of the injection process, and then determine the optimal injection mixture of N2/CO2 for carbon dioxide storage and methane production. Our simulations combine dynamic flash calculations using the Gibbs energy minimization of CSMGEM with 1-d reactive transport modeling. This work provides insight into the efficiency of the guest molecule exchange process in methane hydrate systems.

Keywords: Hydrate, CO2 storage

EG
ECG

Global Full Waveform Inversion using Particle Swarm Optimization

Debanjan Datta
Datta, D., Jackson School of Geosciences
Sem, M., Jackson School of Geosciences

Full Waveform Inversion (FWI) has been traditionally cast as a local optimization problem. This requires the starting model to be fairly close to the true model otherwise the inversion converges to a local minima giving inadequate data fit and incorrect estimation of subsurface properties. Obtaining an optimal starting model is not a trivial task. It requires several levels of data processing and velocity interpretation to come up with a velocity model good enough for FWI. Global methods have not been implemented so far in FWI because they generally take many iterations to converge making FWI computationally prohibitive. We propose and implement a hybrid optimization scheme that combines the salient features of local (gradient) and a Global (Particle) optimization method to invert for P-wave velocity models under the acoustic approximation. This method does not require an optimal starting model and is able to reach close to the true model in a finite number of iterations. In our approach, a population of models is allowed to gradient descent for a few iterations after which each model is updated by combining the fitness information of the population. This helps the algorithm to escape local minima and converge close to the true model in about 20 swarm iterations. We apply our method to two synthetic cases where we are able to accurately reconstruct the true model.

Keywords: Full Waveform Inversion, Swarm Intelligence, Global Optimization

This abstract has been withdrawn

ECG-14

EG
ECG

An Analysis of the Evolution of the Austin Water Network

Tess Haegele
Haegele, T., The Energy Institute, The University of Texas at Austin, Austin, TX

Austin's rapid population growth over the past few decades has given rise to the need for additional water infrastructure and supply. There are limited funds for investment in water infrastructure so it should be spent with the goal of optimizing efficiency and resiliency. It is important for planning to understand the evolution of the network over time and how it has scaled with population growth, funding, socioeconomic status, etc. This research will develop an understanding of the topology and flow of the water network, how it has changed over time, and define the "sweet spot" of resiliency vs. efficiency to allow for the most effective use of funds. The municipal supply, wastewater, and reclaimed water networks can each be defined as an interconnected network with interdependent connections. They will be analyzed using Ulanowicz's information theory to assess resiliency vs. efficiency, and a "failure" analysis looking at pressure and flow rate for customer demand and fire flow.

To address a complimentary component of the water system, supply, this analysis will prove quite useful. Not only is Austin seeing rapid population growth, but Austin (along with the rest of Texas) is seeing a decrease in readily available water resources. This was particularly exacerbated by the drought of 2011, and partly in response, the state water plan indicates Austin will be turning to more reclaimed water use. The analysis of the municipal supply network (and limited reuse network) can be applied to expand reuse capacity with a good balance of resiliency and efficiency and best use of funds.

Keywords: "efficient" vs. "resilient" network, coping with drought, planning of water infrastructure

EG
ECG

Quantifying Natural Fracture Spatial Organization in Horizontal Image Logs: Application in Unconventional Reservoirs

John Li
Li, J., Bureau of Economic Geology, The University of Texas at Austin, Austin, TX
Gale, J., Bureau of Economic Geology, The University of Texas at Austin, Austin, TX
Marrett, R., Department of Geological Sciences, The University of Texas at Austin, Austin, TX
Laubach, S., Bureau of Economic Geology, The University of Texas at Austin, Austin, TX

Hydraulic fracture treatments are necessary for economic production from unconventional reservoirs, yet are challenging to predict due to reservoir heterogeneity. Numerical modeling of hydraulic fractures in heterogeneous material that includes natural fractures is hampered because knowledge of the spatial organization is limited; natural fractures in models are commonly distributed randomly. Fractures may be apparently random, evenly spaced, or arranged in clusters. Here we demonstrate a method for quantifying and predicting the spatial organization of natural fractures at a range of scales. We make use of natural fracture data from horizontal image logs in tight gas sandstones and shales. Horizontal image logs provide an opportunity for characterizing spacing of vertical fractures and faults, which was not previously available when most image logs were taken in vertical wells.

We use a normalized correlation count method to identify different types of spatial arrangement, including periodic, random, and clustered. The method provides a measure of how common given spacings are relative to their occurrence in a randomly spaced fracture set. Fracture spacings, measured normal to the fracture planes and, ideally, kinematic apertures are the input data. Apertures can be measured in outcrops or cores, but are challenging to quantify and calibrate in image logs. For this reason apertures from image log data are input as a single nominal size that is at least an order of magnitude smaller than the smallest spacing. We show examples from the Frontier Formation, a tight gas sandstone from the Green River Basin, Wyoming. In the Frontier Formation, fracture clusters ~25 m wide and spaced ~100 m apart are indicated. Organization within the clusters is perhaps fractal.

Keywords: natural fractures, spatial organization, unconventional reservoirs, horizontal image logs

EG
ECG

The Depositional Evolution of the Terrebonne Basin, Northern Gulf of Mexico.

Patrick Meazell
Meazell, K., Jackson School of Geosciences, The University of Texas at Austin, Austin, TX
Flemings, P., Jackson School of Geosciences, The University of Texas at Austin, Austin, TX

The Terrebonne Basin is a salt withdrawl mini-basin located 400 km south of New Orleans, LA. The area is currently being investigated for methane hydrate deposits due to the presence of discontinuous, bright, seismic anomalies known as bottom-simulating-reflectors that represent the base of the gas hydrate stability zone. The project uses 3D seismic interpretation to investigate the depositional history of the basin in order to identify reservoir quality clasticAccording to our model, the Terrebonne basin has gone through multiple cycles of fill & spill of turbidity currents, resulting in the creation of thick sand and mud packages. Well-sorted sheet sands formed at a low stand as a result of flow stripping followed by additional ponding. Muds formed at high stands and when during ponding phases. Channelized sand deposits formed during bypass and were filled by flow stripping as accommodation space increased. These cycles are the result of changes in accommodation space, which is controlled by the rise of salt on the southern border of the basin.

Keywords: hydrate, depositional systems, basin analysis, seismic interpretation

EG
ECG

Structure-oriented Sobel filter for edge enhancement in seismic images

Mason Phillips
Phillips, M., Bureau of Economic Geology, The University of Texas at Austin

Detection, extraction, and mapping of fault planes and other discontinuities is a major challenge in the interpretation of 3D seismic data. Visually prominent features can easily overshadow smaller features that are critical to understanding the structure and depositional environment. Seismic coherency attributes can accelerate the interpretation process by enhancing edges and providing a quantitative measure of the significance of discontinuities. We propose a modification of the classic Sobel filter by orienting the filter along structures. We find that this modification significantly sharpens faults and demonstrate this by applying the traditional Sobel filter and the structure-oriented Sobel filter to a synthetic model and field data from the Gulf of Mexico.

Keywords: seismic interpretation, seismic attributes, fault detection

ECG-18

EG
ECG

Pore Pressure and Stress Regime at the Macondo Prospect, Gulf of Mexico

Francis W Pinkston
Pinkston, F., Jackson School of Geosciences, The University of Texas at Austin, Austin, TX
Flemings, P., Jackson School of Geosciences, The University of Texas at Austin, Austin, TX

Overpressures likely begin at or near the seafloor in the Macondo Well (Mississippi Canyon Block 252). The overpressure trend continues with depth throughout most of the well. Just prior to reaching the primary target, middle Miocene sands, there is a significant regression (~1200 psi) from ~13,000 psi at ~17725 ft MD (measured depth) to ~11,800 psi at ~18090 ft MD. Overpressures at these depths are ~5240 psi and ~3875 psi respectively. The pressure drop coincides with a drop in the fracture gradient. During drilling operations, margins were determined too narrow to proceed, and total depth was called at 18360 MD. I use well-log and drilling records to describe the pressure and stress in the Macondo Well. Since well log information was not recorded during the first several thousand feet, I've relied on existing literature in this regional setting that suggests overpressures started at or near the seafloor. Drilling data suggest the trend continues with depth as evidenced by direct pressure measurements and kicks taken during drilling. The fracture gradient is also estimated along the well based on analysis of leak-off tests and lost returns. The site is located in Mississippi Canyon block 252, roughly 50 miles offshore Louisiana, in water depths of 5000 feet. The Macondo prospect was the petroleum reservoir target of BP's exploration well at 18,000 feet below sea level. It was deposited in middle Miocene sands as an amalgamated, low-relief, submarine channel levee system. The turbidite deposit overlies a Mesozoic turtle structure, which forms the trapping mechanism with stratigraphic and dip elements. The sediments deposited above the reservoir span the Pleistocene and Upper Miocene, and are largely comprised of siltstone, mudstone, marl and claystone.

Keywords: pore pressure, overpressure, macondo, gulf of mexico, marine geology

EG
ECG

Velocity-Independent Localization of Passive Seismic Events Using Local Slopes

Yunzhi Shi
Shi, Y., Bureau of Economic Geology, The University of Texas at Austin, Austin, TX
Fomel, S., Bureau of Economic Geology, The University of Texas at Austin, Austin, TX

Different from active source seismic exploration, passive seismic events information reveals subsurface information including fault displacement, drilling and hydraulic fracturing process, which mainly consists passive seismic sources locations and activation times. Microseismic monitoring, which includes passive seismic events locating and timing, has already been widely used in hydraulic fracturing activities.

Compared to down-hole arrays setting, surface arrays provide larger aperture thus wider coverage of injection area; however, conventional surface arrays source location methods require velocity model as a priori. In time-domain imaging, effective seismic velocities are picked from coherency scans, which remains one of the most labor-intensive and time-consuming procedures in the conventional approach to seismic data analysis. An alternative approach is velocity-independent imaging, of which the advantage is that local slopes can be measured without picking in the prestack data domain, while local slopes contain complete information about underground velocity geometry.

We proposed that use automated method such as plane-wave destruction to estimate local slopes and decompose prestack data into *t-x-p* domain; after mapping data in *t-x* slices with known slope, or equivalently, velocity information, into time-migrated section, recompose along slopes to build passive events sources localization section. Synthetic and field data tests demonstrate the practical effectiveness of our method.

Keywords: passive seismic, velocity independent, local slope, time imaging

ECG-20

EG
ECG

Integrated Stratigraphic and Structural Evolution of the Guadalupian Seven Rivers Formation, McKittrick Canyon, NM

Benjamin Smith
Smith, B., Department of Geological Sciences, University of Texas at Austin
Kerans, C., Department of Geological Sciences, University of Texas at Austin

Syndepositional to early deformation is recognized as a common process within modern and ancient carbonate platforms. However, the degree to which early faulting and down-to-the-basin tilting affect the final orientation of shelf top strata is not well understood. This ambiguity adds uncertainty to sequence stratigraphic frameworks which often take into account stratal geometries and quantified stratigraphic variables such as progradation/aggradation (P/A) ratios. This study utilizes field data and a lidar-based 3D digital outcrop model (DOM) in order to understand the first order controls on seaward-dipping back reef strata within the Guadalupian Seven Rivers Formation in McKittrick Canyon, NM. Understanding the relative contributions of structural and sedimentological processes to final stratal geometry in carbonate platforms will aid in subsurface reservoir characterization, where stratigraphic frameworks rely heavily on stratal geometries from seismic. Research will focus on constructing a cycle- to cycle-set scale stratigraphic framework which will be used to (1) trace key cycle set boundaries across the outcrop in order to create a detailed quantitative reconstruction of facies dip width distribution and (2) document the effects and timing of faulting and down-to-the-basin tilting by creating cross sections restored to key datums such as accommodation-filled cycle caps.Results from field work and DOM analysis indicate that faults grew syndepositionally with a maximum displacement of up to seven meters during Seven Rivers deposition. Faults are positioned seaward of the antecedent Goat Seep margin, which acted as a fulcrum for deformation of younger back reef strata. Similar deformation features have been documented over terminal shelf margins within the overlying Yates Formation but have not been considered important within the Seven Rivers Formation. Conversely, some geometries have a depositional origin; low curvature, concave upwards benches that thicken seaward are a reliable indicator for the fusilinid-rich outer shelf facies tract. Maximum dip width estimates of this facies tract indicate that it comprises a larger portion (up to 500 m) of the shelf profile within the Seven Rivers relative to the overlying Yates and that the narrowing of the outer shelf through time represents a dynamic sedimentological control on platform morphology and stratal geometry.

Keywords: Sequence stratigraphy, carbonate sedimentology, digital outcrop models, Permian, Seven Rivers, Guadalupe Mountains,

EG
ECG

Reservoir Characterization of an Intrashelf Basin Hybrid Play: Integration of a predictive reservoir model for the Upper Glen Rose, East Texas Basin

Peter Soto-Kerans
Soto-Kerans, P., Jackson School of Geosciences, The University of Texas at Austin, Austin, TX
Loucks, B., Bureau of Economic Geology, The University of Texas at Austin, Austin, TX

In recent years, the need to understand complex, laterally varying lithology and play types of unconventional 'hybrid' plays (such as the Bakken formation) has become a top priority to improve recoverable reserves. In order to achieve this, a predictive depositional model must be constructed through extensive core analysis and log integration. The Upper Glen Rose Formation, a mixed carbonate/siliciclastic hybrid play (Trinity Group) within the East Texas Basin, is a prime case study for exhibiting how integration of a depositional framework model can be used to understand the reservoir heterogeneity of a hybrid reservoir. Deposited within a restricted subtidal lagoon environment behind the Stuart City Reef margin during the Lower Cretaceous, the Upper Glen Rose is characterized by mixed facies varying from ooid grainstone facies to argillaceous mudstones/wackestones. Major oil and gas production within the Upper Glen Rose has been dominated through conventional high porosity ooid grainstone reservoirs (Alabama Ferry, Fort Trinidad), however interest has been directed to understand the unconventional potential of organic rich (up to 2% TOC) source beds (argillaceous mudstones) interbedded throughout. Modeling this distribution of coeval organic mudrocks, porous grainstones, and other potential low permeability reservoir facies is critical in order to understand how potential targets are distributed. Through acquisition/analysis of 10 cores, 100 composite well logs, XRF, pyrolysis, and vitrinite reflectance data, a preliminary predictive depositional model is presented for the Upper Glen Rose in order to gain an understanding of the overall reservoir framework and exhibit how a predictive depositional model can be utilized for other 'hybrid' plays.

Keywords: unconventional, hybrid, oil, east, texas, basin, glen rose

ECG-22

EG
ECG

PROSPECTIVITY MODELING FOR CAMBRIAN–ORDOVICIAN HYDRAULIC FRACTURING SAND RESOURCES AROUND THE LLANO UPLIFT, CENTRAL TEXAS

Rahul Verma
Verma, R., Department of Geological Sciences, The University of Texas at Austin
Elliott, B., The Bureau of Economic Geology, The University of Texas at Austin, University Station, Box X Austin, Texas
Kyle, J., Department of Geological Sciences, The University of Texas at Austin

Cambrian-Ordovician strata in Central Texas are a major source of specialty sand for hydraulic fracturing and have potential to play a bigger role in proppant supply to markets in and around Texas. Sandstone in the Hickory Member of the Riley Formation is suitable in compressive strength, as well as grain size and shape to be used as proppant. The Hickory sandstone forms the basal sequence that non-conformably overlies the Precambrian basement and is a complex succession of terrestrial and transgressive marine arkosic to quartz arenitic sands and silts. The quantity and location of sand resources in the Central Texas Frac Sand district is illustrated through geospatial volumetric techniques and estimated at ~5 billion tons of proppant material. The prospectivity modelling of favorable characteristics in existing resource locations is applied in an effort to determine new sites for resource development, and quantify the abundance of prospective natural sand resource in the Central Texas Frac Sand district. Northern White sand, which has higher compressive strength is also widely used in hydraulic fracturing. The transportation distance for Northern White sands is more than 1,000 miles for hydraulic fracturing sites in Texas, while the Hickory sandstone is located locally within 200 miles from most if the sites. Therefore, wherever applicable, Texas specialty sand would be a more economical alternative. Areas within major shale plays in Texas where basin closure stress is sufficiently low to use Texas specialty sand are also identified.

Keywords: Industrial Sand; Proppant, Mineral Resources; Prospectivity Modelling, Hickory Sandstone, Riley Formation; Llano Uplift, Texas

ECG-23

MG
ECG

Wide-Angle Refraction Tomographic Inversion of Mid Cayman Spreading Center and its Ocean Core Complex, CaySEIS Experiment

Jennifer Harding
Harding, J., The University of Texas at Austin Institute for Geophysics, Austin, TX
van Avendonk, H., The University of Texas at Austin Institute for Geophysics, Austin, TX
Hayman, N., The University of Texas at Austin Institute for Geophysics, Austin, TX
Grevemeyer, I., GEOMAR Helmholtz Centre for Ocean Research Kiel, Kiel, Germany
Pierce, C., Durham University, Durham, DH1 3LE, United Kingdom

The CaySEIS experiment, conducted in April 2015, is a multi-national collaborative seismic study of the Mid Cayman Spreading Center (MCSC), an ultra-slow spreading center [15 mm/yr fr] in the Caribbean Sea. Ultra-slow spreading centers are thought to have very thin crust and a paucity of magmatism due to cooler mantle conditions. However, the suggestion that gabbro-cored ocean core complexes (OCCs), volcanic deposits, and multiple layers of hydrothermal vents are widespread in the MCSC and other ultra-slow spreading centers has led to questions about the relationship between seafloor spreading rates and magmatism. To investigate this further, we conducted the CaySEIS experiment, with five wide-angle seismic refraction lines parallel and perpendicular to the neovolcanic zone. This analysis is based on two east-west oriented 100-km-long seismic refraction lines, which were each occupied by 18 ocean bottom seismometers. Line 2 lies across the central MCSC and an OCC called Mt. Dent. Line 3 crosses the northern end of the MCSC near the Oriente Transform Zone. With the wide-angle OBS data we can image the seismic velocity structure of Mt. Dent and distinguish between two models of OCCs – either Mt. Dent is composed of mostly gabbro with peridotite lenses identified by a low velocity gradient, or it is composed of mostly peridotite with gabbroic bodies identified by a constant velocity gradient. The crustal structure of both lines gives more insight into the asymmetry of the MCSC and the style of seafloor spreading to the east vs. the west. The 2-D velocity models reveal Mt. Dent has thick crust of 8 km with a low velocity gradient, supporting the magmatic gabbroic origin of OCCs. The surrounding crust to the west of the MCSC is highly variable, with areas of very thin crust. The crust to the east of the MCSC has an approximately constant thickness of 4 km. The development of OCCs may contribute to the crustal heterogeneity of ultra-slow spreading centers.

Keywords: tectonics, seismology, oceanic crust

ECG-24

MG
ECG

Architecture of Basin Scale Clinoforms Using Well Logs and Seismic Data in Dacian Basin, Romania

Takonporn Kunpitaktakun
Olariu, C., The University of Texas at Austin, Austin, TX
Fong-Ngern, R., The University of Texas at Austin, Austin, TX

Late Miocene 300 m height clinofroms are easily recognized in 3-D seismic of Dacian Basin, a para-Tethys basin in Romania. The characteristic of clinoform in well logs where is simply distinguishable a 100-150 m thick lower interval with coarse sandy deposits overlain by 300-500 m thick muddy deposits and capped by 50-100 m thick sandy deposits. The sandy muddy pattern appears in most well logs but the inclined features of clinoform are not obvious. This study emphasize the difficulties to recognize the clinoforms using well logs datasets and how subtle thickness changes of the fans and shelf-edge deltas might suffice to suggest clinoforma geometry in the basin. The study is using SP and resistivity logs of closely spaced (hundreds of meters) wells to follow the lithology changes. The proposed method is to create five perpendicular well sections and two parallel well sections to the orientation of the clinoform foreset as recognized on seismic. Well correlation is be guided by seismic interpretation in order to understand the overall trend and extension of clinoform. The results of well log correlation are illustrating inclined subtle lithology changes inside the muddy interval forming clinoforms with little observation of sand units. The lower coarser grained unit interpreted as fan deposits and the upper coarse grained unit interpreted as shelf to shelf edge delta have variable thicknesses. The variable thickness observed on logs combined with erosional geometries (discontinuous reflectors) observed on seismic suggest that the clinoforms have a highly dynamic evolution with deltas (or maybe rivers) at times filling shelf edge incisions. Similarly, sand thickness of the basin floor fans suggest that these are building (aggrading, prograding) stronger at some locations.

Keywords: clinoform, well logs, shelf slope

ECG-25

MG
ECG

Velocity-Effective Stress Relationships at Mad Dog, GoM

Landon Lockhart
Lockhart, L., The University of Texas at Austin, Austin, TX
Flemings, P., The University of Texas at Austin, Austin, TX

I predict pressure in the Green Canyon 826-1 well using a velocity effective stress model that is constrained by direct measurements of pore pressure within reservoir intervals. I demonstrate this technique using the Bowers Method with constants calibrated from direct observations of pressure and velocity. Ultimately, my work will integrate direct measurements of mudstone velocity and pressure with geomechanical modeling to predict pore pressure at the Mad Dog Field and in other locations. My next step will be to devolve a relationship between velocity and effective stress.

Keywords: Pressure, pore pressure, velocity, effective stress

ECG-26

MG
ECG

Deepwater Architecture of the Pliocene Lycium Turbidite Deposits, Fish Creek-Vallecito Mountains Basin, California: Large-Scale Supercritical Bedforms?

Logan West
West, L., Dept. of Geosciences, The University of Texas at Austin, Austin, TX
Olariu, C., Dept. of Geosciences, The University of Texas at Austin, Austin, TX

Recent work has pointed to the previously overlooked role of high-energy processes in offshore, deepwater sediment transport. Flume experiments and numerical modeling have indicated the potential for Froude-supercritical flow to occur in sediment-gravity transport, yet identification and understanding of such deposits in the modern and ancient is limited. This work investigates the Cenozoic Lycium Member turbidites, deposited in a relatively short-lived past northern extension of the Gulf of California, that are now exposed in the Anza-Borrego Desert State Park, California, USA. Initial work interpreted seismic-scale outcrops there as consisting of slope-channel and levee deposits.

The initial aim of this work is to revisit and better understand the two and three-dimensional geometries and characteristics of the Lycium Member turbidites to better understand the stratigraphic architecture and assess whether these bedforms are consistent with the hypothesis that they are the result of supercritical flow processes. For this preliminary work, high-resolution photography is collected and spatially tagged for a more detailed visualization of the outcrop that will be oriented and potentially mapped in three dimensions. Additionally, several sections of the outcrop were measured at the sub-meter scale to better understand the primary facies and their respective lithology, grain size, and centimeter-scale bedforms. Linking the detailed measured sections to the photography allows for better interpretation and mapping of the outcrop and its major bedforms. Future work will look at measuring sections with 3D exposures and to try to determine flow properties that could explain the bedforms present.

Keywords: froude supercritical, Anza-Borrego, high energy bedform

ECG-27

PS
ECG

River meander traverse asymmetry as a paleoflow direction indicator for Martian channel belts

Benjamin Cardenas
Cardenas, B., Jackson School of Geosciences, The University of Texas at Austin, Austin, TX
Mohrig, D., Jackson School of Geosciences, The University of Texas at Austin, Austin, TX

A dataset of measurments of meander traverse asymmetry from active river channels and preserved channel belts demonstrates the effectiveness of that asymmetry as an indicator of paleoflow direction of channel belts at Mars.

Keywords: Mars, fluvial, sedimentary geology

ECG-28

SETP
ECG

Defining the Thermal Evolution of Magma-Poor, Hyperextended Rift Margins, the Err and Tasna Nappes, Eastern Switzerland

Patrick Boyd
Boyd, P., Jackson School of Geosciences, The University of Texas at Austin, Austin, TX
Stockli, D., Jackson School of Geosciences, The University of Texas at Austin, Austin, TX

The Austroalpine and Penninic nappes of Eastern Switzerland expose one of the best-preserved fossil rifted margins in the world and have been critical to the development of tectonic models for magma-poor rift margins. The extended continental margin, which formed during Jurassic rifting between the Adriatic and European plates opening the Alpine Tethys, was exhumed during the Alpine orogeny. The structures related to the Mesozoic rifting between the Adriatic and European plates have been preserved through exhumation and have since been transported as thrust sheets which were delaminated from the upper crust of the Adriatic and currently rest as nappe stacks on the European plate. As many exhumed rift margins have been greatly deformed during their upheavel, and modern rift margins are less accessible due to their deep-marine locality, the preservation and accessibility of the Alpine Tethyan margins provides an excellent opportunity to build on the understanding of the thermal evolution of hyperextended margins. Early hyperextended margins evolve through uniform pure-shear extension acting on the crust and lithospheric mantle which results in symmetrical crustal deformation on either side of the rifting axis. However, low-angle normal faults and asymmetry surrounding the rifting axis that form during the latter stages of extension are now seen in the exhumed and transported Austroalpine and Penninic nappes. The increased geothermal gradient caused by upwelling lithospheric mantle and asthenosphere during the detatchment phase of hyperextension imprint a thermal signature into key mineral grains in the form of quantitative diffusive loss and retention of radiogenic daughter products. This signature allows for the update of the current model of how hyperextended margins evolve throughout time with apatite and rutile high temperature thermochronometry being ideally suited to measure the pre-collisional thermal evolution of the Tethyan rift margin exposed within the Alps. The novel and powerful technique of apatite and rutile U-Pb *depth profiling*, measuring the parent and diffusive daughter concentration ratios in a grain as a function of radial position, gives us access to a temporal and thermal record that was previously inaccessible to traditional radiometric dating techniques. U-Pb zircon geochronology data, a measure of crystallization timing, gives pre-rift Variscan orogenic ages, while zircon and apatite (U-Th)/He low-temperature thermochronometers that record thermal window from 60-200° C have been reset by Alpine metamorphism. With estimates of the thermal overprint caused by hyperextension and mantle upwelling in the fossil Alpine Tethys margin overlapping with the closure temperatures for Pb diffusion in apatite and rutile (~400-600° C) the minerals are ideal high temperature thermochronometers to measure and provide a better understanding of the lithospheric thermal evolution through hyperextension.

Keywords: Geochronology, Thermochronology, Tectonics

ECG-29

SETP
ECG

U-Pb geochronology of modern river sands from wedge-top foreland depo-centers; when sinks becomes the source

Tomas Capaldi
Capaldi, T., Department of Geological Sciences, Jackson School of Geosciences, University of Texas at Austin, TX, USA

This study investigates how Andean river sediments in the flat-slab segment of western Argentina record active mixing of lithologically and geochemically distinct source regions comprising the Principal Cordillera, Frontal Cordillera, Precordillera fold-thrust belt, Sierras Pampeanas basement uplifts, and recycled Neogene basin fill. Detrital zircon U-Pb geochronological results for modern river sands discriminate variations from hinterland source regions, through river tributaries and main trunks of the Bermejo, Jachal, San Juan, and Mendoza rivers, and their respective fluvial megafans within the active foreland basin. Proportions of proximal zircon populations in the hinterland trunk rivers (with extensive Permian-Triassic and Cenozoic igneous exposures) diminish downstream with progressive contributions from the frontal Precordillera fold-thrust belt (dominantly Paleozoic sedimentary rocks) and Pampean basement uplifts. However, this systematic downstream dilution is perturbed in several catchments by significant recycling of older foreland basin fill. The degree of recycling depends on the position and extent of Oligocene–Pliocene exposures within the catchments. To discern the effects of the variable detrital zircon sources, multiple statistical methods are utilized. Quantitative comparisons suggest that variations in detrital zircon age distributions among the modern sands, and with older foreland basin fill and exposed bedrock, are dependent on spatial and temporal variations in exhumation and drainage network evolution within their respective Andean catchments. The present surface area of competing source regions and the configuration of hinterland tributary rivers largely dictate the degree of downstream dilution and/or recycling. This study provides a modern analogue and baseline for reconstructing Neogene shifts in foreland basin provenance, depositional systems, and drainage configurations during a critical transition to flat-slab subduction.

Keywords: Source-to-Sink, foreland basin systems, Andes

ECG-30

SETP
ECG

Pleistocene to recent incision rates for the Rio Grande Gorge, northern New Mexico

Travis Clow
Clow, T., Jackson School of Geosciences, The University of Texas at Austin, Austin, TX
Behr, W., Jackson School of Geosciences, The University of Texas at Austin, Austin, TX
Helper, M., Jackson School of Geosciences, The University of Texas at Austin, Austin, TX
Patterson, D., Jackson School of Geosciences, The University of Texas at Austin, Austin, TX
Stockli, D., Jackson School of Geosciences, The University of Texas at Austin, Austin, TX

The Rio Grande River and other major river systems throughout the western US record a punctuated increase in fluvial incision rates in the middle Pleistocene. Evidence for this includes young, transient features such as knickpoints in longitudinal river profiles, and abandoned river terraces preserved throughout the downstream extent of the system. Despite that apparent increases in incision rates are well documented, the driving mechanisms for incision are poorly understood. Possible mechanisms include: long-term climatic fluctuations, local faulting or regional tectonism, drainage basin integration, or a combination thereof. This study aims to better constrain the rates and driving mechanisms of incision of the northern Rio Grande River gorge from the middle Pleistocene to present day. My approach uses detailed field and digital mapping coupled with cosmogenic 3He surface exposure dating of abandoned river terraces along a ~5km stretch of the Rio Grande River near Questa, NM. This stretch is the only section along the steep-sided northern Rio Grande River where fluvial terraces are preserved. Preliminary digital mapping suggests there are at least 4, and up to 6 terrace levels preserved that span elevations of 2-120 m above the modern river. The terraces are incised into and composed of ~4 m.y. Servilleta basalts of the Taos Plateau, making cosmogenic 3He dating an ideal method for determining the timing of their abandonment. Once gathered, comparing the ages of these terraces and the associated Rio Grande River incision rates to regional climatic and tectonic forcings will allow us to place constraints and gain insight on the driving mechanisms of incision.

Keywords: rapid, incision, rio grande, river, gorge, pleistocene, terraces, climate, tectonics, cosmogenic, surface, exposure, dating, helium, new mexico

ECG-31

SETP
ECG

Basin evolution in northern Peru: Implications for the growth of topographic barriers linking the Central and Northern Andes

Sarah George
Horton, B., University of Texas at Austin, Austin, TX
Moreno, F., University of Rochester, Rochester, NY
Jackson, L., University of Texas at Austin, Austin, TX

The relatively low and narrow Andes of northern Peru and Ecuador record the final establishment of a contiguous topographic barrier along western South America. Establishment of a new drainage divide during the Neogene strongly influenced the creation of an east-flowing Amazon drainage system, aridification of the Andean forearc, and biodiversification of the Amazon Basin. The Bagua Basin, a low elevation (400-600 m) intermontane basin in northern Peru, contains a protracted, semi-continuous record of Triassic through Pleistocene sedimentation. Situated between the Marañon fold-thrust belt of the Western Cordillera, and basement block uplifts of the Eastern Cordillera, the Bagua region offers a unique opportunity to study (1) the poorly constrained Mesozoic record of northern Peru, and (2) a complex history of Cenozoic shortening. We present new measured sections and detrital zircon geochronology on Mesozoic through modern samples to unravel the tectonic history. Detrital zircon geochronology shows evidence for Triassic-Jurassic rifting (marked by unimodal age peaks from 300-150 Ma), Cretaceous post-rift subsidence (dominated by 2000-900 Ma cratonic sources), onset of upper-plate shortening during the late Cretaceous (marked by an influx of syndepositional zircons and a decrease in cratonic sources), and a transition from backbulge to wedgetop deposits from Paleocene to Pliocene.

Keywords: tectonics, Andes, basin evolution, detrital zircon geochronology

ECG-32

SETP
ECG

Early Cenozoic shortening and foreland basin sedimentation in the Marañon fold-thrust belt, central Peruvian Andes

Lily Jackson
Jackson, L., Department of Geological Sciences and Institute for Geophysics, Jackson Sc
Rosell, L., Universidad Nacional San Antonio Abad del Cusco UNSAAC, Av. de la Cultura, 733, Cusco, Peru
Carlotto, V., Universidad Nacional San Antonio Abad del Cusco UNSAAC, Av. de la Cultura, 733, Cusco, Peru
Horton, B., Department of Geological Sciences and Institute for Geophysics, Jackson Sc

The Marañon fold-thrust belt in the western Andes of Peru has long been considered a robust signature of early Cenozoic shortening in the Andean orogenic belt. However, the structural details and potential records of coeval synorogenic sedimentation remain elusive. We report results from new geologic mapping (1:40,000), cross-section construction, and U-Pb geochronology for the Matucana-Ticlio region at 11-12°S along the Lima-La Oroya highway. Zircon U-Pb age data from volcanic rocks and clastic basin fill provide a maximum depositional age of ~43 Ma for a middle Eocene syndeformational unit that we correlate with the Anta Formation of southern Peru, which overlies the Paleocene Casapalca Formation. Sedimentary lithofacies and unconformable relationships within the volcaniclastic Rimac and Millitongo formations (Anta Formation) reveal mixed fluvial, alluvial-fan, and volcanic depositional conditions during shortening accommodated by a NE-verging thrust/reverse fault and corresponding backthrust (here named the Chonta fault system). Our cross-section reconstruction and geochronological data indicate that the region is a critical, possibly unique, zone of the broader NE-directed Marañon fold-thrust belt where pre-Neogene synorogenic sediments and their associated structures are preserved. We interpret this combined structural and basin system as an Eocene-age (Incaic) frontal thrust belt and corresponding foredeep to wedge-top depozone in central Peru. As one of the better-constrained segments of the Marañon fold-thrust belt, this zone provides insight into potential linkages with elusive early Cenozoic (Incaic) structures and foreland basin fill of the Western Cordillera and Altiplano farther south in the central Andean plateau.

Keywords: Peru, Andes, Chonta Fault, Casapalca

ECG-33

SETP
ECG

Depositional and provenance records of Mesozoic basin evolution and Cenozoic shortening in the High Andes, La Ramada fold-thrust belt, southern-central Andes (32-33°S)

Chelsea Mackaman-Lofland
Mackaman-Lofland, C., University of Texas at Austin, Austin, TX
Horton, B., University of Texas at Austin, Austin, TX
Fuentes, F., YPF SA, Buenos Aires, Argentina
Constenius, K., University of Arizona, Tucson, AZ
McKenzie, R., Yale University, New Haven, CT
Alvarado, P., Universidad Nacional de San Juan, San Juan, Argentina
Orozco, P., Universidad Nacional de San Juan, San Juan, Argentina
Stockli, D., University of Texas at Austin, Austin, TX

The Argentinian Andes define key examples of retroarc shortening and basin evolution above a zone of active subduction. The La Ramada fold-thrust belt (RFTB) in the High Andes provides insights into the relative influence and temporal records of diverse convergent margin processes (e.g. flat-slab subduction, convergent wedge dynamics, structural inversion). The RFTB contains Mesozoic extensional basin strata deformed by later Andean shortening. New detrital zircon U-Pb analyses of Mesozoic rift sediments reveal: (1) a dominant Permo-Triassic age signature (220-280 Ma) associated with proximal sources of effective basement (Choiyoi Group) during Triassic synrift deposition; (2) upsection younging of maximum depositional ages from Late Triassic through Early Cretaceous (230 to 100 Ma) with the increasing influence of western Andean arc sources; and (3) a significant Late Cretaceous influx of Paleozoic (~350-550 Ma) and Proterozoic (~650-1300 Ma) populations during the earliest shift from back-arc post-extensional subsidence to upper-plate shortening. The Cenozoic detrital record of the Manantiales foreland basin (between the Frontal Cordillera and Precordillera) records RFTB deformation prior to flat-slab subduction. A Permo-Triassic Choiyoi age signature dominates the Miocene succession, consistent with sources in the proximal Espinacito range. Subordinate Mesozoic (~80-250 Ma) to Proterozoic (~850-1800 Ma) U-Pb populations record exhumation of the Andean magmatic arc and recycling of different structural levels in the RFTB during thrusting/inversion of Mesozoic rift basin strata and subjacent Paleozoic units. Whereas maximum depositional ages of sampled Manantiales units cluster at 18-20 Ma, the Estancia Uspallata basin (~50 km to the south) shows consistent upsection younging of Cenozoic populations attributed to proximal volcanic centers. Ongoing work will apply low-temperature thermochronology to pinpoint basin accumulation histories and thrust timing.

Keywords: basin analysis, Andes, convergent margins, zircon U-Pb geochronology

SETP
ECG

Holocene Geologic Slip Rate for the Mission Creek Strand of the southern San Andreas Fault, Indio Hills, California

Juan Munoz
Munoz, J., Jackson School of Geosciences, The University of Texas at Austin, Austin TX
Behr, W., Jackson School of Geosciences, The University of Texas at Austin, Austin TX
Gold, P., Jackson School of Geosciences, The University of Texas at Austin, Austin TX
Fryer, R., Jackson School of Geosciences, The University of Texas at Austin, Austin TX

The objective of this study is to obtain a Holocene geologic estimate slip rate from an offset alluvial fan located on the Mission Creek strand of the southern San Andreas fault near Indio, CA. The significance is represented by the fact that it will be the only attempt to publish a Holocene slip rate of the Mission Creek strand of the southern San Andreas fault. This will better constrain how slip is partitioned among several strands of the southern San Andreas fault in this complex. Field mapping and observation using airborne LiDAR imagery allows for the precise determination of the amount of offset and the reconstruction of the original catchment area of the alluvial fan. Cosmogenic ^{10}Be surface exposure geochronology will be used on samples taken from the fan surface and from excavated trenches in order to date the timing of fan deposition profiles using amalgamated cobbles to date the original deposition of the alluvial fan and to measure the effect of mixing on this dating method. The cosmogenic dating will be combined with existing minimum depositional ages from U-series pedogenic carbonate dating. A preliminary analysis has determined the offset to be around 80 meters. A mean weighted age of the pedogenic carbonate was determined to be 3.49+/-0.92 ka (95% CI), which is believed to represent a reliable minimum depositional age for the host fan. Field work was done this December to extract samples for ^{10}Be analysis. Results for this method will be resolved in the coming months.

Keywords: southern San Andreas fault, LiDAR, cosmogenic, slip rate,

SETP
ECG

Deep mantle S-wave velocity model under Yellowstone

Peter Nelson
Nelson, P., The University of Texas at Austin, Austin, TX
Grand, S., The University of Texas at Austin, Austin, TX

=12.0ptSince the 1970s, the origin of intraplate hotspots has been hypothesized to come from deep mantle plumes created by thermal instabilities along the core-mantle boundary. Mantle plumes are mushroom shaped warm anomalies that have a spherical “head” and a long narrow “tail”. The plume hypothesis has been used to explain many significant geologic phenomena such as hotspots, large igneous provinces, continental rifting, magnetic pole reversals and even mass extinction events. However, the direct detection of a mantle plume using travel time tomography has remained elusive. The Snake River-Yellowstone Hotspot in the western United States is an intraplate hotspot with exceptional station coverage whose source has been hotly debated. Herein, we present a method using SKS and SKKS waves in conjunction with finite frequency kernels and USArray data to detect a mantle plume under Yellowstone. We demonstrate using a synthetic plume model test the feasibility of our method to image a narrow plume in the lower mantle. Furthermore, we present a preliminary tomographic model which shows a slow anomaly in the lower mantle under the Western United States.

Keywords: Tomography, Yellowstone, SKS waves, Deep Mantle, Mantle Plume

SETP
ECG

Studying tectonic inversion in the eastern Pyrenees using (U-Th)/He and U-Pb bedrock thermochronology

Margaret Odlum
Odlum, M., The University of Texas at Austin, Austin, TX
Stockli, D., The University of Texas at Austin, Austin, TX

Structural and thermal inheritance associated with tectonic inversions are assumed to be important controls on subsequent deformation and strain partitioning, yet the role and extent are poorly understood. The Pyrenean orogen resulted from the tectonic inversion of a rifted margin as the Iberian micro-plate motion reversed from extension and rifting in the early Cretaceous to convergence and collision in the late Cretaceous. The North Pyrenean Zone (NPZ) is a fossilized rift margin along a continental suture where blocks of the entire crustal section and mantle lithosphere exhumed during rifting have been preserved and subsequently deformed during collision and orogenesis. (U-Th)/He and U-Pb thermochronology on crustal sections in the North Pyrenean Zone (NPZ) exhumed during rifting provides insights into the thermal regime and rift margin architecture when Iberia motion reversed to convergence. Understanding the inherited structures, heat and rheology during early convergence and mountain building is critical to understanding the strain partitioning and role of inheritance in mountain building events. Recent studies in the western NPZ have shown that shortening began on a hot paleomargin (~80°C/km) allowing for shallow ductile shortening and significant reactivation of rift structures. A multi-mineral, multi-isotope thermochronology approach in the eastern NPZ, where there was a greater magnitude of rifting and subsequent shortening, will provide a high resolution thermal history through the majority of the crustal section providing insights into rift margin architecture, the thermal regime of rifting and the role of inherited heat in reactivation of structures and shortening. A novel approach to recovering thermal histories by laser ablation depth profiling radiogenic daughter and parent concentrations in single mineral grains is used to recover unique thermal histories. Zircon, rutile and apatite U-Pb (temperature ranges of ~1000-800°, 650-500°C and ~450-370°C respectively) and zircon and apatite (U-Th)/He (temperature ranges of ~180-120°C and 80-40°C respectively) are combined from samples from the Saint Barthélemy and Agly Massifs in the NPZ to recover high-resolution thermal histories that can be used to understand the structural and thermal evolution of tectonic inversions.

Keywords: tectonic inversion, Pyrenees, thermochronometry

SETP
ECG

Longevity of Strain Localization Associated with Dynamic Recrystallization of Olivine in Mantle Rocks

Pamela Speciale
Speciale, P., Jackson School of Geosciences, The University of Texas at Austin, Austin, TX
Behr, W., Jackson School of Geosciences, The University of Texas at Austin, Austin, TX
Hirth, G., Brown University, Providence, RI
Tokle, L., Brown University, Providence, RI

The processes that cause strain localization in the lithosphere are fundamental to our understanding of plate tectonics. Grain size reduction by dynamic recrystallization (DRX) is ubiquitously associated with strain localization in natural shear zones. However, whether DRX-related localization persists to form long-lived, narrow, plate boundaries is debated because of the possible counteracting role of grain growth. If DRX is associated with surface energy-driven grain boundary migration (γGBM), for example, grains are theoretically predicted to grow after recrystallization and localization will be temporary or cyclical. At high stress, low temperature conditions, however, GBM is driven by gradients in strain energy (ρGBM) wherein grain boundaries migrate from regions of low to high dislocation density. At these conditions, grain growth may be suppressed even in monophase aggregates, and localization may persist over geologic timescales. Alternatively, grains oriented such that they accumulate fewer dislocations than adjacent grains may grow by ρGBM. We deformed natural olivine aggregates under axial compression in a Griggs rig to examine the relative contributions of strain energy and surface energy in facilitating grain growth. We conducted 14 experiments in a molten salt cell at 1100 and 1200°C, a strain rate of 10^{-5} s^{-1}, and 1300 MPa confining pressure. After samples reached ~30% strain we relaxed the stress, either with the motor off or at a reduced strain rate of 10^{-6} s^{-1}, for specific time increments before quenching. We performed detailed microstructural analyses to identify the transition from ρGBM to γGBM at these experimental conditions. To evaluate whether the DRX grains grew during the stress relaxation interval, we compared the average flow stress and grain size predicted by the olivine paleopiezometer for that stress, to the final stress and measured grain size. Samples that were allowed to recover after deformation show abundant evidence of γGBM, but average grain size does not increase significantly compared to that in samples quenched prior to annealing. In contrast, samples that continued to deform at a reduced strain rate (for the same time as the annealed samples) show both ρGBM and γGBM, and a larger grain size. These observations indicate that growth is enhanced by continued deformation at low stress, possibly due to preferential migration of low dislocation density grains in favorable orientations.

Keywords: experimental deformation, olivine, stress relaxation, strain localization, Griggs rig

SETP
ECG

Seismiccycle at Sumatra

Xinyue Tong
Tong, X., Institute for Geophysics, Department of Geological Sciences, The University of Texas at Austin, Austin, TX
Lavier, L., Institute for Geophysics, Department of Geological Sciences, The University of Texas at Austin, Austin, TX
Tan, E., Institute of Earth Sciences , Academia Sinica, Taiwan

Subduction zones produce the largest earthquakes. However, our understanding of earthquakes' spatialtemporal occurrence and tectonic deformation at convergent margin is limited. Traditional view for subduction earthquake cycle contain three stages: Interseismic superposition of steady elastic strain accumulation and occasional shortduration aseismic strain release, Coseismic – rapid opposite direction release of accumulated elastic strain, and Postseismic – superposition of afterslips and viscoelastic flow in mantle wedge and lower crust. However, the way strain accumulated interseismically which is related to the generation of longterm deformation and uplift in the forearc region is still a matter of debate. Moreover, when integrated over time, coseismic uplift poorly matches the longerterm vertical deformation. To better understand these relationships, we investigate numerically how coseismic slip and longterm deformation (vertical uplift) accumulate and interact at subduction zones by using a robust, adaptive, multidimensional, finite element method solver, Dynearthsol3D, on a 2D continuum viscoelastoplastic model. We set the conditions in this model to a realistic convergent margin setting that resembles Sumatra region. By introducing bathymetric features, this research also explore mechanisms that could explain how strain accumulation in space and time is modified by the presence of large asperities at the subduction interface.

Keywords: Subduction, earthquake, cycle, Sumatra, Geodynamics, finite element method

ECG-39

SHP
ECG

Multiple Cut and Fill Episodes During the Evolution of the Wilcox Yoakum Canyon

Clarke Clayton
Clayton, C., Jackson School of Geosciences, The University of Texas at Austin, Austin, TX
Olariu, C., Jackson School of Geosciences, The University of Texas at Austin, Austin, TX

The Yoakum Canyon is a large submarine canyon of the Wilcox Group in east Texas. This canyon is a large feature with a depth greater than 1000 meters, length close to 96 km, and a width exceeding 16 km, placing the canyon near the end members of present day large submarine canyons. The previous model of evolution for the canyon by Dingus and Galloway (1990) proposed a single cut and fill episode that occurred during a time frame of 100,000 to 1.5 million years. By mapping sand bodies from well log data of the middle and lower Wilcox, previously thought to be older than the canyon, a trend of sand thickening near the canyon edge can be seen. Additionally core analysis of a sand body in the lower portion of the adjacent Lavaca Canyon from the Wilcox Group gives insight on facies present other than hemipelagic and prodelta muds. From mapping sand bodies and core analysis, a model of multiple cut and fill episodes is proposed.

Studies on other canyons with similar large dimensions have been characterized as having multiple cut and fill episodes. A study by Wonham et al. (2000) on the Baliste-Crecerelle Canyon, offshore Gabon, found the canyon longevity to be +10 million years with cut and fill episodes on a scale of 1 to 2 million years. The Central Canyon of the Qiongdongnan Basin, South China Sea (Gong et al., 2011; Shang et al., 2015) was active for 11.6 million years and had cut and fill episodes on the scale of 600,00 to 1.3 million years. The longevity of other submarine canyons of similar scale to the Yoakum Canyon suggests that the canyon was likely active for a period closer to millions of years rather than the previous model of 100,000's of years.

Keywords: Yoakum Canyon, Submarine Canyon, Wilcox

ECG-40

SHP
ECG

Seasonal Distribution of Mean Temperature and Diurnal Variation for Streams Across the Contiguous United States: A Case Study for Dec. 2012 to Nov. 2013

Stephen Ferencz
Ferencz, S., Jackson School of Geosciences, The University of Texas at Austin, Austin, TX

This study looked at spatial and temporal variations of stream temperatures in the contiguous United States. Despite the importance of stream temperature to ecosystem health, few studies have reported on the distribution of stream temperatures across the entire United States and no previous studies had looked at the magnitude and distribution of diurnal temperature variation. Seasonal data for mean temperature and diurnal variation of approximately 1,000 streams were compiled for a one-year period from December 2012 to November 2013. Stream temperature data was obtained from the USGS National Water Information System Surface-Water Database. Daily stream temperature data was used to calculate the average daily mean temperature and average magnitude of diurnal variation for each season. The 2012-2013 data exhibited clear seasonal trends for both mean temperature and diurnal variation. The magnitude of diurnal variation increased with increasing stream temperature, with the smallest diurnal variation during the winter and the largest in the summer. The spatial distribution of mean temperature and diurnal variation were compared to percent baseflow index and mean air temperature to examine the influence of these two factors. Streams that received a larger percentage of flow from groundwater typically had smaller diurnal variations, and the distribution of mean stream temperature mirrored that of mean air temperature. Understanding the spatial and temporal distributions of stream temperatures can help anticipate the effects that climate change may have on stream temperatures and can be used to indentify where stream biota will be most stressed.

Keywords: stream temperature, diurnal variation, spatial distribution, seasonal variation, aquatic ecology

SHP
ECG

Diurnal Water Characteristics in the Annapurna Himals

Hima Hassenruck-Gudipati
Hassenruck-Gudipati, H., The University of Texas at Austin, Austin, TX

Understanding Nepal's water budget is crucial as hydropower projects are being developed and the climate is changing. The propagation and modification of diurnal characteristics along tributary rivers can tell us something about the upstream river catchments. A major effort is underway to understand the water tower, the Himalayas, of a large part of Southeast Asia. We are contributing to this knowledge space around the Annapurna Himal area, focusing on Modi Khola River, a tributary of the Kali Gandaki River. To understand the diurnal characteristics of the Modi Khola River, we installed six Hobo water loggers to measure water level, conductivity, and temperature. These measurements were supplemented by an isotopic study in the Annapurna Himal including the main Kali Gandaki River. Diurnal signal propagation can be observed from the water logger data as well as isotopic measurements water samples. We hope to understand how much these signal propagations are due to new sources versus upstream signals.

Keywords: Hydrology, diurnal, signal propagation

ECG-42

SHP
ECG

VARIABILITY of TRANSITIONAL FLOWS on SUBMARINE FAN FRINGES

Woong Mo Koo
Koo, W., Department of Geological Sciences, The University of Texas at Austin, Austin, TX
Steel, R., Department of Geological Sciences, The University of Texas at Austin, Austin, TX
Olariu, C., Department of Geological Sciences, The University of Texas at Austin, Austin, TX
Kim, W., Department of Geological Sciences, The University of Texas at Austin, Austin, TX

The vertical and lateral lithofacies variation in the submarine fan-fringes of four clinothem-bottomsets in Washakie Basin, Wyoming, is examined at the scale from bed to submarine fan, using about 96 m of long cores from 4 wells as well as gamma-ray logs of closely spaced 1,585 wells. Cores in Washakie Basin show that there were variable lithofacies patterns in mapped submarine fan-fringes. Multiple transitions of lithofacies occur within the same bed, without significant erosion between high-concentration turbidites (e.g., structureless sandstones) and debrites (e.g., mud-clasts rich muddy sandstones) are identified in distal fringes of submarine fans. In contrast, in the lateral fringes of fans, there is a significantly shorter transition from turbidites to debrites. One explanation of facies variability is correlated with the run-out distance of flow that enhances transitions of flow. The longer axial run-out distance of flows results in deposition of mud-clast rich debrites. The shorter, transverse to lobe run-out distance causes only partial or non-transformed flows, resulting in deposition of muddy and sandy turbidites respectively. In the longitudinally elongated submarine fans in Washakie Basin, developed by long run-out distance of flow, the distal fan-fringes are thus significantly muddier than the lateral fringes, something of importance to hydrocarbon productivity on fan lobes.

Keywords: submarine fan-fringes, transitional flow, run-out distance, mud-clasts

LCMS-1

CCG
LCMS

Taxonomy of Plesioteuthididae and the first Loligosepiina coleoids from North America spanning the Pliensbachian and Toarcian Stages (Early Jurassic), Alberta, Canada

Selva Marroquin
Marroquin, S., Department of Geological Sciences, The University of Texas at Austin, Austin, TX
Martindale, R., Department of Geological Sciences, The University of Texas at Austin, Austin, TX

Octobrachiates (e.g., modern octopods, extinct loligosepiids, teudopseids and prototeuthids, etc.) are found in abundance from the Early Jurassic Posidonia Shale of Germany and other European black shale deposits thought to represent the Toarcian Oceanic Anoxic Event (~183 Ma). Nevertheless, to date, only two North American and two South American fossil Octobrachia specimens have been described outside of Europe. Due to the exceptional conditions required to preserve these organisms, they are typically only found within lagerstätten deposits. Lagerstätten are rare, exceptional fossil deposits that preserve soft tissue and poorly calcified or uncalcified organisms; these deposits capture information about organism physiology typically not preserved (e.g., cephalopod soft parts). Here we present the first comprehensive study of coleoids from outside of Europe for the Early Jurassic. These specimens come from the Ya Ha Tinda Lagerstätte, the first North American Jurassic Lagerstätte and the first Early Jurassic Lagerstätte from outside of Europe. The Ya Ha Tinda Lagerstätte was deposited in the Pliensbachian and Toarcian Stages of the Early Jurassic (Kunae to Planulata ammonite Zone of Western North America or Margaritatus to Bifrons ammonite zone of North Western Europe); this age is well constrained by both chemostratigraphy and ammonoid biostratigraphy. Excavations at Ya Ha Tinda have uncovered twenty new Octobrachiate fossils. Of these, several specimens preserve the subtle growth lines that are critical for taxonomic determinations and some even preserve ink sacs. Eleven of the most well preserved specimens are evaluated in detail and identified to the most specific taxonomic level. Six of these specimens have been identified to the generic and specific level, four [i]Geopeltis simplex[/i] specimens, one [i]Parabelopeltis flexuosa[/i], and one [i]Loligosepia aalensis[/i]. Four of the remaining five are identified as belonging to the suborder Loligosepiina and one to the family Plesioteuthididae. This is the first time these taxa (aside from the Plesioteuthididae) have been found outside of Europe; therefore this study significantly expands their paleogeographic range for the Early Jurassic.

Keywords: Lagerstätte, Octobrachia, Toarcian Oceanic Anoxic Event, Panthalassa

This abstract has been withdrawn

LCMS-2

CCG
LCMS

Investigating multidecadal rainfall variability in the South Pacific Convergence Zone using the geochemistry of stalagmites from the Solomon Islands

Natasha Sekhon
Quinn, T., UTIG,JSG, UT Austin
Partin, J., UTIG,UT Austin

The South Pacific Convergence Zone (SPCZ), which extends southeastward from New Guinea to Tahiti, is the largest perennial rainfall feature in the Southern Hemisphere. The position of the SPCZ and its associated rainfall varies significantly on multidecadal timescales, as documented by instrumental and climate proxy data. For example, stalagmite $\delta^{18}O$ records (rainfall proxy) from Espiritu Santo, Vanuatu (Partin et al., 2013) and Guadalcanal, Solomon Islands (Maupin et al., 2014), document large (~1‰), abrupt changes in stalagmite $\delta^{18}O$ on multidecadal timescales over the past 600 years that arise from internal variability in the climate system. The proxy data agree with the type of rainfall changes observed in the instrumental record, such as the change across 1976/77, but the older changes are larger in relative magnitude.

We expand on these earlier studies of rainfall variability in the SPCZ system using stable isotope variations in stalagmites from two other locations in the Solomon Islands (Munda, New Georgia, 8.3°S, 157.3°E; Suku, Nggela Pile (9.8° S, 160.2° E). These stalagmites range in age from about 400 CE to 1850 CE, based on U-Th dating, and have relatively fast growth rates (60 to 300 μm/yr). Stalagmite $\delta^{18}O$ time series were generated from sub-samples milled every 500 μm, or approximately 1 to 8 years per data point. Initial results from these two new Solomon Island stalagmites not only confirm the presence of multidecadal variability in stalagmite $\delta^{18}O$ identified in previous studies, but suggests that the same amplitude of variability has occurred over several windows of time during the past 1600 years. When complete, these new proxy rainfall records from Munda and Suku will further constrain the pattern and mechanism of SPCZ rainfall variability in western tropical Pacific region.

Keywords: Investigating multidecadal rainfall variability in the South Pacific Convergence Zone using the geochemistry of stalagmites from the Solomon Islands

CCG
LCMS

Testing Proxies to Determine Whether There is Evidence for Photosymbiosis in Fossil Corals

Chiara Tornabene
Tornabene, C., Department of Geological Sciences, The University of Texas at Austin, Austin, TX
Martindale, R., Department of Geological Sciences, The University of Texas at Austin, Austin, TX
Schaller, M., Department of Earth and Environmental Sciences, Rensselaer Polytechnic Institute, Troy, NY

Photosymbiosis is a symbiotic relationship that many corals have developed with dinoflagellates called zooxanthellae. Photosymbiosis is often considered the evolutionary innovation that allowed corals to become major reef-builders. Yet, despite their significance, zooxanthellae are not preserved in the fossil record making it difficult to determine whether ancient reef-building corals had symbionts. Stable isotope geochemistry could serve as a successful indirect proxy for ancient photosymbiosis. The $\delta^{15}N$ of modern zooxanthellate (Z) and azooxanthellate (AZ) coral organic matrices differ due to corals' nutritional lifestyles while the $\delta^{13}C$ and $\delta^{18}O$ of coral skeletons vary due to the influence of zooxanthellae photosynthesis on calcification. Here, we analyzed Modern and Triassic coral skeletons with varying morphologies (i.e. Z-like and AZ-like fossil corals) using the methods outlined by Stanley and Swart (1995) for $\delta^{13}C$ and $\delta^{18}O$ and Muscatine et al. (2005) for $\delta^{15}N$ to test whether these geochemical techniques are applicable to the fossil record. Samples were tested for diagenesis through petrography and scanning electron microscopy (SEM). The $\delta^{13}C$ and $\delta^{18}O$ data displayed high variability and C and O enrichment in fossil corals suggesting that the proxy is unreliable in the fossil record. The $\delta^{15}N$ data failed to identify fossil AZ corals suggesting either that the proxy in unreliable in the fossil record due to diagenesis or that the proxy is viable, but has yet to be tested on AZ corals. While we selected AZ-like fossil corals, all of our samples were collected from shallow water platforms and it is therefore possible that they were zooxanthellate despite of their morphology. Future work will focus on using deep-water Miocene corals to establish whether the $\delta^{15}N$ of fossil coral organic matrix can serve as a reliable proxy for ancient photosymbiosis. The establishment of a successful proxy for photosymbiosis will allow scientists to agreeably define the evolutionary relationship between symbiosis and coral reef-building; this proxy will also provide new insights into the successes and failures of photosymbiosis today.

Keywords: Photosymbiosis, Fossil Corals, Zooxanthellae, Stable Isotopes, Diagenesis

EG
LCMS

Depositional Environment Distribution, Diagenesis and Reservoir Quality of the Middle Bakken Member in the Williston Basin, North Dakota

Oguzhan Ayhan
Ayhan, O., Bureau of Economic Geology, The University of Texas at Austin, Austin, TX
Hammes, U., Bureau of Economic Geology, The University of Texas at Austin, Austin, TX
Fisher, W., Jackson School of Geosciences, The University of Texas at Austin, Austin, TX

The Upper Devonian-Lower Mississippian Bakken formation in the Williston Basin is an important source rock for oil production in North America. The Bakken formation is comprised of three units: upper and lower black shales and middle member. Upper and Lower Bakken shales are high quality source rocks which source reservoirs in the middle Bakken, upper Three Forks and lower Lodgepole formations. The Middle member of Bakken Formation, which consists of gray, interbedded siltstone and sandstone with shale, dolostone and limestone, is under investigation on this study. The goals of this study are to determine the regional distribution of lithofacies and depositional environment of the Middle Bakken Member and explain diagenetic sequence and reservoir quality parameters in the Williston Basin.

The reservoir quality of the Middle Bakken Member is mainly influenced by mineralogy and cementation resulting in low porosity (average ~%5) and permeability (average ~0.04 mD) and linked to facies distribution in the basin. Dolomitization is pervasive throughout the unit; however, we see local concentration of dolomite cement. Moreover, secondary cementation occurred including quartz overgrowths, K-felspar, clay cement and pyrite as both cement and nodules. Not only dolomitization but also pyrite cementation plays an important role in reducing pore spaces in the reservoir. The pore types that we have found are intergranular, intragranular, fracture and vugular porosity. Secondary intragranular porosity generally resulted from dissolution of biogenic fragments.

The distribution of dolomitization and pyrite cementation zones are shown correlating with the lithofacies and depositional environment of the Middle Bakken Member via core and petrographic thin section analysis in the Williston Basin.

Keywords: Depositional Environment, Middle Bakken, Williston Basin

LCMS-5

EG
LCMS

Formation and Evolution of Strandplain Grainstones and Facies Variability Along the Leeward Margin of West Caicos, British West Indies

Nick Danger
Danger, N., Jackson School of Geosciences, The University of Texas at Austin, Austin, TX, United States
Kerans, C., Jackson School of Geosciences, The University of Texas at Austin, Austin, TX, United States
Bachtel, S., Chevron Energy Technology Corporation, Houston, TX, United States
Zahm, C., Bureau of Economic Geology, The University of Texas at Austin, Austin, TX, United States

Pleistocene outcrops of Marine Isotope Stage (MIS) 5e age along the leeward margin of West Caicos show exceptional facies variability along strike (north-south). Diagnostic facies assemblages transition from predominantly skeletal-oolitic strandplain grainstones in the north to reef-dominated facies assemblages in the south. Strandplain grainstones are essential building blocks for many shallow platform carbonate islands. These grainstone assemblages are laterally continuous with good potential reservoir quality at deposition. Understanding the provenance, formation, and evolution of modern strandplain grainstones and their contribution to island formation could prove useful for ancient isolated carbonate platform analogs—particularly those deposited during similar icehouse conditions, such as the Tengiz and Kashagan fields in Kazakhstan. This study attempts to explain the formation and evolution of Pleistocene MIS 5e strandplain grainstones through analysis of facies variability in several representative cross sections, paleocurrent data, and mapped petrographic transects. Cross sections emphasize the overall thinning of the grainstone assemblages from north to south. Thin sections sampled over 16 petrographic transects were taken along the coast at 0.5 km intervals in order to systematically describe the facies petrographically and look for trends in grain size and type. Finally, paleocurrent measurements were taken to demonstrate the persistently southward-directed paleoflow. Mapped cross sections quantify the along strike complexity of these strandplain grainstones. On the northwest coast, the grainstone assemblages are upwards of five meters thick with dip widths on the order of tens of meters. On the southwest coast, the grainstone assemblages are 0-2 meters thick with less continuity (dip widths between 5-10 meters). The along-strike continuity of grainstone units decreases from north to south as reefal facies become predominant. Paleocurrent measurements from upper shoreface troughs support the assertion that these strandplain grainstones form from northern-sourced ooids wrapping around the northwest coast of West Caicos and deposit along the leeward margin. Understanding the nature of modern carbonate platform strandplain grainstones provides insight into the depositional nature and geometry of ancient subsurface isolated carbonate platform reservoirs, which allows for more accurate constraints on exploration plays and prospect assessment.

Keywords: Process Sedimentology, Carbonate Sedimentology, Caicos, Holocene, Pleistocene, Strandplain Grainstones

LCMS-6

EG
LCMS

Southern Gulf of Mexico Paleocene through Miocene Paleogeography: Investigating siliciclastic sedimentation in Mexico Deepwater

Luciana De La Rocha
de la Rocha, L., Institute for Geophysics
Snedden, J., Institute for Geophysics
Tinker, S., Bureau of Economic Geology

Sediment influx from the North American craton shed into the northern Gulf of Mexico basin, creating extensive Paleocene through Miocene deep-water fans which are prolific hydrocarbon reservoirs in US deep-water. Sediment sourcing for northern Gulf of Mexico reservoirs can be linked to drainage catchments developed in the US Laramide tectonic belt; however, less is known about the influence of the southern Laramide sources upon Mexican deep-water sedimentation. Some researchers contend that during the early Cenozoic a foreland system adjacent to the Eastern Sierra Madres had sufficient accommodation space to trap sediments eroded from the nearby Laramide uplands. Moreover, basement-cored Cretaceous carbonate buildups might have created a barrier for potential sediment bypass.This study uses core data, well logs, 2D regional seismic lines, Pemex geologic reports and data from recent literature to synthesize the paleogeographic evolution of the eastern Mexican margin and deepwater systems from Paleocene through Miocene time. Resulting onshore paleogeographic maps define potential entry points for sediment bypass into the Gulf of Mexico. Inferred paleo drainage systems are used to predict deep-water fans. Predictions were based on empirical relationships between length of drainage system and length of deep-water fans. Analysis of onshore paleogeographic trends are then tied to a regional interpretation of 2D seismic lines in the Southern Gulf of Mexico. Paleocene through Miocene structure maps, isochore maps, seismic facies maps, and deep-water paleographic maps highlight areas of interest for oil and gas exploration in the Southern Gulf of Mexico.Results suggest significant deposition of siliciclastic sediments into deepwater southern Gulf of Mexico. Onshore seismic data shows that Paleogene sediments onlap onto Cretaceous carbonate platforms. Nonetheless, data shows at least two Paleogene erosional canyons acting as entry points for sediment bypass into the Gulf of Mexico. Results from drainage systems scaling relationships predict shorter Paleogene deepwater fans than the US counterparts. Accommodation space in the foreland basin is completely filled by Late Oligocene. Offshore Miocene isochore maps show significant thickening towards the eastern Mexican margin. The results of this study improve the current understating of Cenozoic sedimentation in Mexico deepwater.

Keywords: Gulf of Mexico, deepwater, Mexico

LCMS-7

EG
LCMS

An integrated structural and geochemical study of fracture aperture growth in the Campito Formation of eastern California

Natchanan Doungkaew
Doungkaew, N., Bureau of Economic Geology, The University of Texas at Austin, Austin, TX
Eichhubl, P., Bureau of Economic Geology, The University of Texas at Austin, Austin, TX

Processes of fracture formation control flow of fluid in the subsurface and the mechanical properties of the brittle crust. Understanding of fundamental fracture growth mechanisms is essential for understanding fracture formation and cementation in chemically reactive systems with implications for seismic and aseismic fault and fracture processes, migration of hydrocarbons, long term CO2 storage, and geothermal energy production. A recent study on crack-seal veins in deeply buried sandstone of east Texas provided evidence for non-linear fracture growth, which is indicated by non-elliptical kinematic fracture aperture profiles. We hypothesize that similar non-linear fracture growth also occurs in other geologic settings, including under higher temperatures where solution-precipitation reactions are kinetically favored. To test this hypothesis, we investigated processes of fracture growth in quartzitic sandstone of the Campito Formation, eastern California, by combining field structural observations, thin section petrography, and fluid inclusion microthermometry. Field and petrographic measurements of opening-mode cemented fractures show both elliptical and non-elliptical kinematic aperture profiles. In general, fractures that contain fibrous crack-seal cement have elliptical aperture profiles, whereas fractures filled with blocky cement display non-elliptical aperture profiles. Elliptical fracture aperture profiles are consistent with linear-elastic or plastic fracture mechanics. Non-elliptical aperture profiles may reflect aperture growth controlled by solution-precipitation creep, with the aperture distribution controlled by solution-precipitation kinetics. We hypothesize that synkinematic crack-seal cement preserves the elliptical aperture profiles of elastic fracture opening increments. Blocky cement, on the other hand, may form postkinematically relative to fracture opening, with fracture opening accommodated by continuous solution-precipitation creep.

Keywords: fracture aperture profiles, solution-precipitation creep

This abstract has been withdrawn

LCMS-8

EG
LCMS

Sedimentology and Sedimentary Dynamics of the Desmoinesian Cherokee Group, Deep Anadarko Basin, Texas Panhandle

Ningjie Hu
Hu, N., Bureau of Economic Geology, The university of Texas at Austin
Loucks, R., Bureau of Economic Geology, The university of Texas at Austin
Frebourg, G., Bureau of Economic Geology, The university of Texas at Austin

Understanding the spatial variability of deep-water facies is critical to deep-water research because of its revealing information about the relationship between density flow processes and their resultant sedimentary sequences. The Cherokee Group in the Anadarko Basin, northeastern Texas Panhandle, provides an opportunity to investigate an icehouse-greenhouse Pennsylvanian hybrid system that well demonstrates the intricacies of vertical and lateral facies relationships in an unconfined fan-delta fed deep-water slope to basinal setting. The stratigraphic section ranges in thickness from 150 to 460 m. The cyclic sedimentation and foreland basin tectonics resulted in a complex stratal architecture that was sourced by multiple areas of sediment input.
This investigation consists of wireline-log and core data. Five-thousand wireline logs were correlated in an area of over 9500 sq km to map out six depositional sequences that are separated by major flooding events. These events are correlative over the whole area of study. Six cores, that sample nearly the complete section, were described for lithofacies. Lithofacies are recognized based on depositional features and mineralogy:(1) Subarkose, (2) Lithic-arkoses, (3) Sandy siliciclastic conglomerate, (4) Muddy calcareous conglomerate, (5) Crinoid packstone, (6) Ooid grainstone, (7)Peloid grainstone, (8) Ripple laminated mudrock, (9) faint laminated mudrock. The integration of isopachs of depositional sequences with the lithofacies has allowed the delineation of the spatial and temporal evolution of the slope to basin-floor system. Thin-to-thick bedded turbidites, hyperconcentrated density flow deposits (slurry beds), and debris and mud flow deposits were observed and can be used to better predict lithofacies distributions in areas that have less data control. These mixed siliciclastic and carbonate deposits can be carrier beds for the hydrocarbons generated from the enclosing organic-rich (TOC ranges from 0.55 to 6.77wt%), dysaerobic to anaerobic mudstones.

Keywords: Mudrocks, Sedimentology, Stratigraphy

LCMS-9

EG
LCMS

Paleoenvironments of Anchor Mine Tongue and Upper Sego Equivalent Strata in the Rangely Area of Colorado: Tidally-influenced Deposits and Variable Ichnology Along a Complex Coastline

Rebecca Jones
Jones, R., Quantitative Clastics Laboratory, Bureau of Economic Geology, The University of Texas at Austin, Austin, TX
Flaig, P., Quantitative Clastics Laboratory, Bureau of Economic Geology, The University of Texas at Austin, Austin, TX
Hasiotis, S., University of Kansas, Lawrence, KS

Strata in bluffs near Rangely, CO contain a Cretaceous interval found above previously identified Sego equivalent stratigraphy which correlates to those in the Book Cliffs, UT. This interval contains complex sandbody and shale geometries and complex ichnology. We interpret this interval, based on regional subsurface correlations, to be Anchor Mine Tongue and Upper Sego equivalent. Previous research on the Sego in the Book Cliffs and elsewhere typically focused on the sandier intervals, with less emphasis placed on the finer-grained intervals including the Anchor Mine Tongue. The interval of interest for our study contains relatively fine-grained strata which include a maximum flooding surface between the lower and upper Sego and highly variable sandbody and shale geometries typically found along a complex coastline. Five measured sections in the Rangely area contain a succession of facies including combined flow and current ripple laminated to trough cross-stratified sands with abundant organic matter, abundant mud drapes, double mud drapes, flaser, wavy, lenticular bedding, mud balls, mud rip ups, combined flow ripples, oyster and mud lag deposits. Overlying the strata are large scale trough-cross stratified sands containing dinosaur bone and footprints interbedded with coals and paleosols. These observations suggest predominantly tidally influenced paleoenvironments capped by fluvial-coastal plain deposits. Ichnology was critical to identify continental vs. marine deposits. Trace fossils include [i]Teichichnus, Sagittichnus, Ophiomorpha, Macronichnus, Helminthopsis, Crossopodia, Rhizocorallium, Schaubcylindrichnus, Diplocraterion, Teredolites, Asthenopodichnium, [/i]and [i]Rhysoliths[/i]. The majority of trace fossils are indicative of a fully marine to brackishwater setting. [i]Asthenopodichnium [/i]and [i]Rhysoliths[/i] were the only non-marine trace fossils and are associated with the fluvial systems. The combination of ichnology and sedimentology indicates that paleoenvironments likely included tidal channels, tidal bars, and tidal flats, estuarine to lagoonal muds, fluvial channels, levees, splays, swamps, and soil forming environments. The entire succession records the progradation of the fluvial-coastal plain over a complex, tidally influenced coastline.

Keywords: sandbody and shale geometries, transitional stratigraphy, anchor mine tongue, maximum flooding surface

LCMS-10

EG
LCMS

Facies and Cycle Architecture of the Upper Artesia Group in the Gulf PDB-04 Core, New Mexico: Integration of Outcrop Derived Models Into the Subsurface

Kyle McKenzie
McKenzie, K., Jackson School of Geosciences, The University of Texas at Austin, Austin, TX
Kerans, C., Jackson School of Geosciences, The University of Texas at Austin, Austin, TX
Loucks, R., Bureau of Economic Geology, The University of Texas at Austin, Austin, TX

The Artesia Group (Seven Rivers, Yates, and Tansill Formations) form significant oil and gas fields particularly along the western margin of the Central Basin Platform. In 1984, Gulf Research and Development Company drilled the PDB-04 stratigraphic research well in Eddy County, New Mexico, and recovered approximately 4,800 feet of continuous core, the focal point of extensive studies carried out thereafter. Since then, numerous outcrop and reservoir studies have resulted in significant advancements in the structural and stratigraphic framework in the Guadalupe Mountains. A new look at the classic PDB-04 provides a key tie-point and illustrates how the outcrop-based high-frequency sequence framework from core/log patterns can be brought into the subsurface. High resolution core descriptions allowed for detailed facies tracking and the interpretation of the 1D sequence architecture and stacking patterns of complex reservoirs in the Capitan Reef equivalent shelf. Core plugs and a conventional suite of wireline tools from the PDB-04 provide the ability to link the stacking patterns observed in the core to their respective log signatures. Upon building log-facies models, it will be possible to extrapolate the platforms geometric architecture from wells in the nearby subsurface allowing for the generation of an accurate large scale 3-D stratigraphic framework extending from the Guadalupe Mountains to the Central Basin Platform. A total of 111 high frequency cycles (HFC) were interpreted in the core and the range of HFC per high frequency sequence (HFS) ranged from 4-14. The wide range was attributed to syndepositional faulting and missing section near the shelf margin, and a better record of sea level change preserved in the facies in close proximity to the shelf crest, a proxy for the paleoshoreline. HFC patterns tend to be incongruous due to varying positions on the shelf profile between core and outcrop and local controls on sedimentation rate and subsidence. However, cycle sets exhibit strong similarities indicating broad scale mechanisms of accommodation were operating simultaneously across the 70 km area between the outcrop analogs and the core, and the delineation of this trends continuity will be discernable post construction of a log-core facies models.

Keywords: Permain, New Mexico, Stratigraphy, Cyclicity, Core, Outcrop, Subsurface

LCMS-11

EG
LCMS

Coupled Mechanical and Chemical Diagenetic Processes in Deformation Bands: Microstructure and Field Observations from the Entrada Sandstone at the San Rafael Swell, Utah

Casey Obrien
OBrien, C., The University of Texas at Austin, Austin, TX
Eichhubl, P., The University of Texas at Austin, Austin, TX
Elliott, S., The University of Texas at Austin, Austin, TX

Deformation bands in sandstone and other porous rock have been shown to act as barriers or baffles to fluid flow. Changes in flow properties are related to microscale textural changes that occur within the deformation bands through coupled mechanical and chemical diagenetic processes. Cements and other small-scale diagenetic features can control flow through pore throats, and thus affect production from clastic reservoirs that contain deformation bands. Microscale textures relating to flow properties, such as brittle grain deformation, preferred cementation, and the entrainment of fines within bands can be studied using scanning electron microscopy (SEM) imaging techniques. Conventional techniques for imaging deformation bands by SEM involve using mechanically polished thin sections. However, mechanical polishing can cause induced sample damage that limits microstructural observations. To mitigate sample damage, we use large-area and cross-sectional Ar ion beam milling to prepare deformation band samples for SEM imaging. These techniques preserve sample integrity allowing the imaging of cement and pore textures at submicron resolution. Here, we display results from a recent field study of the Entrada Sandstone at the San Rafael Desert, Utah. The outcrop, located in the gently dipping strata just to the east of the Laramide-uplifted San Rafael monocline, records multiple generations of deformation band formation. Early, non-cataclastic bands form first in the cross-bedded sandstone. As deformation continues, bands evolve to become more cataclastic, and continue over larger distances through dune sets and, in some cases, as part of large clusters that form deformation band faults. SEM image analysis and point count results of samples from this outcrop reveal that porosity loss within most bands is dominated by cementational rather than compactional processes, and that quartz cementation increases with cataclasis.

Keywords: deformation bands, diagenesis, San Rafael Swell, scanning electron microscopy

LCMS-12

EG
LCMS

Tying Core Descriptions and Optical Petrography with XRF Geochemical Data for a Detailed Characterization of the Mississippian Barnett Formation in the Southern Fort Worth Basin of North-Central Texas

Lauren Redmond
Redmond, L., Bureau of Economic Geology, Jackson School of Geosciences, The University of Texas at Austin, Austin, TX
Loucks, R., Bureau of Economic Geology, Jackson School of Geosciences, The University of Texas at Austin, Austin, TX
Rowe, H., Bureau of Economic Geology, Jackson School of Geosciences, The University of Texas at Austin, Austin, TX

In the 1960s, the Houston Oil and Mineral Co. drilled 29 cores that penetrated the Barnett Formation in the southern Fort Worth Basin. The cores are located adjacent to the Llano Uplift, throughout McCulloch, San Saba, Brown, and Mills counties. The core collection provides a very dense dataset of the shallow-buried, thermally immature Barnett Formation.The objective of the study is to examine the lateral and vertical heterogeneity of the mudrock facies to better understand its depositional environment. The results of this research can be used to better interpret the geologic history and depositional conditions of the deeper-water Barnett Formation. The methodologies and data manipulation techniques utilized in this study can be applied to other mudrock systems to better understand the depositional environments.For each core in this study a detailed description was recorded with an emphasis placed on the rock fabric, mineralogy, phosphate grain flows, and skeletal debris flows. A dip section, approximately 55 mile long, comprised of eight of the cores was further characterized using x-ray fluorescence at a 2” scanning interval. The distances between the cores in the dip-section ranged between 5 and 14 miles.Distinctive phosphate ooid grainstone beds were used to correlate between wells, taking into account the inherited topography of the Fort Worth Basin. The chemolithofacies that were defined from the geochemical data were also used to correlate between the dip-section wells and to identify down-dip facies changes.The core descriptions and geochemical data capture different features and characteristics of the cores. The core descriptions highlight flow deposits and sedimentary structures that are missed by the geochemical data, such as dilute shell flows or isolated phosphate stringers. And the geochemical data highlights matrix variability and provides insights to the paleoceanographic conditions. The combination of these methods as well as thin section descriptions and XRD analysis has led to a better understanding of the depositional environment of the shallow-buried, thermally immature Barnett Formation.

Keywords: Barnett, Mississippian, stratigraphy, paleoceanographic

LCMS-13

EG
LCMS

Optimizing CMP Stacking Using the Seislet Transform

Kelly Regimbal
Regimbal, K., Bureau of Economic Geology, The University of Texas at Austin, Austin, TX
Fomel, S., Bureau of Economic Geology, The University of Texas at Austin, Austin, TX

CMP stacking is one of the most fundamental routine processes applied to seismic data to improve the signal-to-noise ratio (Yilmaz, 2001). NMO correction is a process that prepares seismic data for stacking by stretching the time axis to the ideal zero-offset. Since NMO correction is not an exact solution, it produces some distortions of a seismic trace called “NMO stretch”, and the corrected trace is always different from the ideal zero-offset trace (Shatilo and Aminzadeh, 2000). Conventional stacking is flawed when there is inaccuracy in NMO correction or stretch muting, resulting in lower amplitude and lower resolution stacks. We present a method that optimizes CMP stacking and reduces the effects of “NMO stretch” by replacing conventional NMO and stack with a regularized inversion to zero offset. We use shaping regularization to achieve a stack that has a denser time sampling and contains higher frequencies compared to the conventional stack. We introduce the 2-D seislet transform (Fomel and Liu, 2010) in the adjoint operator of shaping regularization, which replaces the conventional NMO and stack adjoint operator introduced by Regimbal and Fomel (2015). The resulting seislet stack is a model that best fits the data using additional constraints imposed by shaping regularization. Numerical tests demonstrate that “stretching effects” caused by NMO are reduced and the resulting stacked section contains higher frequencies and preserves shallow reflectors better compared to the conventional stacked section.

Keywords: seislet, stack, regularization

LCMS-14

EG
LCMS

Analysis of Fracture Style and Development Associated with Differential Compaction Around Carbonate Mounds, Sacramento Mountains, New Mexico

Nathan Tinker
Tinker, N., RCRL, Bureau of Economic Geology, The University of Texas at Austin, Austin, TX
Janson, X., RCRL, Bureau of Economic Geology, The University of Texas at Austin, Austin, TX
Zahm, C., RCRL, Bureau of Economic Geology, The University of Texas at Austin, Austin, TX
Kerans, C., RCRL, Bureau of Economic Geology, The University of Texas at Austin, Austin, TX

The effects of early-lithified carbonate mounds on subsequent sediment deposition are well understood. However, the localized deformational impacts of early-lithified mounds during burial have not been well-studied. This project hypothesizes that rigidity differences between early-cemented carbonate mounds and subsequent sediment deposits result in differential compaction and significant fracture development in the overlying sediments. To substantiate the hypothesis, this study characterizes fractured Mississippian strata which overlies Waulsortian-style carbonate mounds that outcrop in the Sacramento Mountains of southeast New Mexico. Understanding such fracture networks could improve production in tight carbonates, tight sands, and unconventional reservoirs. Field work involved vertical and lateral facies mapping (mechanical and stratigraphic), and measurement of fracture spacing along line-transects. Fracture length, orientation, and intensity were compared against mechanical facies, bed thickness, lithology, and stratigraphic architecture of strata overlying the mounds. Thin sections from field hand samples enabled close assessment of facies, petrophyscial characteristics, and diagenetic history, while mechanical properties were measured directly on the outcrop or upon 1-inch core plugs extracted from hand samples. The core plugs were subjected to both uniaxial and triaxial compression tests, which model in-situ confining pressures and gauge corresponding rock strength characteristics. Two- and three-dimensional fracture maps of the study area were generated by combining detailed field mapping with high resolution remote sensing (i.e. ground-based LIDAR as well as high definition images captured from an unmanned aerial vehicle). Fractures range from 0.2 - 48 meters in length, and fractures longer than 2 meters (n=1045; 75% of data) have an average strike of 13 degrees, while those longer than 10 meters (n=85; 6% of data), have a mean strike orientation of 40 degrees. Importantly, the average northeast strike trend aligns with well-documented regional faulting and compression events, implying that tectonically-influenced fractures may be intermingled with local fractures generated by differential compaction. Furthermore, there exists an marked increase in fracture intensity in the strata above carbonate mound cores. Finally, the project develops predictive guidelines regarding fracture development around carbonate buildups, and demonstrates how such fracture networks affect hydrocarbon flow in analogous subsurface reservoirs.

Keywords: carbonate, Waulsortian, Mississippian, mound, fracture, crinoid, stratigraphy, Alamogordo, Sacramento, compaction, differential, UCS, triaxial, early-lithification, sediment, reservoir, oil, gas, tight, production, unconventional, mapping, intensity, diagenesis, remote sensing

This abstract has been withdrawn

LCMS-15

EG
LCMS

Anatomy, Dimensions, and Significance of the Penultimate Yates Tepee-Shelf Crest Complex, G25 Hairpin HFS, Guadalupe Mountains, New Mexico and Texas

Kristopher Voorhees
Voorhees, K., The University of Texas at Austin, Austin, TX
Kerans, C., The University of Texas at Austin, Austin, TX

The Guadalupian Hairpin Member of the Yates Formation in the Guadalupe Mountains is unique in that it reveals pronounced expansion of the shelf crest tepee-pisolite complex compared to the sequences above and below it. This study seeks to document the exceptional development of the Hairpin tepee-pisolite complex and understand the timing and origin of subaerial exposure and its effects on sequence architecture. This requires establishment of a high-resolution cycle-scale stratigraphic model for the Hairpin created through a collection of closely spaced measured sections and bed tracing using gigapan imagery. These sections and bed tracings will document the dramatic facies-tract dip-width expansion of the shelf crest, and will characterize the extensive tepee-pisolite complexes in order to understand their significance and origin.

Data for the study includes six detailed measured sections calibrated to two photomosaics covering ~2.4 km of the north wall in McKittrick Canyon to place high frequency cycles and cycle sets into a sequence stratigraphic framework. The Hairpin shelf crest facies tract width is approximately 1.3 km and 220 m landward of the shelf edge reef. Tepees are best developed in the shelf crest during a HST.

Height of individual tepees ranges from 10s of centimeters to 1-2 m with the larger of these structures occurring near the top of the Hairpin. Crest to crest lateral dimensions for the tepees are approximately 15-20 m but can vary as measured from gigapan and Lidar tracings. Interpretation of the photomosaics reveals that pre-existing tepees tend to act as nucleation sites for newly generated tepees as evidenced by the concentrations of vertically stacked tepees that comprise the tepee-pisolite complexes. Quartz siltstones/sandstones predominately fill tepees at the most landward portion of the study area while carbonate sediments and marine cements dominate tepee infill at the most basinward portion. Applied technology is limited to our understanding of complexities such as lateral variability between wells within Yates reservoirs in the Northwest Shelf and Central Basin Platform. By understanding the interplay between eustatic fluctuation and facies tract development, enhanced recovery strategies can be coupled with improved understanding from this study to ultimately maximize the original oil extracted.

Keywords: Guadalupe Mountains, Yates Formation, Sequence Stratigraphy

LCMS-16

EG
LCMS

Characterizing Bedding-Parallel Fractures in Shale: Aperture-Size Distributions and Spatial Organization

Qiqi Wang
Wang, Q., Bureau of Economic Geology, Jackson School of Geosciences, University of Texas at Austin
Gale, J., Bureau of Economic Geology, University of Texas at Austin

Natural fracture systems are important for production in shale gas reservoirs as they may contribute to permeability of the reservoir, or they may reactivate during hydraulic fracture treatment. However, little is known about their size scaling and spatial distribution. Knowing the aperture-size scaling and spatial organization of bed-parallel fractures may contribute to improved modeling of the combined fracture network (hydraulic and natural). Ten fracture data sets were collected from the Vaca Muerta (7), Marcellus (2) and Wolfcamp (1) shale formations. Bed-parallel fracture attributes such as strike, dip, aperture size, spacing, length and texture were collected from outcrops of the Vaca Muerta Formation in the Neuquén Basin, Argentina. Further fracture aperture-size and spacing data for the Vaca Muerta, and for the Marcellus and Wolfcamp, were collected through measurement direct from cores, and from photographic panels of slabbed core. A total of 1093 fractures were measured along 10 scanlines of total combined length of 629 m. The aperture size of bed-parallel fractures ranges over 4 orders of magnitude, from 15 μm to 87 mm. Nine out of ten datasets follow a negative exponential distribution. Fracture attributes such as intensity and size range are different in the 3 studied shales. Even within the same shale formation, fracture intensity and size range can be variable. Aperture size ranges of bed-parallel and vertical fractures in these shales are comparable as are fracture intensities for the Marcellus examples. Bed-parallel fractures, however, have higher intensities than vertical fractures in the Vaca Muerta examples. Spatial organization of bed-parallel fractures is investigated using a normalized two-point correlation technique that allows distinction between clustering, regular spacing and a random distribution. The relationship between fracture spatial organization and stratigraphy and mechanical interfaces within the host rock is also investigated, with preliminary results suggesting that bed-parallel fractures are more intense in organic-rich layers in some cases, but not in others.

Keywords: Shale, Natural fractures, Size scaling, Spacial distribution, Hydraulic fracturing

LCMS-17

EG
LCMS

Potentially Conductive Channels in Fracture Cements of Low Permeability Rocks

Erick Wright
Wright, E., Bureau of Economic Geology, The University of Texas at Austin, Austin, TX
Landry, C., Bureau of Economic Geology, The University of Texas at Austin, Austin, TX
Eichhubl, P., Bureau of Economic Geology, The University of Texas at Austin, Austin, TX

Natural fractures in shale reservoirs are frequently filled with mineral cement that lacks any residual fracture porosity that is visible under the petrographic microscope. These fully cemented fractures are generally interpreted to be impermeable for fluid flow. Scanning electron microscopy of calcite, dolomite, and barite fracture cements from a variety of shale reservoirs, prepared using broad ion beam milling, provides evidence of open to partially healed elongate pores that are on the order of hundreds of nanometers in aperture. In calcite fracture cement, these pores have consistent apertures of about 100 nm. In dolomite and barite, apertures are up to 500 nm. These pores have been previously overlooked because traditional thin sectioning and polishing destroys sub-micron details of the fracture cement pore structure. Ion milling preserves these details with a minimum of sample damage during sample preparation. Electron backscatter diffraction shows that these pores occur along grain boundaries within the blocky or columnar fracture cement. While partially healed, these pores, arranged along grain boundaries, are frequently sufficiently well connected acting as channels for fluid flow along and across fully cemented natural fractures. In shale reservoirs of ultra-low matrix permeability, these grain boundary channels may thus provide fracture permeability significantly contributing to reservoir production where intersected or indirectly reactivated by hydraulic fractures.

Keywords: Fracture, SEM, EBSD

LCMS-18

EG
LCMS

Stratigraphic Cyclicity and Reservoir Potential of Upper Pennsylvanian Cline Shale, Midland Basin, Texas

Hanyue Zheng
Zheng, H., Bureau of Economic Geology, The University of Texas at Austin, Austin, TX
Fu, Q., Bureau of Economic Geology, The University of Texas at Austin, Austin, TX

The Cline shale, an organic rich mudrocks comprising Cisco and Canyon Group, has recently become an exploration target and production interval. The Cline is distributed and spatially restricted in Midland Basin, and interpreted to have deposited under a deep water environment by pelagic/hemipelagic suspension and mass transport processes varying from debris flow to low-density turbidity flow. Regional stratigraphic sections suggest the Cline updips towards Eastern Shelf, ranging from 117 ft to 530 ft in thickness. Multiple source areas have been identified from Eastern Shelf, Horseshoe Atoll, Central Platform and Ozona Arch.

Gamma ray trend, as an expression of lithology and stacking patterns, illustrates two depositional events during the Cline time. Falling sea level introduces large amount of terrigenous sediments to the basin, which are deposited as mass transport sandstone in the toe of slope and mudstone in central basinal area. Rising sea level diminishes the volume of siliciclastic sediment supply, while biogenic carbonates at platform margin are transported down the slope as skeletal carbonates detritus. Such a transgressive event develops a deepening-upward cycle which is recognized by upward-decreasing gamma ray trend, whereby sandstone and mudstone grade upward into skeletal carbonates detritus in the toe of slope and intrabasinal calcareous mudstone. Likewise, a shallowing-upward cycle is established during a regressive event, and exhibited as upward-increasing trend on gamma ray curve. Eight and seven stratigraphic cycles have been distinguished in the Lower and Upper Cline intervals, respectively. The cyclicity in the basin is correlative to that on the platform, suggesting high-frequency relative sea level fluctuation and regional tectonism affect depositional processes on the platform and further sediment deposition in the basin.

The Cline is a shale-oil resource play containing Type I and Type II kerogen, and various TOC ranging from 0.29% to 9.88%. Massive argillaceous and siliceous mudstone contain relatively higher TOC and porosity and may act as source rocks and reservoir rocks. These two facies are more prevalent and continuous in basinal areas within shallowing-upward cycles, providing implication of locations of potential pay zones.

Keywords: Cline Shale, Cyclicity, Reservoir Potential, Midland Basin

LCMS-19

PS
LCMS

Unraveling Ancient Martian Hydrological Conditions Through Erosional/Depositional Mass Balance Studies of Sedimentary Fans

Katherine Shover
Shover, K., Jackson School of Geosciences, The University of Texas at Austin, Austin, TX
Goudge, T., Jackson School of Geosciences, The University of Texas at Austin, Austin, TX
Levy, J., Institute for Geophysics, The University of Texas at Austin, Austin, TX
Holt, J., Institute for Geophysics, The University of Texas at Austin, Austin, TX

Dozens of landforms on Mars have been interpreted as alluvial fans and deltas, which we generally refer to as sedimentary fans here, indicating fluvial erosion and deposition of sediments. Questions remain regarding the extent to which such deposits have been subsequently modified following deposition. This study seeks to quantify the preservation of these sedimentary fans through a simple mass balance approach; by calculating present volumes of the fans, in addition to the volumes of the valleys feeding them, we can determine the percentage of eroded valley sediment that has remained within the fan. If a volume imbalance exists for fan/valley systems associated with larger valley networks that is unlikely to be explained by post-depositional erosion (i.e., volume valley >> volume fan), it would imply that a distal sediment sink exists for these valley systems, such as a northern hemisphere ocean. We used Mars Reconnaissance Orbiter Context Camera (CTX) stereo-derived digital elevation models (DEMs) to constrain the volumes of the fans and the valleys that feed them, and thus only analyzed fans with appropriate data coverage. Three increasingly detailed methods are used in this study for the volume calculations. The first method calculates the volume between the fan or valley surface and a plane at the average height of the valley rim or the crater floor as measured at the fan toe. The second method fits a segmented, dipping planar surface to the valley rim or the host crater wall and determines the volume between this surface and the fan/valley surface in the DEM. The third method uses a second-order polynomial fit to surrounding topography to model the crater wall surface. Preliminary results from four fans indicate approximately equal volumes for the eroded valley sediments compared to the deposited fan sediments. While the volume of sediments in the fan is always lower than the volume of sediments in the valley, the two values for each deposit investigated thus far have been within the same order of magnitude. Ongoing work involves analysis of a more extensive set of deposits, and we plan to test whether this trend continues. The fact that the fans have a similar volume to the eroded volume of the valley suggests that little landscape erosion has occurred during fan emplacement; rather, nearly all of the sediment in the fans seems to have been derived from the erosion of the valley.

Keywords: Mars, mass balance, fans, deltas, valleys, volume, preservation

LCMS-20

SETP
LCMS

Himalayan thrust belt dynamics, weathering, and Cenozoic seawater chemistry

Cody Colleps
Colleps, C., Department of Geological Sciences, The University of Texas at Austin, Austin, TX
Stockli, D., Department of Geological Sciences, The University of Texas at Austin, Austin, TX
McKenzie, R., Department of Geology and Geophysics, Yale University, New Haven, CT
Hughes, N., Department of Earth Sciences, University of California Riverside, Riverside, CA
Myrow, P., Department of Geology, Colorado College, Colorado Springs, CO
Horton, B., Department of Geological Sciences, The University of Texas at Austin, Austin, TX
Webb, A., School of Earth and Environment, University of Leeds, Leeds, United Kingdom
Singh, B., Center for Advanced Study in Geology, Panjab University, Chandigarh, India

Seawater $^{187}Os/^{188}Os$ and $^{87}Sr/^{86}Sr$ records are utilized as proxies that track Cenozoic global silicate weathering intensity responsible for CO_2 drawdown and climatic cooling. The utility of these records, however, can be complicated by the influence of isotopically anomalous regional sources. The weathering of compositionally unique Himalayan bedrock has been proposed to drive the observed changes in Cenozoic seawater Sr and Os. More specifically, the exhumation of Lesser Himalaya ^{187}Os enriched Cambrian black shale, which have been eroded away across the Himalayan orogen but presently preserved within Lesser Himalaya synforms of Northwest India, has been proposed as the initial primary contributor responsible for an observed abrupt increase in global seawater $^{187}Os/^{188}Os$ starting at ~16 Ma. The timing of initial exhumation of these rocks has, until now, remained poorly constrained and is critical in discriminating what primarily controls these seawater records. Here we present new zircon (U-Th)/He and U-Pb data from distinct Himalayan tectono-stratigraphic bedrock and foreland basin deposits that elucidate major aspects of the exhumation and kinematic evolution of the frontal thrust system. Our data indicate in-sequence southward thrust propagation from the Main Central Thrust to the Tons Thrust, resulting in rapid exhumation of Lesser Himalayan strata enriched in ^{187}Os and less enriched in ^{87}Sr at ~16 Ma, which directly corresponds with coeval shifts in seawater $^{187}Os/^{188}Os$ and $^{87}Sr/^{86}Sr$ at this time. We conclude that weathering of anomalous sources, rather than changes in global silicate weathering intensity, controls these seawater records thus limiting their utility as deep-time weathering proxies.

Keywords: Himalaya, Northwest India, Thermochronology, Geochronology, Seawater Composition

LCMS-21

SETP
LCMS

Initial results of research on gold mineralization in the Surselva district, Switzerland

Dorothy Hinds
Hinds, M., Jackson School of Geosciences, The University of Texas at Austin, Austin, TX
Elliott, B., Bureau of Economic Geology, The University of Texas at Austin, Austin, TX
Kyle, J., Jackson School of Geosciences, The University of Texas at Austin, Austin, TX

Gold in the Surselva district of southeastern Switzerland has been known since Roman times, and the discovery of high-grade gold specimens has prompted exploration and research since the 1980's (e.g. Jaffe, 1989). The main mineralized zone occurs in the Tavetsch schist, a highly sheared zone between the Gotthard and Aar Massifs, and is characterized by sericite and quartz-sericite schists. The protolith of the gold-hosting schists is under investigation, but x-ray fluorescence (XRF) analyses reveal high concentrations of Cr, Mn, Mg, and Fe, as well as relative depletion of Al and Si, that supports a volcanic origin. Roadcuts and outcrops along hiking trails were mapped and systematically sampled, and cores remaining from historic drilling were logged. Sampling of cores was guided by historic gold assays, as well as the presence of sulfide minerals. XRF analyses suggests that gold is associated with concentrations of quartz, arsenopyrite and pyrite, with gold being able to be differentiated in digital radiographs by structure and darker gray-scale values when compared to sulfide grains. Digital radiographs suggest that arsenopyrite is associated with gold grains, which is also supported by higher arsenic, mercury, and tellurium concentrations from XRF analysis. Initial results suggest that gold is associated with S2 foliations, suggesting mobilization of gold during the Alpine orogeny. Computer modeling has denoted a sheared sub- surface ore body, most likely structurally controlled on veins and faults. On-going research involving petrography, geochemistry, and high resolution X-ray computed tomography will attempt to further constrain the nature and origin of the gold concentrations.

Keywords: gold, Switzerland, Computed tomography, x-ray fluorescence

LCMS-22

SETP
LCMS

Investigating the Pathways and P-T-X Conditions of Hydrothermal Fluid Flow Responsible for Cu-Au Mineralization in the Ertsberg East Skarn System, Papua, Indonesia

Matthew Ledvina
Ledvina, M., Department of Geological Sciences, The University of Texas at Austin, Austin, TX
Frelinger, S., Department of Geological Sciences, The University of Texas at Austin, Austin, TX
Young, D., Department of Geological Sciences, The University of Texas at Austin, Austin, TX
Kyle, J., Department of Geological Sciences, The University of Texas at Austin, Austin, TX

The Ertsberg East Skarn System (EESS), a 3-Gt orebody at 0.59% Cu and 0.49 ppm Au, is located in the Ertsberg-Grasberg mining district, a 50km^2 region of world class Cu-Au porphyry and skarn deposits in the highlands of Papua, Indonesia. Subduction of the Australian plate beneath the Pacific plate ca. 12 Ma uplifted and deformed a succession of Upper Cretaceous siliciclastic to Lower Paleogene carbonate strata into which ca. 3 Ma magmatism and episodic hydrothermal fluid flow created stockwork- and skarn-hosted Cu-Au ores. The diorite-wallrock contact, stockwork fracturing within the Ertsberg Diorite, and a major fault have been proposed as possible EESS fluid conduits. Hydrothermal quartz-sulfide veins present the best opportunity to study ore forming fluids by using petrography, SEM-CL and fluid inclusion microthermometry.

SEM-CL images are produced when a quartz crystal is bombarded with high-energy electrons and emits visible light. Individual SEM-CL images are stitched into composite luminescence maps that reveal zonation textures that record changes in P-T-X conditions and crystal growth rates. A total of 17 samples were scanned to create 41 composite images. The eight textures identified in more than one image were used to construct a paragenetic sequence of EESS quartz-sulfide vein architecture as it varies by elevation and host lithology.

Fluid inclusion petrography was completed on 15 carefully selected samples across the EESS to document the fluid inclusion types and distribution within the deposit. Fluid inclusions in eight samples were analyzed with in-situ micro-thermometry to determine salinity and homogenization temperature (T_h) – the minimum temperature at which the fluid was trapped. Four types of fluid inclusion are present in EESS vein quartz. Type 1 is liquid dominant, 2 to 20 wt. % NaCl eq., homogenizes by critical behavior from 330 to 418°C and can contain chalcopyrite daughter crystals. Type 2a is liquid dominant, >26 wt. % NaCl eq., homogenizes to liquid from 280 to 425°C, contains halite and commonly sylvite, anhydrite or opaque daughter minerals. Type 2b is vapor dominated, 1 to 6% NaCl eq., homogenizes to vapor from 364 to 392°C and may contain daughter crystals that do not homogenize. Type 3 inclusions can be liquid- or vapor-dominated, 2 to 23% NaCl eq., homogenize to liquid and may contain an opaque daughter crystal.

The CL textures and fluid inclusion types observed are consistent with other Cu-Au porphyry systems, including the nearby Grasberg intrusive system. All fluid inclusion types were observed over the 2.5 km of elevation sampled – nearly 5x the vertical extent in which similar fluid inclusion types coexist in some other major porphyry systems, e.g. Bingham. No large variation in salinity or T_h corresponds with elevation. Moderate variation in CL textures was observed between high and low elevation diorite veins. Skarn-hosted veins display a greater volume of brittle deformation features than diorite-hosted veins. The majority of veins show evidence of multiple opening and mineralization cycles. A zone of sub-vertical sheeted quartz veining up to 20-m wide that can be traced for at least 150 m along strike and extending from 2550- to 2700-m elevations may record a major fluid pathway. These observations are consistent with fault-controlled fluid migration and dramatic thermal collapse of the system.

Keywords: Ertsberg East Skarn System, hydrothermal quartz, fluid inclusion microthermometry, SEM-CL

LCMS-23

SETP
LCMS

Detrital Zircon Geo- and Thermochronometry of the Eocene Ainsa Basin, South Central Pyrenees, Spain: Insights into Paleodrainage Evolution During Orogenesis

Kelly Thomson
Thomson, K., The University of Texas at Austin, Austin, Tx
Stockli, D., The University of Texas at Austin, Austin, Tx
Clark, J., Statoil Gulf ASA, Austin, Tx
Puigdefabregas, C., University of Barcelona, Barcelona, Spain
Fildani, A., Statoil Gulf ASA, Austin, Tx

South Central Pyrenean foreland basin deposits provide an ideal setting for investigating the interaction between tectonic deformation and basin sedimentation. Early Cenozoic foreland basin deposits preserve the record of hinterland erosion throughout Pyrenean collision. Through high-resolution detrital zircon (DZ) geo- and thermochronometry this study investigates the progressive evolution of sediment provenance and paleodrainages through the stratigraphic record and across different depozones of the foreland basin system. The Ainsa Basin in the South Central Pyrenees contains a secession of Eocene turbidite packages sampled in detail to examine the transition from fluvial to shelf-slope to deep marine environments. New data, congruent with previous DZ studies, indicate the turbidites are mixed from two main sources, Hercynian plutons from the Central Pyrenean axial zone and Cadomian/Caledonian plutonic and metamorphic rocks exposed in the Eastern Pyrenees. Detailed DZ U-Pb-He double dating resolves subtle differences in provenance signatures between stratigraphic packages. These differences likely reflect varying degrees of mixing of multiple sources, and autogenic noise from recycling and sorting during transport. Anomalous DZ U-Pb distributions, potentially indicate an additional source region contributing sediment from the south in the Catalan Coastal Ranges. Studying these anomalies will better our understanding of processes such as sediment bypass in marine canyons and fluvio-deltaic depozones as well as axial vs transverse paleodrainages. Tracing these anomalous signals across proximal to distal depozones in the basin will help to refine stratigraphic correlations. The data, Interpreted in the context of the structural and stratigraphic framework of the Pyrenean foreland basin, provide insights into processes during sediment delivery, paleodrainage networks, and the interplay between tectonic deformation and basin sedimentation.

Keywords: Pyrenees, Basin Analysis, Detrital Zircon, Foreland Basin, Paleodrainage Evolution, Tectonic and Climatic interactions, Source to Sink

LCMS-24

SETP
LCMS

An Evaluation of Predictive Indicators of Mississippi Valley Type Mineralization in Southeast Missouri Using Weights of Evidence

Nathan Williams
Williams, N., Department of Geological Sciences, The University of Texas at Austin, Austin, TX
Kyle, R., Department of Geological Sciences, The University of Texas at Austin, Austin, TX
Elliott, B., Bureau of Economic Geology, The University of Texas at Austin, Austin, TX

The weights of evidence analysis method was used to evaluate the predictive strength of factors spatially associated with Mississippi Valley Type (MVT) Pb-Zn mineralization in southeast Missouri and to predict other areas likely to contain similar mineral concentrations. Publicly available data were used to create binary evidence maps of features suggested by the USGS MVT deposit model to be related to mineralization. These maps were then evaluated by comparing the number of MVT deposits within each area. The best evidence contains the greatest number of deposits in the smallest map area. From best to worst performing, these evidential features are anomalous gravity, anomalous geochemistry, presence of favorable geology, distance from faults, and anomalous magnetic response.

The weights derived from the analysis of these variables were used to generate 18 unique posterior probability maps of mineralization. These models were assessed based on an efficiency of deposit classification score, the percentage of poorly classified deposits, and the conditional independence (CI) ratio. Models with high efficiency scores and low numbers of poorly classified deposits tended to have much greater violations of CI. Conversely, models that violated CI to a lesser degree generally had lower efficiency scores and a greater number of poorly classified deposits. Model 5, which combined weights from the presence of the favorable host Bonneterre Dolomite as well as Pb, magnetic, and gravity anomalies, is presented as an example of a highly performing model with an efficiency score of 81.4%, 30.1% poorly classified deposits, and a CI ratio of 0.67. The three highest posterior probabilities for this model occupied only 1.2% of the total study area, yet contained about 21% of known deposits. Blind testing suggests that these models are also capable of predicting areas of mineralization outside the model area, but with reduced efficiency. The results of this work demonstrate the potential utility of the weights of evidence method in identifying new exploration targets in a mature terrane, and the relative weights of evidence may be useful in understanding controls on MVT mineralization elsewhere.

Geologic similarities between the MVT deposits of southeastern Missouri and minor Pb-Zn occurrences in Paleozoic sedimentary rocks surrounding the Llano Uplift make central Texas an ideal location to apply these results. The favorable geologic setting and evidence from previous work suggests economic MVT deposits could exist in central Texas. An understanding of the spatial relationships and predictive quality of factors associated with mineralization in southeast Missouri may be useful in the generation of a knowledge-driven predictive model of MVT mineralization in central Texas, where a lack of a sufficient number of known mineral deposits prohibits a data-driven evaluation.

Keywords: GIS, Weights of Evidence, mineral potential, prospectivity mapping, MVT deposits, southeast Missouri, central Texas

LCMS-25

SHP
LCMS

Physical Modeling of a Prograding Delta on a Mobile Substrate

Eunsil Jung
Jung, E., Department of Geological Sciences, Jackson School of Geosciences, The University of Texas at Austin, Austin, Texas
Kim, W., Department of Geological Sciences, Jackson School of Geosciences, The University of Texas at Austin, Austin, Texas

Subsurface architecture of a delta that progrades on a mobile substrate (e.g., salt) is a product of complex interplay between depositional process and subsidence. Previous studies mostly focused on structural deformation of a salt layer in response to tectonic forcing, and left the dynamic feedback between sedimentation and subsidence unexplored. We present results from physical experiments of delta progradation on a mobile substrate. Five carefully designed experiments were performed to understand the effects of delta progradation rate on the shape and dimension of salt deformation and associated stratal architecture. All of the runs had constant sediment and water discharge, but the mobile substrate thickness and water depth varied from 2 cm to 4 cm and from 1 cm to 3 cm, respectively. The results showed that the deeper the water depth, the slower the shoreline progradation rate, while the thinner the salt thickness, the faster the delta progradation. The experimental results also provided data over a wide range of shoreline advance and subsidence rates enough to indicate changes in shape and dimension of salt deformation structure. Runs with fast shoreline progradation showed isolated salt domes developed internally into the delta plain and a rough planform pattern in the shoreline due to lobes built by channels flow between upwelled salt structures. However, runs with slow shoreline progradation developed connected long salt ridges around the toe of the delta, limiting sediment to transport beyond the ridges. This overall pattern in salt structures is time dependent. As a delta surface grows larger and the shoreline progradational rate autogenically decreases with time, chances to develop isolated salt domes decrease but more connected long salt ridges occur. The insight from the physical modeling of a delta on a mobile substrate is important to predict the mechanism for large-scale salt basin stratigraphy under a high sediment supply that interact with the substrate actively.

Keywords: delta, mobile substrate, physical modeling

LCMS-26

SHP
LCMS

Comparative Assessment of FWI (Full Waveform Inversion),MASW(Multichannel Analysis of Spectral Waves) and SASW (Spectral Analysis of Surface Waves) method for near surface characterization

Janaki Vamaraju
Sen, M., The University of Texas, Austin,TX

Due to increased power of computers and accurate forward models Full Waveform Inversion (FWI) algorithm has been proved to be a promising technique for seismic imaging of deeper subsurface. Recently more and more developments have been focused on implementing FWI for near surface characterization. This study presents a comparative analysis of FWI and the older established methods such as Multichannel Analysis of Surface Waves (MASW) and Spectral analysis of Surface Waves (SASW). Further integrating these methods can result in extracting more information from recorded surface data. We the help of layered synthetic models the analysis gives us results that shed promising perspectives for using robust FWI along with MASW and SASW to image near surface targets.

Keywords: FWI ,SASW , MASW , near surface

LCMS-27

SHP
LCMS

DOWNSTREAM CHANGES IN THE THERMAL REGIME OF THE HYPORHEIC ZONE OF THE HYDROPEAKED COLORADO RIVER, AUSTIN, TEXAS

Jeffery Watson
Cardenas, M., Jackson school of geosciences, The University of Texas at Austin
Neilson, B., Utah State university
Bennett, P., Jackson school of geosciences, The University of Texas at Austin

The thermal regime of river corridors are critical to many ecological and environmental processes. Thus, in-stream heat transport has been studied for decades. More recently, research has been conducted on in-stream heat transport in regulated rivers subject to hydropeaking, but little work has been done quantifying the effects of downstream attenuation of a single regulated flood pulse in the hyporheic zones of multiple sites. In order to better understand this flood pulse attenuation, we instrumented the hyporheic zone at three sites with temperature probes along a 90 km stretch of the Colorado River downstream of longhorn dam, Austin, TX. Piezometer transectsperpendicular to the river at each site were instrumented with HOBO thermistors over a 1.4 m screened interval within the saturated zone at 20 cm spacing. As flood pulses are attenuated downstream, temperature gradients and distance of lateral temperature pulse penetration into the bank are hypothesized to decrease. The data collected in this investigation will test this hypothesis by providing 2D temperature cross-sections along an attenuating flood pulse, providing detailed spatial data on temperature gradients adjacent to the river.

Keywords: Hydrology, hydrogeology, hyporheic zone

LCPHD-1

CCG
LCPHD

Clumped-isotope Thermometry and Oxygen Isotope Systematics in Speleothem Calcite from a Near Cave Entrance Environment

Peter Carlson
Carlson, P., Department of Geosciences, The University of Texas at Austin, Austin, TX
Banner, J., Department of Geosciences, The University of Texas at Austin, Austin, TX
Breecker, D., Department of Geosciences, The University of Texas at Austin, Austin, TX
Affeck, H., Department of Geology and Geophysics, Yale University, New Haven, CT

Speleothems that grow in well-ventilated zones of caves have not been widely used in paleoclimate studies, yet may provide paleotemperature records., These zones are characterized by low CO2 concentrations year-round and, in temperature climates, large seasonal temperature fluctuations. They are typically avoided for paleoclimate reconstruction due to concerns about kinetic isotope effects (KIE). However, speleothems in general seem to be sensitive to KIE, even in non-ventilated areas and can nonetheless provide useful paleoclimate records. AtWestcave Preserve (Westcave), a shallow, well-ventilated twilight cave in central Texas, we have found seasonal temperature differences recorded in both the oxygen isotope andclumped isotope compositions of speleothem calcite grown on glass-plate substrates harvested from active drips. Although growth rates in this cave are relatively rapid (rangingseasonally 8-40 mg calcite/day), speleothem analogs in Westcave are growing near oxygen-isotopic equilibrium with their drip waters (Feng et al., 2014). The near-equilibriumrelationship (based on Kim and O'Neil, 1997; Coplen 2007; and Tremaine et al., 2011) between the calcite and waters has motivated us to apply the Zaarur et al., (2013) clumped isotope bulk solution thermometer calibration to glass-substrate calcite in the cave. This technique can provide absolute temperatures,independent of drip-water oxygen isotope composition, but is sensitive to kinetic isotope effects, often significantly overestimating growth temperatures of speleothems. When thisthermometer was applied to calcite collected from near the substrate centers where the plates were impacted by drip water, it overestimated measured temperatures by 7.7 ± 4.3°C , showing moderate KIE. When applied to calcite from substrate edges, it overestimated temperatures by 18.7 ± 4.2°C, showing KIE increasing away from the center of the drip. Measured average temperatures in the cave ranged seasonally between 8 and 28°C, and daily temperatures vary significantly. At Westcave, calcite growth rates increase with temperature, and the calcite may therefore preferentially record warmertemperatures. In temperate regions, seasonal temperature records are lacking. Our results suggest near-entrance speleothems may be a valuable proxy for seasonal temperatures, but may overestimate mean seasonal temperatures in seasonally resolved records due to KIE and/or temperature-dependent calcite growth rates.

Keywords: Speleothem, oxygen isotopes, clumped isotopes

CCG
LCPHD

Scale up the influence of aerosols on deep convection derived from GoAmazon/CHUVA measurement to Amazon basin.

Sudip Chakraborty
Chakraborty, S., The University of Texas at Austin, Austin, TX
Fu, R., The University of Texas at Austin, Austin, TX

Although the effects of aerosol on clouds and precipitation have been shown extensively, whether we can detect them on climate and continental scale, especially on convective life cycle, and how can we isolate such effect from the influences of meteorological conditions, are still unclear. To address these challenges, we are analyzing both GoAmazon data and a large suite of instantaneously collocated geostationary and polar orbit satellite datasets over Amazon. The results show consistent increases of rainrate, number of convective cores, and radius of the mesoscale convective systems associated with the aerosols for relatively low and moderate vertical wind shears for various lower tropospheric relative humidity conditions. Our results also suggest that, while the vertical wind shear and lower tropospheric relative humidity dominate the variations of convective system radius and number of convective cores, especially during the growing and mature stage of the convective systems, aerosols dominate the reduction of small hydrometeors, the increase of large hydrometeors, and reduction of convective anvils, especially during the mature and decaying phase of the convective systems. These results derived from a large suite of independent measurements support the hypothesis that aerosols can reduce small hydrometeors and increase hydrometeors, and invigorate convective systems, as shown by their dominant effect during the mature and decay phase of the convection. The meteorological conditions dominate the size and number of convective cores of the convective systems, especially during the growing phase of the convection.We analyze the DOE Atmospheric Radiation Measurement Mobile Facility (AMF) GoAmazon and Brazil led CHUVA field campaign data to evaluate these results from satellite data. Multiple regression analysis of the GoAmazon data generally suggest that aerosols have a comparable influence on cloud ice to those of the lower tropospheric relative humidity and vertical wind shear when the convections are in developing or steady stages in terms of convective top height. The influences also depend on the planetary boundary layer height. We will also report our comparison of the influence of aerosols on deep convection to those on convective congestus and shallow clouds.

Keywords: Cloud, Aerosols.

CCG
LCPHD

DisintegratoR: an upcoming package for evaluating phylogenetic trees while accounting for correlation between character states

William Gelnaw
Gelnaw, W., Jackson School of Geosciences, The University of Texas at Austin, Austin, TX

=12.0pt One of the assumptions of phylogenetic analysis is that all of the characters being assessed evolve independently of one another. However, morphological characters may be linked due to a shared developmental or epigenetic process, or because states are selected together because of shared functional or ecological pressures. The interdependence of characters is referred to as morphological integration and has been the basis for many arguments against using morphology to construct phylogenetic hypotheses. Morphological integration diminishes the reliability of phylogenetic analyses because it draws support for phylogenetic hypotheses from different characters out of proportion to the information that they actually carry. The most common method used to remove the effect of morphological integration has been for the investigator to identify a suite of correlated character changes, usually associated with a particular ecomorph, and then down-weight or delete those characters to reduce their collective contribution to tree length. DisintegratoR is an R package that I developed to evaluate, among other things, the likelihood of a phylogenetic tree topology given a Brownian motion model of evolution. What sets DisintegratoR apart from other programs is that it also uses the tree structure and the distribution of character states to create a model of correlations between characters, which it then uses to transform the original data to the expected set of states if there was no correlation between characters. The likelihood of the tree is then evaluated using the transformed data. DisintegratoR is a step forward for the phylogenetic analysis of morphological data because it accounts for morphological integration in an objective way that diminishes the risk of introduced for investigator bias.

Keywords: R package, phylogenetics, methods

LCPHD-4

CCG
LCPHD

The Wettability of Caprock by CO2 and Its Impact on Geologic CO2 Sequestration

Eric Guiltinan
Guiltinan, E., Jackson School of Geoscience, The University of Texas at Austin, Austin TX
Cardenas, M., Jackson School of Geoscience, The University of Texas at Austin, Austin TX
Espinoza, N., Department of Petroleum Engineering, The University of Texas at Austin, Austin TX

The geologic sequestration of CO2 is widely considered as a potential solution for decreasing anthropogenic atmospheric CO2 emissions. Wettability of fluids within reservoir materials is a critical factor in determining the efficiency of structural and residual trapping, two major mechanisms of geologic sequestration. Individual reservoir minerals are often targeted for wettability studies. Current practice applies these results, recorded under laboratory conditions, to in?situ reservoir rock; however the wide variety of measured contact angles reported in the literature calls this practice into question.

To address these issues and to study the wettability of shale caprock, resedimentation techniques are employed. These techniques allow for the creation of synthetic shales with controlled, homogeneous mineralogies. In addition, the systematic variation of the mineralogy allows for the characterization of shale wettability as a function of mineralogical composition. A novel design has been developed and used to conduct wettability experiments at reservoir conditions using high resolution X-ray computer tomography. Using this technique the wettability of resedimented shales and natural shales are compared at different reservoir conditions. Next, Lattice Boltzmann modelling methods are used to simulate capillary entry pressure into a shale capillary. Adhesion parameters along the wall are tuned to the results of the synthetic shales and heterogeneity is incorporated to estimate the capillary entry pressure into a natural shale. Understanding the mineralogical components of shale wetting allows for the prediction of capillary entry pressure based on shale mineralogy which can be used to help select secure CO2 storage sites.

Keywords: CO2 sequestration, wettability

LCPHD-5

CCG
LCPHD

Using solar-induced fluorescence measurements from the space to estimate global and time-resolved land photosynthesis and to monitor droughts in the United States

Maryia Halubok
Halubok, M., Jackson School of Geosciences, The University of Texas at Austin, Austin, TX

Our ability to understand how global vegetation uptakes the atmospheric CO_2 is crucial for closing the Earth's carbon budget and predicting feedbacks under a changing climate, but this understanding has been poor primarily due to limited observations and analyses. Historically, satellite observations have been focused on reflectance at different wavelengths, from which vegetation structure and potential photosynthesis can be inferred. Recently, satellite solar-induced chlorophyll fluorescence (SIF) retrievals have become available using a technique which previously was considered not possible, namely, in-filling of solar absorption lines. Thus, satellite observations now provide a highly credible opportunity to use SIF as a direct probe into photosynthesis for better understanding and resolving the terrestrial carbon cycle processes over much larger areas and longer periods of time.

When a plant absorbs energy from the sun, there are two main ways of how this energy can be used. A plant uses most of the energy to grow via photosynthesis and dissipates unused energy as heat. In addition, about 1-2% of solar energy captured by plants is re-emitted by chlorophyll molecules as fluorescence. Thus, SIF is essentially a distinct 'glow' at wavelengths of ~690–800 nm that is quite specific to green plants.

As such, SIF is an excellent proxy for the photosynthesis process which is of paramount importance to the Earth's carbon, water and energy cycles. It was also demonstrated that SIF may detect the development of stress in vegetation before traditional reflectance-based vegetation indices (VIs) become capable of capturing it. Hence, solar-induced chlorophyll fluorescence might be a useful tool for early identification of physiological effects of drought on vegetation and serve for drought monitoring purposes.

This study intends to investigate how global photosynthesis estimates can be improved with the use of SIF and how useful SIF and SIF-based gross primary production (GPP, or gross photosynthesis) can be in capturing drought onset, time to peak and demise. We have received new GPP estimates over the contiguous USA based on multiple linear regression analysis of SIF, which was previously shown to have better predictive skill than VIs and even some carbon models, and other parameters influencing GPP such as precipitation and soil moisture. The results were then compared to already existing GPP data from satellite and ground-based observations and were found to be in accordance with them. Thus, we can potentially use this simple and computationally efficient method based on derived linear equations linking SIF, precipitation, soil moisture and potentially other parameters to GPP, with the aim of providing a new dataset of global time-resolved GPP.

As for using SIF for drought monitoring, preliminary results indicate that on monthly scale SIF, SIF-based GPP and precipitation anomaly as well as Palmer Drought Severity Index values all show a significant downward trend. The further research will be shifted to finer temporal scale to reveal the drought onset, evolution, and recovery. The results of this study may have implications for drought management over the USA and globally.

Keywords: solar-induced chlorophyll fluorescence, gross primary production, drought monitoring.

LCPHD-6

CCG
LCPHD

Improving the Radiance Assimilation Performance in Estimating Snow Water Storage Across Snow and Land Cover Types in North America

Yonghwan Kwon
Kwon, Y., Jackson School of Geosciences, The University of Texas at Austin, Austin, TX
Yang, Z., Jackson School of Geosciences, The University of Texas at Austin, Austin, TX
Toure, A., Hydrological Sciences laboratory, Code 617, NASA GSFC, Greenbelt, MD; Universities Space Research Association (USRA), Columbia, MD
Hoar, T., The National Center for Atmospheric Research, Boulder, Colorado
Zhao, L., Jackson School of Geosciences, The University of Texas at Austin, Austin, TX
Rodell, M., Hydrological Sciences laboratory, Code 617, NASA GSFC, Greenbelt, MD

Data assimilation of microwave brightness temperature ([i]T_[/i]B) observations (i.e., radiance assimilation (RA)) has been proven to improve snowpack characterization at relatively small spatial scales. However, global climate and water cycle studies require large-scale snow datasets and hence a large-scale RA research, which demands a considerable amount of further efforts. Our objective in this study is to improve the continental-scale RA performance in estimating snow water storage for various snow classes and land cover types. Our RA system is comprised of the Community Land Model version 4 (CLM4), the Data Assimilation Research Testbed (DART), and two snowpack radiative transfer models (RTMs), i.e., the Dense Media Radiative Transfer–Multi Layers model (DMRT-ML) and the Microwave Emission Model for Layered Snowpacks (MEMLS). Vertically polarized 18.7 and 36.5 GHz [i]T_[/i]B from the Advanced Microwave Scanning Radiometer–Earth Observing System (AMSR-E) is assimilated into the RA system using the ensemble adjustment Kalman filter (EAKF). The results of snow depth estimation over North America are evaluated for six snow classes (i.e., tundra, taiga, maritime, ephemeral, prairie, and alpine) and five land cover types (i.e., bare soil, forest, shrub, grass, and crop) using the Canadian Meteorological Centre (CMC) daily snow depth data. The use of different RTMs for snowpack [i]T_[/i]B in the coupled RA system shows different performance in estimating snow depth for different snow classes and land covers. DMRT-ML and MEMLS exhibits better performance for tundra and taiga snow classes, respectively. Regardless of the snowpack RTMs, the RA performance is degraded for vegetated areas, in particular for forest and crop land covers. This may be attributed to the use of a simple empirical equation to estimate the vegetation effect on [i]T_[/i]B at the top of the atmosphere. To enhance the performance of the RA system for vegetated areas, several different vegetation RTMs are tested.

Keywords: Snow water storage, Radiance assimilation, Brightness temperature, Community Land Model, Radiative transfer model, Data Assimilation Research Testbed

LCPHD-7

CCG
LCPHD

The role of Northern Hemisphere snow data assimilation in seasonal predictions of surface air temperature

Peirong Lin
Lin, P., UT-Austin
Wei, J., UT-Austin
Zhang, Y., UT-Austin (Now at U. Washington)
Yang, Z., UT-Austin

Land initializations (i.e., snow, soil moisture, leaf area index) have been recognized as important sources of seasonal climate predictability besides ocean and atmosphere initializations. However, studies focusing on assessing how land data assimilation (DA) contributes to seasonal forecast skills are still lacking due to the limited number of large-scale land DA studies. In this study, taking advantage of the snow outputs from a multivariate global land DA system (i.e., DART/CLM), we systematically investigated the role of large-scale snow DA in influencing seasonal forecasts of surface air temperature. Three suites of ensemble seasonal forecast experiments were performed using the Community Earth System Model (CESM v1.2.1), in which three different snow initialization datasets were used. They are (1) CLM4 simulation without DA, (2) CLM4 simulation with MODIS snow cover DA, and (3) CLM4 simulation with joint GRACE and MODIS snow DA. Each suite of the experiment starts from multiple initialization dates of seven years from 2003 to 2009 and has three-month lead times. All experiments used the same atmosphere initializations from ERA-Interim (perturbed to get 8 ensembles) and the same prescribed SSTs. Our results show that snow DA plays an important role in surface air temperature predictions in regions such as Mongolia Plateau, Tibetan Plateau, Siberia, and the Rocky Mountains. The analyses also account for multiple lead times as snow can influence the atmosphere through immediate snow-albedo effect and through delayed snow hydrological effect after snow melts and wets the soil. This is a first study to quantify the impacts of snow initializations on seasonal forecasts of surface air temperature with an emphasis on large-scale snow DA. The insights are helpful to both land DA studies as well as research on seasonal climate forecasts.

Keywords: snow data assimilation, seasonal climate prediction

LCPHD-8

CCG
LCPHD

Development of an empirical model for predicting dust aerosol optical depth using satellite and reanalysis data

Sagar Parajuli
Parajuli, S., Jackson School of Geosciences
Yang, L., Jackson School of Geosciences
Kocurek, G., Jackson School of Geosciences

[color=black]Despite the increasing availability of satellite and ground-based aerosol optical depth (AOD) data, their application in dust modeling is limited because these data do not differentiate locally mobilized dust from remotely advected dust and other aerosols. In this work, we extract the locally mobilized dust signal from historical AOD data through a principal component analysis of wind and AOD time series. We then develop an empirical regression model for predicting dust optical depth (DOD) based on key environmental variables related to DOD, namely wind, soil moisture, soil temperature, vegetation, and boundary layer height. Principal component analysis is shown to be capable of separating the dust signal from AOD data and producing reconstructed DOD values. The developed DOD regression model is robust to represent the reconstructed DOD with overall R-squared (RMSE) of 0.72 (0.23). Initial results are presented using our reconstructed DOD to evaluate simulations from a global-scale dust model. [/color]

Keywords: Aerosol Optical Depth, Dust

LCPHD-9

CCG
LCPHD

Evaluating and Improving the Performance of Common Land Model Using FLUXNET Data

Xiangxiang Zhang
Zhang, X., The University of Texas At Austin, Austin, TX

Common Land Model(CoLM), combined the best features of LSM, BATS, and IAP94, has been widely applied and shown its good quality. However, land surface processes are crucial for weather and climate model initialization, hence it's necessary to constrain land surface model performances using observational data. In our preliminary work, eddy covariance measurements from 20 FLUXNET sites with over 100 site-years were used to evaluate CoLM while simulating energy balance fluxes in different climate conditions and vegetation categories. And the results show CoLM simulates well for all four energy fluxes, with sensible heat flux(H) better than latent heat flux(LE), net radiation (Rnet) the best. In terms of different vegetation categories, CoLM performs the best on evergreen needle-leaf forest among the 8 selected land cover types, and shows significant priority at evergreen broadleaf forest. Although a good agreement of simulation and observation is found on seasonal cycles at the 20 sample sites, it produces extreme bias mostly at summer noon, but not shows consistent bias among different seasons. This underestimate was associated with the weakness in simulating of soil water in dry seasons and incomplete description of photosynthesis as well, that's why we will first focus on implementing mesophyll diffusion in CoLM to improve the physical process of photosynthesis.

Keywords: Common Land Model, Energy Fluxes, Evaluation

LCPHD-10

EG
LCPHD

Trans-dimensional Seismic Inversion

Reetam Biswas
Biswas, R., Institute for Geophysics, The University of Texas at Austin, Austin, TX
Sen, M., Institute for Geophysics, The University of Texas at Austin, Austin, TX

Pre-stack or angle stack gathers are inverted to estimate pseudo-logs at every surface location for building reservoir models. Recently several methods have been proposed to increase the resolution of the inverted models. All of these methods, however, require that the total number of model parameters be fixed a priori. Here, we investigate an alternate approach in which we allow the data to choose model parameterization. In other words, in addition to the layer properties, the number of layers is also treated as a variable in our formulation. Such trans-dimensional inverse problems are generally solved by using the Reversible Jump Markov Chain Monte Carlo (RJMCMC), which is an effective tool for model exploration and uncertainty quantification.. Here we introduce a new gradient based RJMCMC, called the Hamiltonian Monte Carlo, where the model perturbations are generated according to the birth-death approach. Model updates are computed using gradient information and the Metropolis-Hastings criterion is used for model acceptance. We have applied this technique to pre-stack (angle stack) AVA inversion for estimating acoustic and shear impedance profiles. Our results demonstrate that RJHMC converges rapidly and can be a practical tool for inverting seismic data.

Keywords: AVO/AVA, resolution, prestack, poststack, inversion

LCPHD-11

EG
LCPHD

INFLUENCE OF SPATIAL VELOCITY DISTRIBUTION ON SEISMIC IMAGING OF MIXED CARBONATE-SILICICLASTIC CLINOFORMS, THE PERMIAN SAN ANDRES FORMATION, LAST CHANCE CANYON, NM

Yawen He
He, Y., Department of Geological Sciences, Jackson School of Geosciences, The Univeristy of Texas at Austin
Zeng, H., Bureau of Economic Geology, Jackson School of Geosciences, The Univeristy of Texas at Austin
Janson, X., Bureau of Economic Geology, Jackson School of Geosciences, The Univeristy of Texas at Austin
Kerans, C., Department of Geological Sciences, Jackson School of Geosciences, The Univeristy of Texas at Austin

Facies-averaged acoustic impedance is the most common in forward stratigraphic and seismic modeling workflow. In a previous paper, we highlighted challenges to accurately interpreting geologic time lines from seismic models characterized by impedance models with high lateral heterogeneity. Herein, we extend this study to a strongly prograding mixed siliciclastic-carbonate system from the Permian upper San Andres Formation. We illustrate the impact of facies-specific velocity assignments to the resultant seismic models, and the associated challenges in interpreting both time-significant high frequency cycle boundaries and diachronous lithofacies boundaries separating these zones of contrasting petrophysical properties.

We applied an alternative approach (Janson and Fomel, 2011) to populate velocity values across a grid of Kenter et al. (2001)'s modified LCC lithofacies model, and tested different combinations of velocity distribution and continuity based on analysis of petrophysical measurements from Kenter et al. (1997 and 2001). As a result, either changes in the velocity distribution or the velocity continuity can make a difference in seismic models, and different interpretations. Therefore, seismic images and interpretation strategies are closely related to complexity of local geologic models, this makes the petrophysical measurements even more necessary, before building a seismic model to study small-scale heterogeneity.

Keywords: Seismic modeling, Stratigraphy, Interpretation, Impedance

LCPHD-12

EG
LCPHD

3D simulation of seismic wave propagation in fractured medium using an integral method accommodating irregular geometries

Han Liu
Liu, H., Department of Geological Sciences, The University of Texas at Austin, Austin, TX
Sen, M., Institute for Geophysics, Jackson School of Geosciences, University of Texas at Austin, Austin, TX
Spikes, K., Department of Geological Sciences, The University of Texas at Austin, Austin, TX

Fractures are the most abundant visible structural features in the Earth's upper crust. They also strongly influence seismic wave propagation, which give rise to fracture induced anisotropy and scattering. Precise identification of fractures and their associated properties from seismic data has significant impact on reservoir management and hydrocarbon recovery. 3D simulation is necessary for a comprehensive understanding of azimuthal seismic wave propagation across the fractures. We model seismic wave propagation in fractured medium using integral method with tetrahedral grid cells. The integral approach is derived from the finite element and finite difference methods in heterogeneous medium. It is flexible in modeling irregular interface and surface topography. It also has low computational cost and memory requirement, which is essential in 3D simulation. The fractures are explicitly treated as displacement discontinued interfaces using linear slip model. We implemented the 3D explicit interface scheme on an irregular mesh. Arbitrary fractures can be accurately modeled in the numerical discretization. This approach can provide detailed wave propagation phenomena resulting from spatially complicated fractures. Different seismic signatures induced by various fracture length, fracture spacing, and fracture density are compared.

Keywords: seismic, fracture, elastic, modeling

LCPHD-13

EG
LCPHD

Effect of Chemical Environment and Rock Composition on Fracture Mechanics Properties of Reservoir Lithologies in Context of CO2 Sequestration

Jonathan Major
Major, J., Bureau of Economic Geology, The University of Texas at Austin, Austin, TX
Eichhubl, P., Bureau of Economic Geology, The University of Texas at Austin, Austin, TX

The coupled chemical and mechanical response of reservoir and seal rocks to injection of CO2 have major implications on the short and long term security of sequestered carbon. Many current numerical models evaluating behavior of reservoirs and seals during and after CO2 injection in the subsurface consider chemistry and mechanics separately and use only simple mechanical stability criteria while ignoring time-dependent failure parameters. CO2 injection irreversibly alters the subsurface chemical environment which can then affect geomechanical properties on a range of time scales by altering rock mineralogy and cements through dissolution, remobilization, and precipitation. It has also been documented that geomechanical parameters such as fracture toughness (KIC) and subcritical index (SCI) are sensitive to chemical environment. Double torsion fracture mechanics testing of reservoir lithologies under controlled environmental conditions relevant to CO2 sequestration show that chemical environment can measurably affect KIC and SCI. This coupled chemical-mechanical behavior is also influenced by rock composition, grains, amount and types of cement, and fabric. Fracture mechanics testing of the Aztec Sandstone, a largely silica-cemented, subarkose sandstone demonstrate it is less sensitive to chemical environment than Entrada Sandstone, a silty, clay-rich sandstone. The presence of de-ionized water lowers KIC by approximately 10% and SCI 30% in the Aztec Sandstone relative to tests performed in air, whereas the Entrada Sandstone shows reductions on the order of 70% and 90%, respectively. These results indicate that rock composition influences the chemical-mechanical response to deformation, and that the relative chemical reactivity of target reservoirs should be recognized in context of CO2 sequestration. In general, inert grains and cements such as quartz will be less sensitive to the changing subsurface environment than carbonates and clays.

Keywords: fracture, geomechanics, CO2 sequestration, coupled processes

LCPHD-14

EG
LCPHD

Path-Integral Diffraction Imaging

Dmitrii Merzlikin
Merzlikin, D., Bureau of Economic Geology, The University of Texas at Austin, Austin, TX
Fomel, S., Bureau of Economic Geology, The University of Texas at Austin, Austin, TX

Diffraction imaging aims to emphasize small-scale subsurface heterogeneities such as faults, pinchouts, fracture swarms, channels, etc., and, therefore, might play an important role in unconventional reservoir characterization. Existing diffraction imaging techniques are based on conventional migration algorithms, which are not optimal in terms of spatial resolution. We apply sparse inversion approach to increase diffraction imaging resolution limits. Path-integral diffraction model weighting is performed to increase inversion result stability. Velocity model building is performed automatically via double-path-integral approach. Resolution and uncertainty of produced diffraction images are analyzed. Synthetic and real data examples illustrate the efficiency of the proposed approach.

Keywords: Diffraction Imaging, Velocity Analysis, Unconventional Reservoirs

LCPHD-15

EG
LCPHD

Methane hydrate formation in a saturated, coarse-grained sample through the induction of a propagating gas front

Dylan Meyer
Meyer, D., The University of Texas at Austin, Institute for Geophysics, Austin, TX
You, K., The University of Texas at Austin, Institute for Geophysics, Austin, TX
Borgfeldt, T., The University of Texas at Austin, Institute for Geophysics, Austin, TX
Flemings, P., The University of Texas at Austin, Institute for Geophysics, Austin, TX
DiCarlo, D., The University of Texas at Austin, Petroleum and Geosystems Engineering, Austin, TX
Kneafsey, T., Lawrence Berkeley National Laboratory, Berkerley, CA

We generate methane hydrate in the laboratory in a coarse-grained, brine-saturated, vertically-oriented sample through gas injection. The sample (5.125 inch length; 2 inch diameter; 0.383 porosity) was initially pressurized to 12.24 MPa (1775 psi), cooled to 1 degree Celsius, and saturated with a 7 wt% NaBr solution. A syringe pump was filled with methane gas and connected to the top of the sample at a constant pressure. Another pump was used to withdraw brine from the base of the sample at a constant rate (0.003 mL/min), pulling methane into the sample and initiating hydrate formation. Based on mass balance calculations, derived from the mass of water withdrawn and the mass of methane consumed, the bulk saturations of water, hydrate, and gas reached final values of 0.683, 0.278, and 0.038, respectively. The computed-tomography (CT) scans confirm a downward-propagating low density front, which we interpret as the front of the region where hydrate is forming and free gas is replacing withdrawn water. Assuming that hydrate formation and gas presence is limited to the region behind this front increases the hydrate and gas saturations to 0.452 and 0.062, respectively. Additional analysis of the CT scans indicates a heterogeneous distribution of gas, hydrate, and water within the core and provides insight into hydrate formation behavior and the thermodynamic state of hydrate in gas-rich, coarse-grained systems.

Keywords: methane hydrate, fluid flow, computed tomography

LCPHD-16

EG
LCPHD

Spatial and Temporal Characterization of Mechnical Rock Properties From West Caicos, BWI

Andrea Nolting
Nolting, A., The Jackson School of Geosciences, The University of Texas at Austin, TX
Zahm, C., Bureau of Economic Geology, The University of Texas at Austin, TX
Kerans, C., The Jackson School of Geosciences, The University of Texas at Austin, TX
Donnie, B., Bureau of Economic Geology, The University of Texas at Austin, TX

Early brittle deformation is a key component in the structural, stratigraphic and diagenetic evolution of steep-rimmed carbonate platforms common to many major petroleum systems (e.g., pre-Caspian, Stuart City, and Scotian Abenaki). The goal of this study is to gain an understanding of the early response of carbonates to loading, deformation, and potential margin collapse or failure and to incorporate the variability of mechanical properties that are critical to the early deformation process. Samples were collected and unconfined compressive strength (UCS) field measurements were taken on West Caicos, where the eustatic history is tightly constrained, and detailed facies successions and fractures have been mapped. Key locations for sampling and UCS field measurements on West Caicos were chosen based upon the exposure of reef and grainstone facies and their relationship to the four major glacial-interglacial sea-level fluctuations. Facies successions include a base that is characterized by reef deposits abruptly transitioning into grainstone facies (e.g. foreshore, upper shore face, eolianite) and is often capped by an exposure surface. Three different analyses were completed: (1) detailed petrographic descriptions of grain type, texture, sorting, and cementation; (2) Porosity and Permeability measurements were completed on 1” diameter plugs; and (3) triaxial compression testing to ascertain mechanical rock behavior of samples and compare against in situ UCS readings. A Schmidt hammer was used to take 295 field rock hardness measurements to further constrain the mechanical behavior of facies within a stratigraphic framework. Thin section analysis and porosity and permeability data from 125ka and 400ka eolianite ooid grainstones reveals that cementation increases through time, indicating UCS is a function of porosity and age. Initial triaxial compression testing reveals a 125ka eolianite ooid grainstone has UCS of 4 MPa, similar to, but slightly lower than the in situ UCS of 9 MPa. Results from in situ UCS measurements illustrate that with increasing age, overall rock strength increases. Measurements collected from West Caicos also demonstrate that rock strength is dependent upon proximity to exposure surfaces, where UCS increases. The temporal and spatial variation in UCS across West Caicos illustrates that rock strength of young carbonates must be considered when evaluating syndepositional deformation of ancient steep-rimmed carbonate platforms.

Keywords: Carbonate platform, Syndepositional deformation, rock properties,

LCPHD-17

EG
LCPHD

Greedy Annealing Importance Sampling Inversion Method, an application on Eagle Ford Formation

Qi Ren
Ren, Q., Jackson School of Geosciences
Sen, M., Jackson School of Geosciences
Spikes, K., Jackson School of Geosciences

Seismic inversion is the mathematical technique to estimate the reservoir properties (impedance) as a function of two way travel time or depth, from the observed seismic data. It is an important part of reservoir modeling. For the high-dimension non-linear seismic inversion problem, there are two types of inversion methods: stochastic inference methods and global optimization methods. The stochastic methods, like important sampling methods, provide unbiased results; however, in order to converge efficiently, it requires that the initial model can statistically represent real earth model. On the other hand, the global optimization methods, like simulated annealing methods, can provide optimized results based on simple initial model; however, the results might be biased.In this work, we developed a new inversion methods named as greedy annealing importance sampling (GAIS), which is a combination idea of stochastic methods and global optimization methods. This method at runs multiple independent very fast simulated annealing (VFSA), whose results are applied as initial models for greedy important sampling (GIA) as the next step. Finally the GIA results are weighted average to provide the final estimation of the real earth model. This new developed GAIS method is applied on Eagle Ford Formation.

Keywords: seismic inversion, shale, reservoir modeling

LCPHD-18

EG
LCPHD

Muir-Dellinger parameters for anisotropic signatures analysis in shales

Yanadet Sripanich
Sripanich, Y., Bureau of Economic Geology, The University of Texas at Austin, Austin, TX
Fomel, S., Bureau of Economic Geology, The University of Texas at Austin, Austin, TX
Spikes, K., Department of Geological Sciences, The University of Texas at Austin, Austin, TX
Stovas, A., Norwegian University of Science and Technology (NTNU), Norway

The effect of seismic anisotropy is generally described via a set of anisotropic parameters instead of the direct stiffness tensor coeficients due to the conciseness in the resulting expressions and their abilities to describe meaningful quantities important in seismic data processing. We revisit one of such set, namely the Muir-Dellinger parameters, and demonstrate their advantages in characterizing the effect of anisotropy on seismic waves in shales. We emphasize that the Muir-Dellinger parameters have a strong linear relationship between a pair of its members, aneliiptic parameters, which govern the deviation of the wavefront from an ellipse when the vertical or horizontal axis is considered. This relationship is observed from laboratory measurements on many different shale samples from various geographical locations and depths and it provides a mean to reduce the total number of parameters for qP-wave analysis while maintianing high accuracy in transversely isotropic (TI) and orthorhombic media from four to three and from nine to six respectively. In this study, we use both the Backus' average and the self-consistent rock physics modeling to explain this linear behavior in a simple manner.

Keywords: Seismic anisotropy

LCPHD-19

EG
LCPHD

Imaging microseismic and diffraction events with cross-correlation imaging condition

Junzhe Sun
Sun, J., Bureau of Economic Geology, The University of Texas at Austin, Austin, TX
Zhu, T., Bureau of Economic Geology, The University of Texas at Austin, Austin, TX
Fomel, S., Bureau of Economic Geology, The University of Texas at Austin, Austin, TX

Passive microseismic events and active diffraction events share the similarity that seismic waves are initiated from a single source location. Therefore, the back propagated events should focus at zero time that corresponds to the start time of the recorded event. Using this property, we propose a new imaging condition that a true seismic source must correspond to the location where all the backward-propagated events coincide in both space and time. For microseismic imaging, instead of simply stacking the backward-propagated seismic wavefields, as suggested by time-reversal imaging, we cross-correlate wavefields back-propagated using different groups of record to compute a high-resolution micro-seismicity map. The map has an extra dimension of time, indicating the start times of different events. For diffraction imaging, we improve the reverse-time migration imaging condition by also cross-correlating different groups of receiver wavefields, which effectively removes conventional imaging artifacts and enhances resolution. Using synthetic models in both 2D and 3D, we test the robustness of the proposed method in the presence of velocity errors. We conclude that the cross-correlation imaging condition is an effective way to constrain source location and enhance image resolution.

Keywords: microseismic, diffraction, imaging condition

LCPHD-20

EG
LCPHD

Simultaneous Inversion of Velocity and Attenuation Models with Adaptive Matching Filter

Zhiguang Xue
Xue, Z., Bureau of Economic Geology, The University of Texas at Austin, Austin, TX
Zhu, T., Bureau of Economic Geology, The University of Texas at Austin, Austin, TX
Fomel, S., Bureau of Economic Geology, The University of Texas at Austin, Austin, TX
Sun, J., Bureau of Economic Geology, The University of Texas at Austin, Austin, TX

Because of the conversion of elastic energy into heat, seismic waves are attenuated and dispersed as they propagate. The attenuation effects can reduce the resolution of velocity models obtained from waveform inversion or even cause the inversion to produce incorrect results. Attenuation should be taken into account in the process of inverting for velocity model. We propose to simultaneously invert for velocity and attenuation models. To mitigate the cycle-skipping problem of waveform inversion, we fist use misfit function based on adaptive matching filter to build a starting model, and then switch to use conventional least-squares misfit function to refine small-scale features in velocity and attenuation models. Numerical examples verified the effectiveness of the proposed method in recovering the velocity and attenuation models.

Keywords: Waveform inversion, Attenuation effect, Cycle-skipping, Simultaneous inversion

LCPHD-21

EG
LCPHD

Reciprocity and Double Plane Wave Migration

Zeyu Zhao
Zhao, Z., Institute for Geophysics
Sen, M., Institute for Geophysics
Stoffa, P., Institute for Geophysics

A plane wave dataset is optimal if it records seismic energy for both positive and negative ray-parameter. Such optimal plane wave data are assumed to be required to properly implement plane wave migration schemes, since viewing angles on both sides of targets are illuminated. Traditionally, split-spread gathers are preferred over one-sided gathers for plane wave migration because seismic waves coming from both sides of source locations can be captured using split-spread acquisition geometry. One-sided or end-on gathers produced by marine acquisition geometry is generally believed to be inadequate for producing optimal plane wave data without preprocessing. Such one-sided gather usually need to be gathered into common receiver gathers, and reciprocity need to be invoked to approximate the same subsurface coverage. In this study, we investigate the applicability of the reciprocity principle in the double plane wave (DPW) domain. We demonstrate two methods by which optimal reciprocal DPW datasets can be easily generated using originally one-sided shot gathers. An optimal reciprocal DPW dataset transformed from one-sided gathers is shown to approximate a DPW dataset generated from split-spread shot gathers. Based on this study, under the ideal acquisition conditions, we suggest that one-sided acquisition geometries should be extended to the largest possible offsets and reciprocity should be invoked to improve subsurface illumination. Further, we show that migration efficiency can be improved for DPW reverse time migration (RTM) with the help of the reciprocity principle. Proposed methods are tested on synthetic examples to demonstrate their effectiveness.

Keywords: Seismic Acquisition, Imaging, Reciprocity, Plane Wave

LCPHD-22

MG
LCPHD

New Somali Basin Magnetic Anomalies and a Plate Model for the Early Indian Ocean

Joshua Davis
Davis, J., Institute for Geophysics, The University of Texas, Austin, TX
Lawver, L., Institute for Geophysics, The University of Texas, Austin, TX
Norton, I., Institute for Geophysics, The University of Texas, Austin, TX
Gahagan, L., Institute for Geophysics, The University of Texas, Austin, TX

The oldest portions of the Indian Ocean formed via the breakup of Gondwana and the subsequent fragmentation of East Gondwana. We present a constrained plate model for this early Indian Ocean development for the time period from Gondwana Breakup until the start of the Cretaceous Normal Superchron. The motions of the East Gondwana terranes are determined using new geophysical observations in the Somali Basin and existing geophysical interpretations from other coeval Indian Ocean basins. Within the Somali Basin, recent satellite gravity data clearly resolve traces of an east-west trending extinct spreading ridge and north-south oriented fracture zones. A thorough compilation of Somali Basin ship track magnetic data allows us to interpret magnetic anomalies M24Bn through M0r about this extinct ridge. Our magnetic interpretations from the Somali Basin are similar in age, spreading rate, and spreading directions to magnetic anomalies previously interpreted in the neighboring Mozambique Basin and Riiser Larsen Sea. The similarity between the two magnetic anomaly datasets allows us to match both basin's older magnetic anomaly picks by defining a pole of rotation for a single and cohesive East Gondwana plate. However, following magnetic anomaly M15n, we find it is no longer possible to match magnetic picks from both basins and maintain plausible plate motions. In order to match the post-M15n geophysical data we are forced to model the motions of Madagascar/India and East Antarctica/Australia as independent plates. The requirement to utilize two independent plates after anomaly M15n provides strong circumstantial evidence that suggests East Gondwana breakup began around 135 Ma.

Keywords: Somali Basin, Magnetic Anomalies, East Gondwana, Indian Ocean Tectonics

LCPHD-23

MG
LCPHD

Seafloor Changes Offshore Northern Sumatra from 1997-2008 Bathymetric Data

Marina Frederik
Frederik, M., Institute for Geophysics, The University of Texas at Austin, Austin, TX
Gulick, S., Institute for Geophysics, The University of Texas at Austin, Austin, TX
Austin, J., Institute for Geophysics, The University of Texas at Austin, Austin, TX
Bangs, N., Institute for Geophysics, The University of Texas at Austin, Austin, TX
Udrekh, U., Badan Pengkajian dan Penerapan Teknologi, Jakarta, Indonesia
Duncan, D., Institute for Geophysics, The University of Texas at Austin, Austin, TX

We present the first regional study of seafloor changes offshore of northern Sumatra, covering from the northwest of northern Sumatra to west of the Simeulue Island, 1-6.5°N and 93-96.5°E. The pre-earthquake dataset was from Dec 1997-Jan 1998 and the post-earthquake datasets were from the multiple surveys between Jan 2005 and Aug 2008. Using a cell size of 50 m and sample interval of 100 m, we focused our observation on three 20 km long, NE-SW transects, of the toe of the accretionary prism comparing the 1997-1998 data with the more recent surveys. We investigate changes in slope instead of absolute depth because of uncertainties resulting from the missing parameters of the 1997-1998 data. Furthermore, the slopes are less affected by differences in sound velocity profiles between the surveys. On Crossing 1, we observe evidence of a gravitationally driven mass wasting feature, and on Crossing 2 and 3, we observe thrust fault activity related to the 2004 event. For northern Sumatra, we propose that the seaward dipping thrust faults of the frontal folds are active in response to major earthquake. This study also highlights the need to establish fundamental time series datasets for hazard mitigation.

Keywords: Bathymetric differences, 2004 Sumatra-Andaman earthquake, 2005 Sumatra earthquake

LCPHD-24

MG
LCPHD

Geomechanical Modeling in Fold-and-Thrust Belts Systems

Baiyuan Gao
Gao, B., Institute for Geophysics, The University of Texas at Austin
Flemings, P., The University of Texas at Austin

We present a large-strain poro-mechanical model to investigate the evolution of stress and strain in fold and thrust belt systems. We impose horizontal shortening in the model and observe that a tapered wedge develops. Inside the accrecionary wedge, the horizontal effective stress increases to about 2.3 times the vertical effective stress. The maximum principle stress direction rotates gradually from the initial vertical direction to the horizontal direction as sediment gets closer to the backstop. We use stress paths to illustrate how the stresses evolve during the thrust loading. We find the sediment stress path starts from uniaxial condition and moves towards critical state condition. We categorize the thrust belt into 3 zones according to their stress conditions from the backstop to the farfield: critical state region, transition region, and uniaxial region. We show that the sediments within the accretionary wedge are at critical state, which indicate they lost their strength to resist deformation. The sediment porosity decreases dramatically within the wedge due to high mean effective and differential stress. We observe that the shear-induced compression also plays a key role which can not be neglected for compression analysis. We built the model in finite element program Elfen. The sediments are modeled as poro-elastoplastic materials with a critical state soil model. Overall, our results provide insights of stress and porosity evolution in compressional regimes and can assist field stress and pressure predictions.

Keywords: thrust belts, stress path, compression

LCPHD-25

MG
LCPHD

Revisiting the 1899 Earthquakes of Yakutat Bay, Alaska Using New and Existing Geophysical Data

Maureen Walton
Walton, M., Institute for Geophysics, The University of Texas at Austin, Austin, TX
Gulick, S., Institute for Geophysics, The University of Texas at Austin, Austin, TX
Haeussler, P., U.S. Geological Survey, Anchorage, AK

North of Yakutat Bay in southeastern Alaska, the subducting Yakutat Block intersects with the Fairweather transform fault system. A series of large earthquakes occurred in the region in September of 1899, including a Mw 8.2 event on 10 September that resulted in >14 m of coseismic uplift and a 6 m tsunami in Yakutat Bay. Despite recurrence risk of the 1899 or similar events in the region, the fault(s) that ruptured in 1899 remain unidentified. Previous efforts to map active Yakutat Bay faults carried out by Plafker and Thatcher (2008) used post-1899 bedrock uplift measurements to infer the location of potentially important structures, including the Esker Creek and Bancas Point thrusts. As measurement error was not assessed in their study, we revisit the uplift measurements by quantifying uncertainty; effects of glacial isostatic adjustment (GIA), in particular, are significant. We also combine new seismic reflection data with existing topography, bathymetry, GPS, and satellite photo data to update earlier fault maps. Our reevaluation of uplift measurements suggests that primary slip and uplift during the 10 September earthquake was limited to northwest of Yakutat Bay. Additionally, a high-resolution seismic reflection survey we conducted in Yakutat Bay during August 2012 constrains faulting to on- or near-shore based on the absence of bay-crossing faults. Collectively, our results imply that predominantly strike-slip and transpressive horsetail-type faults are southeast of Yakutat Bay, with compressional structures related to Yakutat Block subduction/collision to the northwest. We interpret the 10 September 1899 event to be the result of complex rupture somewhere within the Yakutat subduction/collision system. Based on our updated map of coseismic uplift and fault structure, we favor a rupture model where primary slip occurred along the Esker Creek system locally with possible induced coseismic slip along the neighboring Boundary transpressive fault system. Future work targets imaging offshore connections between Yakutat Bay fault systems and the Pamplona Zone subduction deformation front, which will assist with assessing potential hazards related to recurrence of an 1899-type event.

Keywords: tectonics, Alaska, marine geophysics, seismic reflection, earthquake

LCPHD-26

MG
LCPHD

Point-bar scaling and application to the Lower Miocene drainage system of the Gulf of Mexico basin

Jie Xu
xu, J., Institute for Geophysics, The University of Texas at Austin, Austin, TX
Snedden, J., Institute for Geophysics, The University of Texas at Austin, Austin, TX
Galloway, W., Institute for Geophysics, The University of Texas at Austin, Austin, TX
Milliken, K., Emerald Mountain Geoscience, LLC
Blum, M., Department of Geology, The University of Kansas
Fulthorpe, C., Institute for Geophysics, The University of Texas at Austin, Austin, TX

Fluvial systems are major sediment conveyers from source terranes to basinal sinks. Fluvial channel geometry results from interaction between fluid flow and sediment particles, and scales with water discharge and sediment flux. Point bar deposits formed in bends of meandering rivers provide a good proxy to estimate the depths of paleochannels (Ethridge and Schumm, 1978; Blum et al., 2013). Modern observations show that bankfull channel depth (or point bar thickness) well correlates with bankfull discharge and drainage area (Blum et al., 2013). However, this scaling relationship has not been rigorously tested in ancient rock records, especially for large passive margin basins that have diverse climate, tectonic, topographic, lithological, and geomorphic regimes. In this study, we try to test whether this scaling relationship applies to the large drainage systems in the Gulf of Mexico in early Miocene time. Point bar thickness data were collected from subsurface well logs that are within major paleo-fluvial axes. Point bar data from each major fluvial axis display a wide range of thickness and a combination of different river types, including point bar thickness from trunk stream, local small streams, and valley fills. The Paleo-Mississippi and Red rivers in eastern Texas-Louisiana have the thickest point bar deposits (25 m and 21 m), while Paleo Houston-Brazos and Guadalupe rivers in central Texas deposited the thinnest point bars in early Miocene (12.8 m and 13 m). Paleo-Rio Grande River has intermediate values, 17m. The results show a clear scaling relationship between the point bar thickness and paleo-drainage area, length of channel, and sediment supply rate. This study indicates that such point bar scaling relationship can be used to ancient sedimentary rock to constrain paleodrainage system size. In addition, the sediments deposited in point bars can be applied to predict the fan run out length and size where the seismic image quality does not allow one to detect such features beneath a salt canopy (e.g. lower Miocene subsalt reservoir in GOM deep-water basin).

Keywords: Point bar, Scaling relationship, source-to-sink, lower Miocene, Gulf of Mexico

LCPHD-27

PS
LCPHD

3D measurement of fine-grained rims in CM Murchison using XCT

Romy Hanna
Hanna, R., University of Texas at Austin, Austin, TX
Ketcham, R., University of Texas at Austin, Austin, TX

Previous work using X-ray computed tomography (XCT) of a 44 g sample of CM Murchison (USNM 5487) has revealed an impact-derived foliation and weak lineation defined by partially altered chondrules. The coarse scan resolution (29-58 μm per voxel) did not allow for the discrimination of fine-grained rims (FGRs) around the chondrules but BSE imaging of sections from the sample suggest that the rim thickness around the chondrules is irregular and that the shape and orientation of deformed chondrules differs when including the FGR. If the FGR thickness is variable around each chondrule and correlates with the macroscopic foliation or lineation, it may suggest that the FGRs were initially uniform in thickness but had a different strain response to the impact stress than the interior chondrule. Alternatively, if the thickness of FGRs are found to be variable with no correlation to the macroscopic petrofabric, it will suggest that geometry of the rim is an inherited property related to the origin of the rim or perhaps subsequent alteration.

The origin of FGRs in CM chondrites is intensely debated with arguments and evidence for both nebular and parent body formation. In particular researchers have argued whether there is or is not a correlation between rim thickness and the size of the enclosed object, with the former scenario argued as evidence of a nebular origin of formation. These measurements were made using 2D thin sections and therefore only a portion of the rim and chondrule were measured. Further, any deformational strain would have altered the shape of the chondrule and/or the rim and therefore complicate the interpretation of the rim thickness and geometry. In our study we will test for a correlation between average rim thickness and the size of the enclosed object in 3D and will also determine if the rim has any regular relationship to macroscopic petrofabric.

A high-resolution (5.5 μm pixel) XCT scan of a 0.143 g chip of USNM 5487 at low energy (70 kV) has allowed discrimination of the FGRs around the deformed chondrules. Using Avizo we are manually segmenting each chondrule twice: both with and without the FGR. The segmented data is then imported into the Blob3D program that measures the chondrule size and orientation as well as the rim thickness in 3D.

Preliminary results suggest that the FGRs are variable in thickness around each chondrule. The orientations of the deformed chondrules are generally the same regardless of inclusion of the FGRs but the measured 3D aspect ratio and elongation of the chondrule is on average lower when including the FGR. This could indicate that the FGRs are thicker in the direction perpendicular to the foliation or that the variability in rim thickness is much less than the size of the enclosed object. In addition, we see evidence for a moderately strong positive correlation between rim thickness and the size of the enclosed chondrule.

Keywords: Meteorite, chondrite, chondrule, X-ray computed tomography

LCPHD-28

SETP
LCPHD

Thermokinematic modeling of fold-thrust belts: Bitlis-Zagros orogen, Kurdistan, Iraq

Douglas Barber
Barber, D., Jackson School of Geosciences, The University of Texas at Austin, Austin, TX
Stockli, D., Jackson School of Geosciences, The University of Texas at Austin, Austin, TX
Koshnaw, R., Jackson School of Geosciences, The University of Texas at Austin, Austin, TX

Crustal-scale balanced cross-section reconstruction is a useful approach for constraining the structural-kinematic development of orogenic belts. Such kinematic reconstructions require an integration of all available geological and geophysical data to produce the most accurate model, and can be further supplemented by thermochronometry results to provide independent temporal markers of deformation as well as burial estimates. However, the direct association of thermochronometric ages with tectonic and exhumational processes can be ambiguated in orogenic settings due to complexities in fault-motion geometries, shortening rates, and rock characteristics (e.g., thermal conductivity). Advances in thermochronology and numerical modeling allow for the quantitative linkage of deformation kinematics and material properties to the time-temperature pathway of a rock or structure, thus providing a more accurate assessment of a particular kinematic reconstruction. In this study we apply 2-D thermokinematic modeling to competing forward-modeled balanced 2-D cross sections of a fold-and-thrust belt in Bitlis-Zagros Mountains. The east-west trending Bitlis-Zagros belt is an active orogenic system in northern Iraq and southeastern Turkey that formed as a result of incremental collision associated with late Mesozoic-Cenozoic convergence of the Arabian and Eurasian continents and final closure of Neotethys. Balanced cross-sections (>70 km length) of this region are constructed based on surface measurements, existing geologic map data, and limited seismic sections. Kinematic restoration software Move™ (Midland Valley) is used to determine a set of velocity vectors that represent each model's deformation kinematics. These velocity vectors are then input into FETKIN (thermokinematic modeling code) to calculate expected thermochronometric ages along the topographic surface of each cross-section line. We compare these predicted thermochronometric ages with a set of new and previously published thermochronometric data in southeastern Turkey and northern Iraq to test the validity of the timing, rate, and fault motion geometry associated with each reconstruction. Together, (U-Th)/He and fission-track ages of apatite and zircon indicate that Bitlis-Zagros thrusting in southeastern Turkey commenced by early Miocene time and sequentially propagated southward into northern Iraq through middle and late Miocene time. Deformation later shifted towards the hinterland as manifested by Plio-Pleistocene reactivation of the Ora Thrust basement uplift near the Iraq-Turkey border. We find that our FETKIN modeled results are similar to that of observed data. However, in contrast to predicted results, the presence of partially reset zircon (U-Th)/He ages in Paleozoic basement rock of the Ora Thrust region show that the area was not affected by Neogene sediment burial, likely indicating that this region was a paleohigh by this time and perhaps uplifted by pre-Neogene deformation. Limited seismic data indicate that the Bitlis-Zagros structures in northern Iraq are controlled by reactivated Early Cretaceous normal faults. In the future we plan to integrate vitrinite reflectance data into the modeling program to better constrain maximum burial temperatures in our reconstructions. This approach can be adapted for other deformed regions of various tectonic settings to evaluate the consistency of proposed kinematic reconstructions in terms of their fault-motion geometry, timing of exhumation, and burial history.

Keywords: fold-thrust belt, structural geology, thermochronology, thermokinematic modeling

LCPHD-29

SETP
LCPHD

Constraints from Xenoliths on the Rheology of the Mojave Lower Crust and Lithospheric Mantle

Rachel Bernard
Bernard, R., Department of Geological Sciences, The University of Texas at Austin, Austin, TX
Behr, W., Department of Geological Sciences, The University of Texas at Austin, Austin, TX

We use xenoliths from young (3 Ma to present) cinder cones in the tectonically active Mojave region of southern California to characterize the rheological properties of the lower crust and upper mantle beneath the Eastern California Shear Zone. The xenoliths, which include spinel and plagioclase facies peridotites and lower crustal rocks (representing a depth range of ~25-60 km), were collected from two localities roughly 80 km apart: the Cima and Dish Hill volcanic fields. We document how stress, temperature, water content, deformation mechanism, lattice preferred orientation (LPO), and style of localization vary spatially and with depth. Key findings include the following:

(1) Both xenolith suites exhibit a wide range of deformation textures, ranging from granular, to protogranular, to porphyroclastic and mylonitic. Higher strain fabrics show no evidence for static annealing, thus are likely reflecting youthful deformation and strain gradients at depth.

(2) Both xenolith suites show abundant dynamic recrystallization and other evidence for dislocation creep as the dominant deformation mechanism.

(3) A- and E-type olivine LPOs occur in both xenolith suites. In general, E-type LPO is associated with higher strain fabrics than A-type.

(4) Water contents—found using Fourier transform infrared spectroscopy (FTIR) and Secondary Ion Mass Spectrometry (SIMS)—range from 117-370 ppm for clinopyroxene, 57-217 ppm for orthopyroxene, and less than 10 ppm for olivine. We have found no correlation between water content and olivine LPO, despite experimental work associating higher water content with the development of E-type LPO, compared to A-type.

(5) Deformation in most lower crustal gabbros is weak, but some show strong fabrics associated with plagioclase-rich zones. Water content from clinopyroxene in one highly-deformed gabbro is <1 ppm.

(6) Paleopiezometers for olivine and plagioclase indicate stress magnitudes of 11-21 MPa for the uppermost mantle, and 0.1 MPa for the lowermost crust.

Keywords: mantle, rheology, xenoliths, deformation

LCPHD-30

SETP
LCPHD

The effects of chemical alteration on fracture mechanical properties in hydrothermal systems

Owen Callahan
Callahan, O., Bureau of Economic Geology, The University of Texas at Austin, Austin, TX
Eichhubl, P., Bureau of Economic Geology, The University of Texas at Austin, Austin, TX

Fault and fracture networks often control the distribution of fluids and heat in hydrothermal and epithermal systems, and in related geothermal and mineral resources. Additional chemical influences on conduit evolution are well documented, with dissolution and precipitation of mineral species potentially changing the permeability of fault-facture networks. Less well understood are the impacts of chemical alteration on the mechanical properties governing fracture growth and fracture network geometry.

We use double-torsion (DT) load relaxation tests under ambient air conditions to measure the mode-I fracture toughness (K_{IC}) and subcritical fracture growth index (SCI) of variably altered rock samples obtained from outcrop in Dixie Valley, NV. Samples from the Box Canyon site in southern Dixie Valley include weakly altered granodiorite and diorite, characterized by minor sericite and incomplete replacement of biotite with chlorite, as well as granodiorite from an area of locally intense propylitic alteration (chlorite-calcite-hematite-epidote). Samples from the Dixie Meadows site include tuff with moderate argillic alteration and silicified bladed calcite fault breccia associated with active fumaroles and hot springs. Samples from the Dixie Comstock epithermal gold deposit include propylitically altered gabbro, calcified gabbro, and massive silicification.

Weakly altered granodiorite has a K_{IC} between 1.1 and 1.6 MPa√m, and SCI ranges from 48 to 78. By contrast, K_{IC} in propylitically altered granodiorite is reduced to 0.5 MPa√m, and SCI increases to 76-100. In both cases, the altered materials have lower fracture toughness and higher SCI than is reported for common geomechanical standards such as Westerly Granite (K_{IC} ~1.7 MPa√m; SCI ~48). Fracture toughness of calcified breccia from Dixie Meadows is indistinguishable from the argillic tuff, K_{IC} = 1.4 and 1.5 MPa√m, respectively, but from tuff to cemented breccia the SCI nearly doubles from 69 to 119. Massive silicified fault zone material from the Dixie Comstock Mine shows a significant increase in K_{IC} (2.9 MPa√m) and SCI (126-147) compared to the surrounding propylitically altered and calcified gabbro (K_{IC} = 0.5 and 1.6 MPa√m, SCI = 55 and 67, respectively).

These results suggest that mineralogical and textural changes associated with different alteration assemblages may result in spatially variable rates of fracture initiation and growth in different parts of hydrothermal systems. Contrasting fracture mechanical properties between alteration assemblages may constitute new mechanisms of chemical-mechanical feedback that contribute to the localization of conduits in hydrothermal systems.

Keywords: hydrothermal alteration, fracture mechanics

LCPHD-31

SETP
LCPHD

LATE CRETACEOUS-CENOZOIC EVOLUTION of the CENTRAL ANDEAN FORELAND BASIN SYSTEM in the EASTERN CORDILLERA to SUBANDEAN ZONE, SOUTHERN BOLIVIA

Amanda Calle
Calle, A., Institute for Geophysics and Department of Geological Sciences, The University of Texas at Austin, Austin, TX
Horton, B., Institute for Geophysics and Department of Geological Sciences, The University of Texas at Austin, Austin, TX
Anderson, R., Washington State University, School of the Environment, Pullman WA; University of Nevada, Reno, Reno, NV
Long, S., Washington State University, School of the Environment, Pullman WA; University of Nevada, Reno, Reno, NV
Stockli, D., Department of Geological Sciences, The University of Texas at Austin, Austin, TX

Evaluation of foreland basin deposystems and provenance across southern Bolivia reveals punctuated growth of the central Andean orogenic wedge.New and published sedimentology, provenance data, stratigraphy, subcrop mapping, and apatite (U-Th)/He thermochronometry along two transects (19.5, 21°S) from the easternmost Eastern Cordillera (EC) to the western Subandean Zone (SAZ) shed light on Late Cretaceous–Miocene thrust belt and foreland basin dynamics. Sediment dispersal patterns are constrained by paleocurrents, detrital zircon U-Pb geochronology, sandstone petrography, and conglomerate clast compositions. Spatial and temporal changes in the Andean thrust belt are recorded in asymmetric foreland basin thicknesses, facies distributions, and provenance within the EC (Incapampa and Camargo synclines) and SAZ (El Rosal and Entre Rios synclines). The >4 km uppermost Cretaceous–lower Miocene EC succession and ~2.5 km upper Oligocene–Miocene SAZ clastic successions record a shift from fluvial backbulge to pedogenic forebulge deposition. Braided, meandering, and lacustrine foredeep deposition records the most-rapid subsidence, with a later shift to progradational braided and alluvial fan deposition in the wedge-top zone. Growth strata preserved in EC and SAZ wedge-top deposits suggest unsteady eastward advance of the deformation front. Distal foreland deposits show west-directed paleocurrents with >1 Ga detrital zircon populations. Emerging Andean sources are indicated by east-directed paleocurrents, 36-25 Ma), Interandean Zone (IAZ, ~22-7 Ma) and SAZ (

LCPHD-32

SETP
LCPHD

Direct U-Pb dating of skarn garnets: A case study from Black Rock Mine skarn, eastern California

Michelle Gevedon
Gevedon, M., Jackson School of Geosciences, University of Texas at Austin
Seman, S., Jackson School of Geosciences, University of Texas at Austin
Barnes, J., Jackson School of Geosciences, University of Texas at Austin
Stockli, D., Jackson School of Geosciences, University of Texas at Austin
Lackey, J., Pomona College
Kitajima, K., WiscSIMS, University of Wisconsin Madison
Valley, J., WiscSIMS, University of Wisconsin Madison

Oxygen isotope compositions of skarn garnet can be used to trace hydrothermal fluid sources; regional and small-scale (inter-skarn and intra-grain) variation in $\delta^{18}O$ values may potentially resolve magmatic flare-ups, fluid pulses, and relative depths of emplacement. Laser fluorination (LF) garnet $\delta^{18}O$ data from 19 skarns (n = 136) associated with the Sierra Nevada arc vary by ~20‰. These data provide insight to the depth and dominant fluid regime associated with Sierra Nevada plutonism through time and space.

Values of $\delta^{18}O$ data (LF and ion probe [SIMS]) from multiple skarns from the Jurassic Mojave segment of the arc vary from −9.6‰ to +5.5‰ VSMOW, and are interpreted to reflect mixing of meteoric and magmatic-derived hydrothermal fluid sources. SIMS analysis of two Mojave skarn garnets with oscillatory zoning reveals cores with $\delta^{18}O$ values of −9.6‰, internal variations of −9.4‰ to −3.3‰, and rims of −2.2‰ and −2.9‰ (precision ±0.3; 2σ). In general, $\delta^{18}O$values do not correlate with Fe in the mostly andraditic garnet.

The preponderance and magnitude of negative $\delta^{18}O$ values from Jurassic Mojave skarn garnets preclude skarn formation below the Jurassic sea and corroborate the presence of a large, shallow, sub-aerial hydrothermal system as documented by Solomon and Taylor (1991) and Battles and Barton (1995). In contrast, Jurassic skarns of the eastern Sierra Nevada generally lack low-$\delta^{18}O$ values, and may indicate formation at greater crustal depths below the depth at which brittle deformation in hydrothermal systems would allow infiltration of surface water. Instead $\delta^{18}O$ values of the Jurassic eastern California skarns suggest a component of sedimentary-derived fluid.

New methods for laser ablation inductively coupled plasma mass spectrometry (LA-ICP-MS) U-Pb dating of grossular-andradite garnet provide the ability to determine the absolute timing and longevity of skarn formation, and to monitor regional changes in the fluid composition through time. Garnet U-Pb dates from Black Rock skarn (203±7 Ma) match the age of the causative pluton (~196 Ma) within in error. Skarn grossular-andradite is typically uranium-rich (1 – 100ppm); common Pb is highly heterogeneous at the micron scale, which allows for the construction of robust Discordia lines in Tera-Wasserburg space with relatively few analyses over a small area.

Keywords: U-Pb, garnet, skarn, oxygen isotope, Sierra Nevada, laser ablation

LCPHD-33

SETP
LCPHD

New Geologic Slip Rates for the Agua Blanca Fault, Northern Baja California, Mexico

Peter Gold
Gold, P., Department of Geological Sciences, University of Texas, Austin
Behr, W., Department of Geological Sciences, University of Texas, Austin
Fletcher, J., Centro de Investigación Científica y de Educación Superior de Ensenada
Hinojosa-Corona, A., Centro de Investigación Científica y de Educación Superior de Ensenada
Rockwell, T., San Diego State University

Within the southern San Andreas transform plate boundary system, relatively little is known regarding active faulting in northern Baja California, Mexico, or offshore along the Inner Continental Borderland. The inner offshore system appears to be fed from the south by the Agua Blanca Fault (ABF), which strikes northwest across the Peninsular Ranges of northern Baja California. Therefore, the geologic slip rate for the ABF also provides a minimum slip rate estimate for the offshore system, which is connected to the north to faults in the Los Angeles region. Previous studies along the ABF determined slip rates of ~4-6 mm/yr (~10% of relative plate motion). However, these rates relied on imprecise age estimates and offset geomorphic features of a type that require these rates to be interpreted as minima, allowing for the possibility that the slip rate for the ABF may be greater. Although seismically quiescent, the surface trace of the ABF clearly reflects Holocene activity, and given its connectivity with the offshore fault system, more quantitative slip rates for the ABF are needed to better understand earthquake hazard for both US and Mexican coastal populations.

Using newly acquired airborne LiDAR, we have mapped primary and secondary fault strands along the segmented western 70 km of the ABF. Minimal development has left the geomorphic record of surface slip remarkably well preserved, and we have identified abundant evidence meter to km scale right-lateral displacement, including new Late Quaternary slip rate sites. We verified potential reconstructions at each site during summer 2015 fieldwork, and selected an initial group of three high potential slip rate sites for detailed mapping and geochronologic analyses. Offset landforms, including fluvial terrace risers, alluvial fans, and incised channel fill deposits, record displacements of ~5-80 m, and based on minimal soil development, none appear older than early Holocene. To quantitatively constrain landform ages, we collected surface and depth profile samples for ^{10}Be cosmogenic exposure dating. We also identified sites for new paleoseismic excavations, and documented evidence of the last two earthquakes, each of which produced ~2.5 m of surface displacement. We expect new Holocene slip rates for the Agua Blanca Fault to be forthcoming in fall of 2015.

Keywords: active tectonics, slip rate, Agua Blanca fault, San Andreas fault, lidar, cosmogenic dating

LCPHD-34

SETP
LCPHD

Zircon (U-Th)/He: Effects of Radiation Damage on 4He diffusion and Age

Adam Goldsmith
Goldsmith, A., The University of Texas at Austin Austin, TX
Stockli, D., The University of Texas at Austin Austin, TX
Ketcham, R., The University of Texas at Austin Austin, TX
Waffforn, S., The University of Texas at Austin Austin, TX

Interpretation of cooling ages from the increasingly popular zircon (U-Th)/He (or ZHe) thermochronometry is sometimes complicated by zircon having experienced high radiation doses, due to high U and Th concentrations and/or slow, protracted exhumation histories. Such highly damaged zircons record cooling ages which can vary over tens to hundreds of millions of years from a single rock, and yielding a negative correlation with effective U (eU = [U] + 0.23[Th]) concentration, here as a proxy for radiation damage. Although more rare, some researchers also observe positive age-eU correlations for low-eU, low-damage ZHe datasets. Inverse modeling is often used to interpret these data, however, an understanding of the dynamic diffusion kinetics of ^{4}He from zircon is critical to accuracy. This research seeks to better understand how the diffusivity of ^{4}He from zircon changes with the progressive destruction of the crystal lattice by radioactivity, with the end goal being improved inverse modeling of the thermal histories recorded by ZHe data with age-eU correlations. To address low-dose, positive age-eU correlations, we also present step-heated diffusion experiments from the Grasberg Igenous Complex, using three zircons from the Main Grasberg Intrusion (U-Pb age: ~3.2 Ma) and three from the Dalam Intrusion (U-Pb age: ~3.5 Ma). To address high-dose, negative age-eU correlations, we present ZHe ages and diffusion experiment results from the Sinai Peninsula of Egypt and the Hall Peninsula of Baffin Island, Canada, with complimentary measurements of crystallinity by Raman spectroscopy and U/Th zonation by laser ablation ICP-MS. The Hall Peninsula of Baffin Island is a slow-cooled Archaean craton (U-Pb ages: ~2.7 Ga) composed of assorted felsic igneous rocks; borehole samples of assorted igneous and metamorphic rocks from the Sinai Peninsula basement are younger but more eU-rich with an active but relatively well-constrained thermal history, whose ZHe ages cluster around known tectonic events. Both settings show distinct log-normal decreases in ZHe ages with increasing eU beyond clearly defined eU thresholds, with the maximum potential doses at these thresholds—$\leq 1 \times 10^{18}$ α-decays/g on the Hall Peninsula, and $\leq 5 \times 10^{17}$ on the Sinai Peninsula—being below the currently accepted threshold of changes in diffusivity of 2×10^{18} α-decays/g. Furthermore, step-heated ^{4}He diffusion experiments show Arrhenius diffusivity parameters, activation energy E_A, and the pre-exponential factor $ln(D_0/r^2)$, both increasing with increasing dose. These results are in direct contradiction with the current high-damage ZHe model, which decreases E_A with increasing dose while D_0 is held constant beyond the α-recoil damage percolation threshold of $\sim 3 \times 10^{16}$ α-decays/g. We interpret increasing $ln(D_0/r^2)$ with increasing dose as reflecting either decreases in effective diffusion domain size r, or increases in ionic porosity related to D_0; furthermore, increases in E_A with increasing damage is consistent with the apatite (U-Th)/He system, wherein damage zones function as helium 'traps'. Although the result of both approaches is a reduction in effective closure temperature (T_C) recorded by the ZHe system with increasing damage, these results will be the foundation of an improved model capable of more accurately extracting the thermal histories recorded by high-damage zircon.

Keywords: zircon, (U-Th)/He, thermochronometry

LCPHD-35

SETP
LCPHD

A New Approach to Date Serpentinites with Magnetite (U-Th)/He Thermochronology

Emily Hernandez Goldstein
Cooperdock, E., Department of Geological Sciences, The University of Texas at Austin
Stockli, D., Department of Geological Sciences, The University of Texas at Austin

Serpentinization is a widespread and fundamental process that occurs along plate boundaries during hydrous alteration of mantle rocks. The timing of serpentinization is critical for understanding the evolution of rheological strength of the mantle and chemical exchange between fluids and ultramafic rocks during tectonic processes, but direct dating of serpentinites has been challenging or impossible. We present the first application of magnetite (U-Th)/He thermochronology to date stages of alteration in ultramafic rocks. In order to prove the viability of magnetite He dating in these lithologies, magnetite ages were obtained from two ultramafic matrix lithologies of the Kampos melange belt, a high-pressure low-temperature subduction complex on the island of Syros, Greece. Magnetite (U-Th)/He measurements from internal fragments of large grains within a chlorite schist and a serpentinite schist record Mid-Miocene exhumation-related cooling ages, whereas smaller grains from the serpentinite schist record Pliocene magnetite growth. These results are evidence for multiple episodes of late-stage fluid alteration, which has implications for the cooling history and local geochemical exchanges of this HPLT terrane. This method provides a new tool that may be expanded to investigate the processes and timescales of serpentinization from a variety of tectonic settings.

Keywords: thermochronology, geochronology, serpentinites, magnetite

LCPHD-36

SETP
LCPHD

Rheological Heterogeneity Along the Deep Subduction Interface: Insights From Exhumed HP Metamorphic Rocks Exposed on Syros Island, Greece

Alissa Kotowski
Kotowski, A., The University of Texas at Austin, Austin, TX
Behr, W., The University of Texas at Austin, Austin, TX
Stockli, D., The University of Texas at Austin, Austin, TX
Ashley, K., The University of Texas at Austin, Austin, TX

The rheological properties of subduction interface shear zones control several aspects of subduction zone dynamics, including shear tractions along the plate interface, rates and amounts of exhumation, and depths and styles of seismicity. We document the rheological properties of a deep subduction interface using exhumed eclogite and blueschist facies rocks from Syros Island, Greece. These rocks were subducted to ~60 km depth during the Eocene, were exhumed part way along the top of the subducting slab, and were then ultimately exhumed to the surface beneath Miocene detachment faults. Localization of strain during exhumation allowed prograde fabrics to be preserved. The PT conditions (400-550C, 12-16kb) of these fabrics are comparable to conditions of episodic tremor and slow slip (ETS) observed in some modern subduction zones, including Cascadia. Two types of prograde fabrics were distinguished after analyzing macro-scale distributions of strain and microphysical mechanisms of creep in metamafic rocks. Type 1 fabrics contain eclogite pods boudinaged within a blueschist matrix. The eclogites show brittle deformation with cross-cutting veins containing abundant high pressure minerals. Deformation in matrix blueschists is accommodated by rigid rotation of amphibole and diffusion creep in plagioclase. Type 2 fabrics contain blueschists and eclogites that are isoclinally folded at similar wavelengths, thus are approximately isoviscous. Deformation is again accommodated by diffusion creep in blueschists, but by dislocation creep of omphacite in eclogites. We interpret these deformation types to reflect varying amounts of finite strain, but work is in progress to establish whether they also record different PT conditions. The transition from Type 1 to 2 fabrics represents a significant change in both bulk viscosity and seismic anisotropy, and may correspond to a transition from ETS-type behavior—a coupled seismic (brittle failure)-aseismic (ductile creep) phenomena—to fully ductile aseismic creep. Rheological heterogeneity appears to be an inherent feature of subduction terranes, involving changes in deformation mechanisms from subduction to exhumation and strain partitioning between lithologies in the subduction shear zone.

Keywords: subduction zone, rheology, blueschist, eclogite, seismicity

LCPHD-37

SETP
LCPHD

Extensional Evolution of the Lower Crust with Orogenic Inheritance: Observations from the Basin-and-Range and the Pyrenees

Rodrigo Lima
Lima, R., Institute for Geophysics, University of Texas at Austin, Austin, TX
Hayman, N., Institute for Geophysics, University of Texas at Austin, Austin, TX
Kelly, E., University of Texas at Austin, Austin, TX
Lavier, L., Institute for Geophysics, University of Texas at Austin, Austin, TX

Continental margins exhibit a range of widths and symmetries defined by the patterns of localization during extension and rifting. The formation of such crustal-scale zones of localized strain occurs early in rift evolution, and the rheology of the lower crust plays a large role in this localization. In particular, domains of low viscosity can control the bulk lower crustal strength relative to the upper crust and lithospheric mantle. Many rifted margins inherit earlier orogenic structures, fabrics, and metamorphic/igneous mineral assemblages, and even though these can predate the rift by 10' to 100's myr, there are hypothesized mechanical linkages between such inherited crustal fabrics and subsequent rift propagation. In the study I used microstructural observations coupled with phase equilibria modeling to further evaluate the role of preexisting orogenic fabrics in continental extension. Exposures of mid- to lower-crustal rocks were investigated in this study; the Funeral and Black Mountains of the Death Valley region, California, and from the Mauleon Basin of the Western Pyrenees. The Death Valley region sits within the Basin-and-Range region of broadly distributed Cenozoic extension, over a relatively flat and deep (~30-35 km) moho. In contrast, in the Mauleon basin Cretaceous extension was more localized in older Hercynian orogenic crust, which appears to have accommodated mantle exhumation early in the rifting evolution. In both areas, lower crustal rocks are characterized by inherited migmatitic fabrics overprinted by zones of localized, extensional-related fabrics consisting mineral assemblages that define an overall P-T cooling path. The high-temperature fabrics record decompression-melting following late- to post-orogenic collapse. Yet, these areas show contrasting retrograde assemblages and microstructures, inferred to reflect differences in melt segregation and loss at the km-scale, which affected lower crustal fertility and mechanical properties. At subsequent extensional stages, mid- to lower crustal deformation was controlled by high-strain zones consisting retrograde reaction products from the inherited (post-orogenic) fabrics. The transposition of the inherited fabrics associated to crustal thinning over a cooling path is documented with c-axis fabrics analysis in quartz; while in the Death Valley extensional fabrics are characterized by interconnected "weak" layers, the Mauleon rift-related deformation show minor fluid-assisted reactions and more high-T embrittlement. Therefore, weakening and strain localization during extensional stages is directly controlled by the preexisting, post-orogenic thermal evolution, compositional and fabric development.

Keywords: Extension, Rifting, Lower Crust, Rheology, Microstructural, Metamorphic Petrology

LCPHD-38

SETP
LCPHD

The Effect of Subducting Slabs in Global Shear Wave Tomography

Chang Lu
Lu, C., Department of Geological Sciences, The University of Texas at Austin, Austin, TX
Grand, S., Department of Geological Sciences, The University of Texas at Austin, Austin, TX

Subducting slabs represent strong short wavelength seismic anomalies in the upper mantle where much of Earth's seismicity is located. As such, they have the potential to bias longer wavelength seismic tomography models. To evaluate the effect of subducting slabs in global tomography, we performed a series of inversion tests using a global synthetic shear wave travel time dataset for a theoretical slab model based on predicted thermal anomalies within slabs. The spectral element method (SEM) was applied to predict the travel time anomalies produced by the 3D slab model for paths corresponding to our current data used in actual tomography models. Inversion tests have been conducted first using the raw travel time anomalies to check how well the slabs can be imaged in global tomography without the effect of mislocation. Our results indicate that most of the slabs can be identified in the inversion result but with smoothed and reduced amplitude. The recovery of the total mass anomaly in slab regions is about 84%. We then performed another inversion test to investigate the effect of mislocation caused by subducting slabs. We found that source mislocation significantly degrades the imaging of subducting slabs – potentially reducimg the recovery of mass anomalies in slab regions to only 39%. We tested two source relocation procedures – an iterative relocation inversion and joint relocation inversion. Both methods partially recover the true source locations and improve the inversion results, but the joint inversion method worked significantly better than the iterative method. In all of our inversion tests, the amplitude of artifact structures in the lower mantle caused by the incorrect imaging of slabs (up to ~0.5% S velocity anomalies) are comparable to large scale lower mantle heterogeneities seen in global tomography studies.

Keywords: Subducting Slabs, Global Tomography, Inverse Theory, Earthquake Mislocation

LCPHD-39

SETP
LCPHD

Numerical Modeling of Initial Slip and Poroelastic Effects of the 2012 Costa Rica Earthquake

Kimberly McCormack
McCormack, K., Department of Geosciences, The University of Texas At Austin, Austin,TX
Hesse, M., Department of Geosciences, The University of Texas At Austin, Austin,TX
Stadler, G., Courant Institute, New York University, New York, NY

Remote sensing and geodetic measurements are providing a new wealth of spatially distributed, time-series data that have the ability to improve our understanding of co-seismic rupture and post-seismic processes in subduction zones. We formulate a Bayesian inverse problem to infer the slip distribution on the plate interface using an elastic finite element model and GPS surface deformation measurements. We present an application to the co-seismic displacement during the 2012 earthquake on the Nicoya Peninsula in Costa Rica, which is uniquely positioned close to the Middle America Trench and directly over the seismogenic zone of the plate interface. The results of our inversion are then used as an initial condition in a coupled poroelastic forward model to investigate the role of poroelastic effects on post-seismic deformation and stress transfer. From this study we identify a horseshoe-shaped rupture area with a maximum slip of approximately 2.5 meters surrounding a locked patch that is likely to release stress in the future. We model the co-seismic pore pressure change as well as the pressure evolution and resulting deformation in the months after the earthquake. The results of the forward model indicate that earthquake-induced pore pressure changes dissipate quickly near the surface, resulting in relaxation of the surface in the seven to ten days following the earthquake. Near the subducting slab interface, pore pressure changes are an order of magnitude larger and may persist for many months after the earthquake.

Keywords: Poroelasticty, post-seismic deformation, Bayesian inversion

LCPHD-40

SETP
LCPHD

Kinematic Linkages Among Fold-thrust Belt Advance, Drainage Network Evolution, and Foreland Basin Development in the Zagros Fold-thrust Belt and Foreland Basin, Northern Iraq, Kurdistan

Renas Mohammed
Koshnaw, R., Department of Geological Sciences, The University of Texas at Austin, TX
Horton, B., Department of Geological Sciences and Institute for Geophysics, The University of Texas at Austin, TX
Stockli, D., Department of Geological Sciences, The University of Texas at Austin, TX
Barber, D., Department of Geological Sciences, The University of Texas at Austin, TX
Kendall, J., Department of Geosciences, The University of Arizona, AZ

The Zagros orogenic belt is the Middle Eastern segment of the Alpine-Himalayan system and is the most recent continental collision zone on Earth. However, due to diachronous and incremental deformation the precise ages and kinematics of shortening and deposition remain poorly understood. The Kurdistan region of the Zagros fold-thrust belt and foreland basin contains well-preserved Neogene wedge-top and foredeep deposits that include clastic units of Upper Fars, Lower Bakhtiari, and Upper Bakhtiari Fms. These preserved strata record variations in sandstone mineralogy, pebble clast type, bed thickness, bed geometry, and a major shift from distal fine-grained to proximal coarse-grained deposition. This research seeks to constrain the timing and geometry of shortening, exhumation, sedimentation, and mechanisms of foreland basin fill by addressing the following hypotheses: (1) deposits of smaller wedge-top basins and the broader foreland basin are (1A) genetically connected, showing comparable provenance signatures, depositional ages, and thermal history, or (1B) they formed as separate compartmentalized basins with different geologic histories; (2) foreland basin fill clastic sediments delivered by (2A) axial rivers carrying distal fine-grained sediments rather than (2B) proximal transverse rivers with coarse sediments from the adjacent thrust belt; (3) the Zagros orogenic wedge (3A) advanced steadily under critical to supercritical wedge conditions involving in-sequence thrusting or (3B) propagated intermittently under subcritical condition involving out-of-sequence deformation. To assess these hypotheses, we employed apatite (U-Th)/He thermochronometry, detrital zircon U-Pb geochronology, magnetostratigraphy and various basin analyses techniques. Stratigraphic measurements from the wedge-top and foredeep basins suggests development of depositional systems from meandering to anastomosing for Upper Fars Fm. and from braided to low sinuosity channel system for Lower Bakhtiari Fm. Magnetostratigraphic analysis from the wedge-top deposits of Dinarta and the foredeep deposits of Kifri constrained the depositional timing of Upper Fars Fm. and Lower Bakhtiari Fm. to 12.5 to 7.8 Ma and 7.8 to 5 Ma respectively. Provenance data form thin section petrography and detrital zircon U-Pb populations shows that the Upper Fars Fm. was sourced form Pan-African basement and Paleozoic strata (~600 Ma), Eastern Anatolian Accretionary Complex (~300 Ma), ophiolitic terranes (~100 Ma), and Walash-Naopurdan arc system (43-24 Ma), whereas the Lower and Upper Bakhtiari formations were derived solely from the Walash-Naopurdan arc system to the northeast of the study area. The U-Pb age spectra advocate a sharp shift from axial (Upper Fars Fm.) to transverse drainage (Lower and Upper Bakhtiari Fms.) and commencement of a topo-barrier and no unique age signature among the depozones. Apatite (U-Th)/He ages from the Zagros Main Thrust, the Mountain Front Flexure (MFF), and the frontal thrusts suggest rapid exhumation by ~10 Ma, ~5 Ma, and ~8 Ma respectively. Field observations and seismic sections indicate progressive limb rotation and development of growth strata within Lower Bakhtiari adjacent to the frontal thrusts and within Upper Bakhtiari nearby the MFF. These relationships indicate out-of-sequence deformation of MFF and intermittent hinterland uplift postdating initial collision. Ultimately, these findings suggest that upper-crustal shortening pattern is a major controller of the drainage network, in which determines the foreland basin fill stratigraphy.

Keywords: Zagros, fold thrust belt, foreland basin, Mountain Front Flexure, drainage, axial, transverse, thermochronology, provenance, detrital zircon

LCPHD-41

SETP
LCPHD

Miocene extensional development of the Harquahala Mountains core complex, west-central Arizona: Magnitude and rates of slip along the Eagle Eye Detachment

Michael Prior
Prior, M., Department of Geological Sciences, University of Texas at Austin, Austin, TX
Stockli, D., Department of Geological Sciences, University of Texas at Austin, Austin, TX
Singleton, J., Department of Geosciences, Colorado State University, Fort Collins, CO

Metamorphic core complexes (MCC) in the Colorado River extensional corridor (CREC) contain numerous exposures of low-angle normal faults (detachments) that exhumed mid-crustal mylonites. This study focuses on the Harquahala Mountains MCC, at the southern edge of the Whipple tilt domain, where extension was accommodated along the Eagle Eye detachment (EED). We present new geo-thermochronometry data on Miocene deformation in the Harquahala Mountains to determine timing, displacement magnitude, and slip rates along the EED. Zircon and apatite (U-Th)/He ages from 31 samples along a ~55 km extension-parallel transect (~N60E) display 3 distinct trends when plotted versus distance from the EED: 1) samples in the SW, furthest from the EED, show the oldest ZHe ages of ~50-40 Ma; 2) a middle segment where ZHe ages decrease from ~40 to 22 Ma over ~15 km; 3) a third segment of 22 ZHe ages ranging from ~22-16 Ma record rapid cooling during detachment slip. The second and third segments of ZHe ages are clearly separated by an inflection point ~34 km SW of the EED, recording a minimum displacement estimate and initial exhumation of deeply buried rocks at ~22-20 Ma. Linear regression of ZHe and AHe ages yields slip rates of 8.9 +5.5,-2.5 km/Myr and 4.7 +0.9, -0.7 k/Myr, respectively.A lithologic correlation has been proposed between distinct plutonic footwall rocks in the Little Harquahala Mountains (LHQ1) and preserved clasts (AR1) within Tertiary breccia (Tcb) exposed near Bullard Peak at the NE end of the Harcuvar Mountains (Reynolds and Spencer, 1985). Underlying ash-flow tuffs constrain the maximum age for Tcb suggesting active syn-extensional deposition by ~23 Ma. Identical U-Pb ages of 164.3 ± 1.4 (LHQ1) and 164.4 ± 1.1 Ma (AR1) and lithologic similarity between these units strongly support this correlation, indicating ~45 km of offset across the detachment system. Exhumation of the zircon partial retention zone in the breakaway zone requires ~8-12 km of displacement (for a 60-35° fault dip) in addition to the ~34 km derived from the spatial extent of reset ZHe ages, yielding ~45 km of total displacement. The EED displacement estimate shows clear agreement between lithologic and geo-thermochronometric offset constraints, thus providing a rare opportunity to fully resolve timing, rates, and total displacement magnitudes in the CREC.

Keywords: Eagle Eye detachment, slip rates, (U-Th)/He dating, metamorphic core complexes, Harquahala Mountains

LCPHD-42

SETP
LCPHD

(U-Th)/He and U-Pb double dating constraints on the interplay between thrust deformation and basin development, Sevier foreland basin, Utah

Edgardo Pujols
Stockli, D., The University of Texas at Austin, Austin, TX
Brian, H., The University of Texas at Austin, Austin, TX
Steel, R., The University of Texas at Austin, Austin, TX
Constenius, K., Independent researcher

The degree of connectivity between thrust-belt deformation and foreland basin evolution has been a matter of debate for decades. This is in part due to the lack of temporal constraints on the relationship between thrust-belt deformation and associated deposition. New high-resolution zircon (U-Th)-(Pb-He) double dating of pre- and syn-tectonic sedimentary strata along the Sevier thrust front and basin provide an unprecedented geochronological framework to temporally and spatially link the Sevier foreland basin stratigraphy to deforming hinterland sources. Results improve constraints on timing and magnitude of deformation, depositional ages, sediment dispersal and sources. In Late Cretaceous proximal deposits of the Indianola Group (IG) and Canyon Range Conglomerates (CRC), detrital zircon U-Pb (zUPb) and (U-Th)/He ages (ZHe) chronicle the sequential unroofing of the Charlestone-Nebo Salient (CNS) and Canyon Range (CR) duplexes. Furthermore, short ZHe depositional lag-times indicate rapid hinterland exhumation (>1km/my) associated with active thrusting during Cenomanian and Coniacian-Santonian times as supported by bedrock ZHe ages in the CNS and CR thrust sheets. Detrital zircon analyses on the Late Cretaceous Book Cliffs strata suggest a more complex source-to-sink evolution compared to the time-equivalent proximal basin strata due to mixing of multi-source detrital zircons, sediment recycling and more prominent volcanic input. Nonetheless, the overall cooling history recorded in the Book Cliffs clearly reflects three hinterland exhumational phases, an early phase derived from the frontal thrusts and two additional phases with more integrated hinterland ZHe signatures. These three short lag-time phases correlate with fast clastic progradational wedges in the Sevier foreland. These results strengthen the role played by hinterland deformation on clastic progradation and elucidate the temporal aspects between thrusting and foreland basin architecture.

Keywords: Foreland basin evolution, thrusting, (U-Th)/(He-Pb) double dating

LCPHD-43

SETP
LCPHD

The km-scale structure of the Cycladic Blueschist Unit on Syros Island, Greece

Spencer Seman
Seman, S., Department of Geological Sciences, The University of Texas at Austin, Austin, TX
Stockli, D., Department of Geological Sciences, The University of Texas at Austin, Austin, TX
Soukis, K., Geoscience Faculty, National and Kapodistrian University of Athens, Greece

At the km-scale, coherent high-pressure low-temperature metamorphic belts are viewed in two disparate manners: 1) As chaotic, mega-scale mélanges where the distribution of rock units does not correlate with timing of subduction or P-T conditions experienced. 2) As truly coherent terranes where the structural position of units reflects progressive subduction and underplating of portions of the down-going plate. These conflicting models exists due to our generally poor understanding of the large-scale structure of HP-LT metamorphic terranes. The pervasive retrograde metamorphism common in these settings, lack of unmetamorphosed equivalent rocks, as well as the absence of fossils to constrain depositional age all contribute to this problem. We employ detrital zircon geochronology to constrain the maximum depositional ages and provenance of metamorphosed sediments within the Cycladic Blueschist Unit (CBU) exposed on Syros Island, Greece. Triassic volcanic rocks are repeated at least three times in the ~12 km structural section of Syros. Maximum depositional ages for intervening metasediments range from Jurassic to Late Cretaceous and possess several distinct provenances. The repetition of Triassic rocks confirms Syros Island is composed of a series of imbricate thrust or nappe sheets as proposed by other workers. The shift in metasediment composition and provenance from structurally higher to lower units suggests progressive underplating of more distal to more proximal portions of a passive margin sedimentary sequence. We argue that the distribution of rock units on Syros Island is not chaotic, but reflects their original paleogeographic arrangement on the downgoing plate.

Keywords: blueschist, eclogite, detrital zircon, U-Pb, Cycladic Blueschist Unit, Greece

LCPHD-44

SETP
LCPHD

Duration of Ore Formation and Rate of Deep-seated Cooling in the Ertsberg-Grasberg Mining District, Papua, Indonesia

Stephanie Wafforn
Wafforn, S., Department of Geological Sciences, University of Texas at Austin, Austin, TX
Cloos, M., Department of Geological Sciences, University of Texas at Austin, Austin, TX
Stockli, D., Department of Geological Sciences, University of Texas at Austin, Austin, TX

Isotopic dating of intrusions and hydrothermal alteration from porphyry copper deposits worldwide is rarely able to constrain the duration of ore formation with a resolution better than one million years. Zircon U/Pb dating of intrusions that host and cross-cut ore grade mineralization at the supergiant Grasberg deposit, located in Papua, Indonesia, provides a constraint on the maximum duration of hydrothermal fluid flow. Porphyry copper-type mineralization is hosted in the Grasberg Igneous Complex (GIC), which comprises three pulses of magmatism: the Dalam Phase, the Main Grasberg Intrusion (MGI), and the Kali Dikes. Main phase copper mineralization initiated following intrusion of the MGI (3.21±0.04 Ma, n=102) and predates the Late Kali Dikes (3.09±0.05 Ma, n=88). These ages have been corrected for initial Th disequilibrium and common lead. Based on these ages the maximum time window for deposition of the Grasberg orebody is between 30 and 210 k.y. Cross-cutting relationships have also been identified in the Big Gossan skarn: an altered dike (3.04 ± 0.11 Ma, n=54) cuts high grade skarn mineralization. The age of the Big Gossan skarn is constrained by this contemporaneous dike. Furthermore, the age range of the Ertsberg pluton (3.09 to 2.83 Ma) constrains the timing of Ertsberg porphyry mineralization and the super-giant Ertsberg East Skarn system. These data indicate that each of the mineralizing centers in the Ertsberg-Grasberg district was spatially and temporally distinct.

Apatite and zircon (U-Th)/He (aHe and ZHe) ages provide additional insight into the low-temperature thermal history associated with ore formation. Samples were collected from a vertical profile in the Kali Dikes spanning 2 km. Near-surface samples cooled almost immediately following crystallization (3.1±0.2 Ma zHe age), whereas samples at 2 km depth cooled more slowly (2.1±0.3 Ma zHe age). Throughout the vertical profile aHe ages are less 0.9 m.y. younger than the than the zHe ages. Based on these ages the calculated cooling rate from 750-200°C was 30°C/10 k.y. near the surface, 10°C/10 k.y. at 1 km depth, and 4°C/k.y. at 2 km depth. The cooling rate from 200-110°C was 1-2°C/k.y. Collectively these results indicate Grasberg ore formation occurred immediately following MGI emplacement, was short-lived, and the system rapidly cooled. The high cooling rates to temperatures below 110°C at both surface and 2 km depth indicate the wall rock was cold and preclude the presence of a 2 km tall volcanic structure over the orebody. High cooling rates and steep thermal gradients along the edges of the stock would cause rapid deep-seated crystallization of quartz and feldspars. This led to the formation of copper-rich fluid bubbles in mobile magma that rose to collect beneath a cupola before ascending to form the Grasberg orebody

Keywords: Grasberg, Porphyry Copper Deposit, Ore Formation, Cooling Rate

LCPHD-45

SHP
LCPHD

Toe-of-Slope: Definition, Trajectory and Significance to Basin Margin Architecture

Rattanaporn Fong-Ngern
Fongngern, R., Department of Geological Sciences, The University of Texas at Austin, Austin, TX
Olariu, C., Department of Geological Sciences, The University of Texas at Austin, Austin, TX
Steel, R., Department of Geological Sciences, The University of Texas at Austin, Austin, TX

A toe-of-slope is a zone where the slope gradient becomes gentler toward the basin floor. This change in gradient triggers deceleration of sediment gravity flows and deposition of the transported sediment that bypasses or is removed from the updip locations. Thus besides the shelf edge, the toe-of-slope is critical to understanding depositional history and predicting sediment dispersal within margin-accreting sedimentary wedges. This research proposes 'Toe-of-Slope' trajectory analysis as a complimentary tool to the 'shelf-edge' trajectory, a method proven to be powerful in predicting an interplay between shelf-accommodation and sediment supply. 'Toe-of-Slope' trajectory can be classified based on the angle it makes with a horizontal, basinward pointing vector into three main classes; falling, rising, and back stepping. In turn, the trajectory angle is controlled by the amount of sediment deposited on the slope versus on the basin floor. In contrast to the shelf-edge trajectory, the 'Toe-of-Slope' trajectory is not affected by the shelf accommodation and thus this method allows focused investigation on sediment supply and deepwater processes and their controls. A working hypothesis "Toe-of-slope migration path reflects intrinsic controls of slope gradient, sediment supply and depositional processes on sediment accumulation on the slope and basin floor and thus changing in the trajectory classes, essentially associated with altering clinothem shape/geometry, implies temporal variation in sediment supply and depositional processes." is being test on the deep-lake Dacian clinoforms and published seismic transects from other basin margins of various tectonic settings. In addition to a history of sediment supply and depositional processes on the clinoforms, grain size and sediment gravity flow efficiency are expected to be anticipated by this type of analysis.

Keywords: Toe-of-slope, clinoforms, deepwater processes

LCPHD-46

SHP
LCPHD

Mass Loss Down Under: Distributed Subglacial Discharge Drives Significant Submarine Melt at a Tidewater Glacier

Mason Fried
Fried, M., Institute for Geophysics, The University of Texas, Austin, TX
Catania, G., Institute for Geophysics, The University of Texas, Austin, TX
Bartholomaus, T., Institute for Geophysics, The University of Texas, Austin, TX
Duncan, D., Institute for Geophysics, The University of Texas, Austin, TX
Davis, M., Institute for Geophysics, The University of Texas, Austin, TX
Stearns, L., Department of Geology, University of Kansas, Lawrence, KS
Nash, J., College of Earth, Ocean & Atmos. Sciences, Oregon State University, Corvalis, OR
Shroyer, E., College of Earth, Ocean & Atmos. Sciences, Oregon State University, Corvalis, OR
Sutherland, D., Department of Geological Sciences, University of Oregon, Eugene, OR

Submarine melt can account for substantial mass loss at tidewater glacier termini. However, the processes controlling submarine melt are poorly understood due to limited observations of submarine termini. Here, at a tidewater glacier in central West Greenland, we identify subglacial discharge outlets and infer submarine melt across the terminus using direct observations of the submarine terminus face. We find extensive melting associated with small discharge outlets. While the majority of discharge is routed to a single, large channel, outlets not fed by large tributaries drive submarine melt rates in excess of 3.0 m d-1 and account for 85% of total estimated melt across the terminus. This pattern suggests distributed subglacial discharge drives significant submarine melt. Nearly the entire terminus is undercut due to submarine melt, which may intersect surface crevasses and promote calving. Severe undercutting constricts buoyant outflow plumes and may amplify melt. The observed morphology and melt distribution motivate more realistic treatments of terminus shape and subglacial discharge in submarine melt models.

Keywords: glaciology, glacier hydrology, mass loss

SHP
LCPHD

A Numerical Model of Armor Development in Flash Flood-Dominated Channels: Sensitivity to Sediment Supply, Hydrograph Shape, and Base Flow

Kealie Goodwin
Goodwin, K., University of Texas at Austin, Austin, TX
Johnson, J., University of Texas at Austin, Austin, TX
Viparelli, E., University of South Carolina, Columbia

Most gravel-transporting rivers with perennial base flow are armored, with bed surface grain size distributions that are coarser than the subsurface. In contrast, ephemerally flowing rivers, which are commonly flash flood-dominated, are typically unarmored. Both high sediment supply and elevated shear stresses have been identified as processes that may prevent armor development. We use a two-dimensional morphodynamic model that conserves mass and momentum, and tracks grain size distributions of bedload, surface, and subsurface stratigraphy independently. Model inputs include hydrograph, initial condition grain size distributions, bed slope, and input sediment supply. Using the model, we explored the parameter space of armor ratio (Surface D50 / Subsurface D50) varying sediment supply, flood peak magnitude, flood duration, and base flow magnitude, including ephemeral hydrographs with no base flow. The base case sediment supply, grain size distribution, and hydrograph is chosen based on the Nahal Yatir, an ephemerally flowing river in the Negev Desert. Sensitivity analysis was conducted to quantitatively rank the importance of each input parameter. We found that armor ratio was the most sensitive to changes in base flow magnitude. In perennially flowing rivers, base flows can preferentially transport smaller grain sizes. In ephemerally flowing rivers, the modeling suggests that a large percentage of flow occurs above the threshold of motion for all grain sizes, transporting all grain sizes nearly equally, resulting in minimal armor development. We find that sediment supply rate and hydrograph shape have measurable but smaller influences on armoring.

Keywords: Sediment Transport, Flash Floods, Numerical Models, Geomorphology

LCPHD-48

SHP
LCPHD

Large-Scale Inflections in Slope Angle Below the Shelf Break: A First Order Control on the Stratigraphic Architecture of Carbonate Slopes; Delaware Basin

Gregory Hurd
Hurd, G., The University of Texas at Austin, Austin, TX
Kerans, C., The University of Texas at Austin, Austin, TX
Janson, X., Bureau of Economic Geology, The University of Texas at Austin, Austin, TX
Fullmer, S., ExxonMobil Upstream Research Company, Spring, TX
Frost, N., Matador Resources, Dallas, TX

A large-scale inflection (LSI) in the slope profile may develop as a carbonate platform is drowned and abandoned basinward of the active shelf break. The impact of LSIs on the sediment dispersal patterns and stratigraphic architecture of carbonate slopes remains understudied.

Outcrops of the Early-Middle Permian Cutoff Formation in the Guadalupe Mountains National Park provide an oblique-dip view of a mixed carbonate and siliciclastic slope system modified by an LSI during a 2-4 m.y. composite sequence (Permian Composite Sequence, PCS9). Processes of channelization, bypass, and slope failure associated with the LSI contributed to the development of basin-restricted carbonate, shale, and sandstone strata which demonstrate apparent onlap to the relic platform. Correlation of high frequency sequences between the slope and shelf-equivalent strata demonstrates that channels incising the relic platform LSI served as conduits for confined gravity flows and depocenters for organic-rich shale throughout the transgression and much of the ensuing highstand of PCS9. In the latest highstand regression, an increase in the production of carbonate mud by the active shelf system contributed to the complete filling of channels across the LSI and accumulation of carbonate mud-dominated mass-transport deposits basinward of the LSI.

One-dimensional gamma ray profiles collected on the outcrop and an extensive subsurface dataset allow for detailed mapping of the LSI-modified slope system across the northern margin of the Delaware Basin. Well log correlations reveal that the gradient of the slope profile basinward of the LSI is comparatively steeper on the northeast side of the basin compared to the northwest side. The dip-parallel distance of the active shelf margin is also about 20 km closer to the LSI in the northeast compared to the northwest. Shale-rich strata associated with the transgressive stage of PCS9 thin updip gradually along the shallow profile and abruptly along the steep profile. Interbedded carbonates and shales associated with the early highstand stage of PCS9 transition from linear to strike-elongate geometries at the base of the shallow slope and exhibit only strike elongate, apron geometries at the base of the steep slope. Carbonate strata deposited during the latest highstand stage represent a thin, isopachous sheet-like deposit across the shallow slope and a thick, strike-elongate apron at the base of the steep slope.

A critical review of previous studies reveals that LSIs are common in the geologic record, across multiple basins and time periods. LSIs that developed due to drowning of carbonate platforms demonstrate dimensions and stratal patterns comparable to the relic Leonardian platform. LSI development in the identified examples occurred in association with 1) the transgressive stages of 10 – 100 m.y. (2^{nd} order) sequences, 2) ocean anoxic events, or 3) times of concomitant sea level rise and ocean anoxic events

Keywords: Carbonate Slope, Permian, Delaware Basin, Sediment gravity flow deposits

LCPHD-49

SHP
LCPHD

The Dynamic Response of Hyporheic Redox Zonation After Surface Flow Perturbation

Matthew Kaufman
Kaufman, M., Department of Geological Scienes, The University of Texas at Austin, Austin, TX
Zheng, L., Department of Geological Scienes, The University of Texas at Austin, Austin, TX
Cardenas, M., Department of Geological Scienes, The University of Texas at Austin, Austin, TX

As water in a stream or river flows over ripples and other bedforms, differential surface pressures create bedform-induced hyporheic exchange. The oxygen, carbon, and nutrients carried into the bed by the surface water as well as those already existing in the bed material form the basis for microbial communities in the sediment.The resulting dissolved oxygen conditions are a critical control on the ecological function of the hyporheic zone (HZ), from both micro- and macro-biological habitat perspectives. Because hyporheic exchange rates are controlled by surface flow velocity, variations in surface flow have significant impact on the subsurface oxygen conditions. Most rivers are subject to flow velocity variations due to natural forcing including precipitation and variations in evapotranspiration as well as anthropogenic forces like dam releases. We use a large (10m x 0.7m x 0.3m) programmable flume instrumented with a bedform-scale high-resolution planar optode dissolved oxygen imaging system to observe the distribution of oxygenated sediment within the HZ over time. Using this system we characterize the rate at which hyporheic oxygen conditions reconfigure in response to changes in the surface flow velocity, particularly the time it takes for conditions to recover after a pulse of increased flow velocity. In addition, we make use of numerical models to further identify critical response time drivers. With these tools, we develop equations to describe the post-disturbance recovery time as a function of relative pulse magnitude and duration. Using these equations we can predict the time scale over which the hyporheic zone will recover following both natural and anthropogenic flow regime disturbances. Being able to predict the magnitude and duration of dissolved oxygen changes in the wake of flow perturbing events allows us to better understand the impact these disturbances have on the ecology of the hyporheic zone.

Keywords: hydrology, hyporheic zone, redox, biogeochemistry

LCPHD-50

SHP
LCPHD

Spatio-temporal variation in bed-material load using dune topography collected during a severe flood on the coastal Trinity River, east TX, USA

Jasmine Mason
Mohrig, D., UT Austin

A series of 5 repeat surveys along 27 river kilometers of the coastal Trinity River in east Texas, USA, reveal the temporal and spatial changes in bed material during and following a historically large flood. The river event was above the NWS flood stage for 55 days at the Liberty USGS station, and had a maximum discharge of about 80,000 cfs. As a community, we are beginning to understand how fluvial geomorphology is influenced by backwater hydraulics, but we still lack an understanding of how the bed-material transport adjusts to accommodate larger-scale changes in river bend pattern and kinematics. Survey data from this project includes sidescan sonar along the channel centerline, multibeam bathymetry, and channel bed sediment samples. In combination, this data set provides new insight into how and when bed material, primarily medium sand with some pebbles, moves through this region, and how this connects to previously observed changes in channel geometry (including downstream decreases in channel width to depth ratio, bar form volume and surface area, and lateral migration rates of river bends). Preliminary results show groups of similarly-sized bedforms advecting downstream together, an observation that has never before been made for large scale field studies. Maximum bedform height correlates well with river discharge. Grain size data collected during the low flow survey shows a decrease in the maximum grain size with distance downstream, likely due to spatial decelerations associated with the backwater effect. This presentation will discuss these results with respect to backwater dynamics and sediment supply and transport and will have implications for coastal geomorphology as well as sediment delivery into deltaic systems.

Keywords: bedforms, sediment transport, geomorphology, backwater

LCPHD-51

SHP
LCPHD

Controls on Arctic groundwater flow and its impacts on carbon processing

Michael O'connor
O'Connor, M., Department of Geological Sciences, The University of Texas at Austin, Austin, TX
Cardenas, M., Department of Geological Sciences, The University of Texas at Austin, Austin, TX
Neilson, B., Utah Water Research Lab, Department of Civil and Environmental Engineering, Utah State University, Logan, UT
Kling, G., Department of Ecology and Evolutionary Biology, University of Michigan, Ann Arbor, MI

Vast reservoirs of organic matter become accessible each summer when Arctic soils thaw. Groundwater transports this organic matter into streams, where it can be respired into CO2. However, we know little about how groundwater moves through the shallow and temporary aquifer exposed by thawing soils. Further understanding of these flowpaths is required to accurately understand the Arctic terrestrial carbon budget.Here we present findings from field data and numerical groundwater flow models that help discern where and how flowpaths develop in the Arctic shallow subsurface. We monitored temperature, specific conductance, soil hydraulic conductivity, and thaw during Summer 2015. This was a low precipitation year and thus allowed us to observe hillslope groundwater dynamics without the added input of precipitation. Radon observations highlight a unique groundwater signature within the hillslope and flow path connections between the hillslope and stream. Head and thaw observations show that groundwater flow paths mimic land surface topography on the hillslope scale, yet often depart from surface topography, following ice topography instead, at a finer scale. Hydraulic conductivity decreases with depth, but appears to be uniform laterally. Time-series and spatial snapshots of specific conductance suggest that it could be a useful tracer of preferential flowpaths within this shallow aquifer system.These data will be critical for the further development of flow models that accurately represent aquifer properties, preferential flowpaths, and residence times in this and other Arctic watersheds. With an accurate understanding of water movement, we will be better able to understand the constituent profile that is advected and the reactions that occur during that process. This allows us to mechanistically understand the role of Arctic hillslopes as the primary suppliers of DOM to streams.

Keywords: carbon, permafrost, arctic, groundwater

LCPHD-52

SHP
LCPHD

The Effect of Tides on Deltaic Morphology and Stratigraphy in River-Dominated Conditions

Valentina Rossi
Rossi, V., Department of Geological Sciences, The University of Texas at Austin
Kim, W., Department of Geological Sciences, The University of Texas at Austin
Hiatt, M., Department of Civil, Architectural and Environmental Engineering and Center for Research in Water Resources, The University of Texas at Austin
Passalacqua, P., Department of Civil, Architectural and Environmental Engineering and Center for Research in Water Resources, The University of Texas at Austin
Edmonds, D., Department of Geological Sciences and Center for Geospatial Data Analysis, Indiana University
Leva-Lopez, J., Department of Earth and Space Sciences, Lamar university
Geleynse, N., Water and Environment Division, ARCADIS
Olariu, C., Department of Geological Sciences, The University of Texas at Austin
Steel, R., Department of Geological Sciences, The University of Texas at Austin

Deltas are dynamic and sensitive systems that undergo changes of morphology, channel network, and stratigraphic architecture in response to variations in coastal processes, e.g., waves and tides. These changes need to be properly understood in order to make reliable subsurface predictions.
Numerical modeling has been extensively used to study delta evolution in response to a single dominant coastal forcing, but rarely to examine the sensitivity of delta to mixed energy forcing. Therefore predictions on reservoir modeling based on conventional models could be highly misleading when used in mixed-energy delta systems. This study uses Delft3D to investigate the influence of tidal currents on river-dominated deltas in terms of deltaic stratigraphic architecture and sediment partitioning. We conducted 24 modeling runs with a range of tidal amplitude and initial sediment composition of the substrate.
The modeling results show that deltas formed under river-dominated condition without tidal currents (control runs) develop delta foresets with concave profiles, whereas with increasing tidal amplitude the delta foreset profiles become more convex or have compound geometries. In the control runs, distributary channels avulse and bifurcate frequently, resulting in the complete reworking of deltaic lobes. As a result, coarse sediment is stored in the proximal delta plain. In contrast, the presence of strong tidal currents creates deeper and stable distributary channels. These channels do not rework previously deposited deltaic lobes, but act as an efficient conduit for ebb-current sediment to bypass across the delta. Furthermore, the analysis of sediment fluxes across the delta shows that ebb tidal currents increase suspended and bedload sediment fluxes by at least 3 times compared to cases without tidal currents. The enhanced sediment transport leads to deposits with higher net-to-gross ratios than in their river-dominated counterparts.
This study highlights how tidal currents, even under river-dominated conditions, have strong effects on delta surface morphology, stratigraphic architecture, and sediment partitioning. Therefore it is critical when trying to model paralic reservoirs to consider the changes that varying tidal influence may have in reservoir geometry, net-to-gross distribution, and flow path barriers.

Keywords: Tides, River-dominated deltas, Delft3D

CCG
U

Obliquity (41kyr) paced SE Asian Monsoon variability following the MCT

Emma Heitmann
Heitmann, E., Jackson School of Geosciences, The University of Texas at Austin, Austin, Tx
Ji, S., Lanzhou University, Lanzhou, Gansu, China
Breecker, D., Jackson School of Geosciences, The University of Texas at Austin, Austin, Tx
Nie, J., Lanzhou University, Lanzhou, Gansu, China

Middle Miocene climate had boundary conditions similar to those predicted for Earth's future including substantial Antarctic ice cover but no northern hemisphere ice sheets. Pleistocene Asian monsoon variability is well-studied, yet there is a need to study Miocene monsoon variability as it is likely a good analog for future climate. High-resolution chemical analysis and stratigraphic observation of the Yanwan Section in the Tianshui Basin, China, was conducted to interpret climatic changes in central Asia following the Miocene Climate Transition (MCT; ~13.9-12.9Ma). Pedogenic carbonates and occluded organic matter were analyzed for stable carbon and oxygen isotopes. We describe in detail a 12m subsection of the Yanwan Section near Sun Jia. It consists of CaCO3 horizons (Munsell color 7.5YR 6.5/4) with root-pore cements and clay nodules, inter-bedded at ~1m intervals with siltstones (7.5YR 5.5/6 or 5YR 4.5/6) with well-preserved roots, clay films, and variable abundances of 0.1–2cm diameter CaCO3 nodules. Roots extend ~10-40cm in the sediment and found in well-cemented horizons filled in with silt material. This occurs in environments with seasonal wetting and drying where the root is cemented in CaCO3, dies, and is filled in with matrix. Well-cemented horizons are typical of late-stage carbonate accumulation that occurs during slow sedimentation rates. Pedogenesis has destroyed primary sedimentary structures so depositional environment is difficult to interpret. From previously determined sedimentation rates it is concluded that the observed cycles are obliquity-paced (41kyr). Accumulation rate controls the cycles, which would likely be controlled by the winter monsoon (aeolian) or summer monsoon (fluvial). ?13C and ?18O values of carbonate nodules become lighter from the bottom of a well-cemented horizon to the top of the overlying siltstone horizon, indicating climatic change. Obliquity–paced (41kyr) monsoon variability is likely controlled by the meridional temperature gradient.

Keywords: Miocene, Asian Monsoon, Paleoclimate, Astronomical Cycles

EG
U

PETROGRAPHIC AND ISOTOPIC EVIDENCE FOR MICROBIAL INFLUENCE IN THE ORIGIN OF THE BOLING SALT DOME CALCITE CAP ROCK, HOUSTON DIAPIR PROVINCE, TEXAS

John Hill
Hill, J., Jackson School of Geosciences, University of Texas at Austin, Austin, TX
Kyle, J., Jackson School of Geosciences, University of Texas at Austin, Austin, TX
Caesar, K., Department of Geological Science, California State University at Fullerton, Fullerton, California
Loyd, S., Department of Geological Science, California State University at Fullerton, Fullerton, California

Boling dome is a large Gulf of Mexico Basin onshore salt structure developed from the Mid-Jurassic Louann Salt. The Boling dome cap rock hosts one of the world's largest native sulfur concentrations with more than 80 million tonnes of production. Extensive cap rock drilling provides subsurface data and samples to systematically investigate the cap rock nature and origin. Conventional and cathodoluminescent petrography of Boling cap rock cores reveals a complex history of calcite paragenesis. The dome has a complex upper calcite cap rock zone that grades into an underlying anhydrite zone that rests on and is residual from the salt diapir. The upper cap rock is dominated by gray fine-crystalline calcite with irregular segregations and complex veins of pale to amber coarse-crystalline calcite. Native sulfur, and locally sulfides, is associated with veins and late-stage pores commonly filled with scalenohedral pale calcite. Historic and new cap rock calcite ?13C data are isotopically depleted with a large range of values from –3 to –32‰, reflecting a mixture of various carbon sources potentially including a substantial methane component. These depleted carbon isotope compositions and the presence of abundant sulfur minerals have led to interpretations that invoke microbial sulfate reduction as an important calcite cap rock process. Sulfur isotope analysis of carbonate-associated sulfate (CAS) provides a means to directly identify sulfate reduction. Reconnaissance CAS analyses yield ?34SCAS values to 42‰, significantly higher than mother salt sulfates (?34S ~ 20‰), suggesting cap rock carbonate formation via microbial sulfate reduction under closed-system conditions. The most depleted carbonate ?13C values combined with the enriched ?34SCAS values may reflect sulfate-dependent anaerobic oxidation of methane, particularly for the early generation gray calcites. Fluid inclusions in early coarse-crystalline calcite commonly have positive melting temperatures, suggesting the presence of methane within low-salinity inclusion fluids; later calcite veins contain high-salinity brines with local oil inclusions. These data collectively suggest that a prolonged history of fluid and microbial processes produced the current calcite cap rock and its sulfur concentrations.

Keywords: Microbes, Hydrocarbons, Sulfur

MG
U

The Evolution of the Surveyor Fan and Channel System, Gulf of Alaska Based on Core-Log-Seismic Integration at IODP Site U1417

Susannah Morey
Morey, S., Jackson School of Geosciences, The University of Texas at Austin, Austin, TX
Gulick, S., Jackson School of Geosciences, The University of Texas at Austin, Austin, TX
Walton, M., Institute for Geophysics, The University of Texas at Austin, Austin, TX
Swartz, J., Institute for Geophysics, The University of Texas at Austin, Austin, TX

The transition to quasi-periodic ~100-kyr glacial cycles during the mid-Pleistocene transition (MPT, 0.7-1.2 Ma) saw an acceleration of sediment delivery from the St. Elias orogen. Eroded sediment from the St. Elias Mountains is transferred to the deep sea via glacially carved shelf troughs and eventually to the Aleutian Trench via the Surveyor Channel and Fan system. By analyzing the submarine sediments in this Fan, we can evaluate the source-to-sink relationship between the erosion of an orogen and deep-sea deposition and inform our understanding of the impact of climate on local tectonics. Our work seeks to update depositional models of the unique sedimentary sequences, architecture, and origins of the glacially-fed Surveyor Fan using core-log-seismic integration and new data from Integrated Ocean Drilling Program (IODP) Expedition 341. We specifically look at site U1417, the most distal borehole location from Expedition 341. An integrated velocity model allowed us to perform an integrated analysis of seismic facies, log data (gamma ray and density), and lithologic units. This analysis revealed that the initiation of the Surveyor Fan exists as the Sequence I/II boundary (~300 mbsf) at this site and this boundary corresponds with the intensification of northern hemisphere glaciation at ~2.8 Ma. The Surveyor Channel then reaches this distal location not long after. Channel deposits rest just above a unit of ice-rafted debris at ~260 mbsf. These deposits indicate a transition from wide aggradational channel deposits into narrow erosional channel deposits at the Sequence II/III boundary (~160 mbsf), which is at ~1.3 Ma—just before the beginning of the MPT. Integration with provenance studies can address potential changes in orogen response to deformation and erosion patterns and changes in fan evolution to changing sediment flux.

Keywords: Alaska, Surveyor Fan, Surveyor Channel, Gulf of Alaska, core, log, seismic, integration, IODP, mid-Pleistocene transition, deep sea, Expedition 341

SETP
U

Holocene geologic slip rate for Mission Creek strand of the southern San Andreas Fault

Rosemarie Fryer
Fryer, R., The University of Texas at Austin, Austin, TX
Behr, W., The University of Texas at Austin, Austin, TX
Sharp, W., BGC Berkeley Geochronology Center, Berkeley, CA
Gold, P., The University of Texas at Austin, Austin, TX

The San Andreas Fault (SAF) is the primary structure accommodating motion between the Pacific and North American plates. The Coachella Valley segment of the southern SAF has not ruptured historically, and is considered overdue for an earthquake because it has exceeded its average recurrence interval. In the northwestern Coachella Valley, this fault splits into three additional fault strands: the Mission Creek strand, which strikes northwest in the San Bernardino Mountains, and the Banning and Garnet Hill strands, which continue west, transferring slip into San Gorgonio Pass. Determining how slip is partitioned between these faults is critical for southern California seismic hazard models. Recent work near the southern end of the Mission Creek strand at Biskra Palms yielded a slip rate of ~14- 17 mm/yr since 50 ka, and new measurements from Pushawalla Canyon suggest a possible rate of ~20 mm/yr since 2.5 ka and 70 ka. Slip appears to transfer away from the Mission Creek strand and to the Banning and Garnet Hill strands within the Indio Hills, but the slip rate for the Garnet Hill strand is unknown and the 4-5 mm/yr slip rate for the Banning strand is applicable only since the mid Holocene. Additional constraints on the Holocene slip rate for the Mission Creek strand are critical for resolving the total slip rate for the southern SAF, and also for comparing slip rates on all three fault strands in the northern Coachella Valley over similar time scales. We have identified a new slip rate site at the southern end of the Mission Creek strand between Pushawalla and Biskra Palms. At this site, (the Three Palms Site), three alluvial fans sourced from three distinct catchments have been displaced approximately 80 meters by the Mission Creek Strand. Initial observations from an exploratory pit excavated into the central fan show soil development consistent with Holocene fan deposition and no evidence of soil profile disruption. To more precisely constrain the minimum depositional timing of the most well-defined alluvial fan, we are currently processing samples for U-series analysis of pedogenic carbonate. We expect this to result in a maximum bound of the Holocene slip rate on the Mission Creek Strand. Future Be-10 exposure age measurements from surface cobbles will independently constrain fan age yielding a complementary Holocene slip rate.

Keywords: Mission Creek, San Andreas Fault, Slip rate

U-5

SETP
U

Sediment dispersal during rift to drift transition in the central North Atlantic – Insights from U-Pb-He provenance data from the Lusitania Basin, Portugal

Dylan Hart
Hart, D., Dept. of Geological Sciences, University of Texas at Austin
Stockli, D., Dept. of Geological Sciences, University of Texas at Austin
Odlum, M., Dept. of Geological Sciences, University of Texas at Austin
Thomson, K., Dept. of Geological Sciences, University of Texas at Austin
Fildani, A., Statoil RDI, Austin, Texas
Moscardelli, L., Statoil RDI, Austin, Texas

The Iberian Atlantic continental margin, together with the Newfoundland conjugate margin, forms one of the prototypical magma-poor continental margins. Triassic extension formed widespread continental half-grabens during diffuse continental extension, resulting in deposition of red beds and evaporites. In contrast to Nova Scotia/Morocco, Triassic extension did not lead to Early Jurassic continental break-up and seafloor spreading. Renewed Late Jurassic continental rifting along the Newfoundland-Iberia margin ultimately led to necking, subcontinental mantle exhumation, and development of a hyperextended margin and culminating in early Cretaceous seafloor spreading. The sedimentary record of Triassic and Jurassic to Cretaceous continental extension is accessible in the Lusitania Basin of central Portugal. The Lusitania Basin exposes the record of the protracted history of Atlantic rifting related to opening of the central Atlantic (Nova Scotia-Morocco), renewed continental extension in the Late Jurassic, and break-up in the Early Cretaceous in response to Grand Banks-Iberia separation. The western margin of the Lusitania basin, spectacularly exposed along the Atlantic coast of Portugal, allows access to the stratigraphic succession related to post-Triassic thermal sag, Late Jurassic rifting, and Cretaceous break-up. For this study, a siliciclastic succession between the S. Martinho do Porto and Nazaré that spans Kimmeridgian rifting to Albian-Cenomanian break-up was measured and sampled for zircon U-Pb and (U-Th)/He provenance analysis. Paleocurrent data clearly show that the sediments were sourced to the west (not Iberia). Hence, fundamental questions remain regarding paleogeography, sediment dispersal, source-to-sink dynamics prior and during Grand Banks-Iberia separation. What is the provenance of Jurassic to Cretaceous sandstones? Were they sourced from local footwall blocks or from much farther west (Canada)? When did a super-regional drainage network get disrupted and result in isolated and locally sourced rift basins during asymmetric and diachronous rifting and breakup in the central North Atlantic? These are fundamental questions relevant to both the better understanding of the multi-stage tectonic evolution of the Newfoundland-Grand Banks-Iberia magma-poor rift system as well as the prediction of Jurassic-Cretaceous reservoir distribution and quality in petroliferous rift basins of the central North Atlantic.

Keywords: Structural geology, sedimentary geology, geochronology, U-Pb, Uranium-lead, (U-Th)/He, conjugate margins, rift basins, sediment dispersal, Iberia, provenance, Portugal, Lusistanian basin,

SETP
U

Petrogenesis of Cycladic Serpentinites: Understanding the Tectonic History Preserved in Metamorphic Rocks in Syros, Greece

Natalie Raia
Raia, N., Department of Geological Sciences, The University of Texas at Austin, Austin, TX
Cooperdock, E., Department of Geological Sciences, The University of Texas at Austin, Austin, TX
Barnes, J., Department of Geological Sciences, The University of Texas at Austin, Austin, TX
Stockli, D., Department of Geological Sciences, The University of Texas at Austin, Austin, TX

The Cycladic archipelago of Greece represents a metamorphosed subduction complex that has been exhumed by a combination of syn-orogenic (e.g. extrusion wedge) and extensional mechanisms (e.g. detachment faulting). The best preserved high-pressure unit in the Cyclades is the Cycladic Blueschist Unit (CBU) in Syros, Greece, which includes metamorphosed remnants of subducted oceanic crust in close association with serpentinized ultramafic rocks. We present preliminary bulk trace element and stable isotope data from the island of Syros in order to determine the protolith origin and tectonic setting of serpentinization in this high-pressure fossil subduction zone. All samples are completely serpentinized, variably deformed, and no relict grains are observed. The dominant mineral assemblage for all samples consists of serpentine, talc, and carbonate. Bulk rock serpentinite samples have high REE concentrations, compared to typical mid-ocean ridge serpentinites, as well as relatively flat REE patterns (La_N/Sm_N = 0.1-5.1; La_N/Yb_N = 0.1-3.2; Sm_N/Yb_N = 0.5-1.4; N = C1-chondrite normalized). These high REE concentrations are consistent with small degrees of melt depletion expected for abyssal peridotites, compared to fore-arc mantle peridotites. The REE patterns are similar to serpentinites from passive margin settings (e.g. Galicia Margin and areas of the Eastern Alps). In addition, bulk trace element concentrations are also high when compared to typical mid-ocean ridge serpentinites, supporting a passive margin setting. δD and δO values of bulk rock serpentinite powders and chips, respectively, reflect typical seafloor serpentinites hydrated by seawater at low T. Based on bulk rock geochemistry, serpentinites located in the Greek Cyclades exhibit geochemical characteristics of serpentinites from passive rifted margins.

Keywords: Syros, serpentinites, geochemistry, stable isotopes

SETP
U

Testing Mechanisms and Scales of Equilibrium Using Textural and Compositional Analysis of Porphyroblasts in Rocks with Heterogeneous Garnet Distributions

Rachel Ruthven
Ruthven, R., Jackson School of Geosciences, The University of Texas at Austin, Austin, TX
Ketcham, R., Jackson School of Geosciences, The University of Texas at Austin, Austin, TX
Kelly, E., Jackson School of Geosciences, The University of Texas at Austin, Austin, TX

Three-dimensional textural analysis of garnet porphyroblasts and electron microprobe analyses can, in concert, be used to pose novel tests that challenge and ultimately increase our understanding of metamorphic crystallization mechanisms. Statistical analysis of high-resolution X-ray computed tomography (CT) data of garnet porphyroblasts tells us the degree of ordering or randomness of garnets, which can be used to distinguish the rate-limiting factors behind their nucleation and growth. Electron microprobe data for cores, rims, and core-to-rim traverses are used as proxies to ascertain porphyroblast nucleation and growth rates, and the evolution of sample composition during crystallization. MnO concentrations in garnet cores serve as a proxy for the relative timing of nucleation, and rim concentrations test the hypothesis that MnO is in equilibrium sample-wide during the final stages of crystallization, and that concentrations have not been greatly altered by intracrystalline diffusion. Crystal size distributions combined with compositional data can be used to quantify the evolution of nucleation rates and sample composition during crystallization.This study focuses on quartzite schists from the Picuris Mountains with heterogeneous garnet distributions consisting of dense and sparse layers. 3D data shows that the sparse layers have smaller, less euhedral garnets, and petrographic observations show that sparse layers have more quartz and less mica than dense layers. Previous studies on rocks with homogeneously distributed garnet have shown that crystallization rates are diffusion-controlled, meaning that they are limited by diffusion of nutrients to growth and nucleation sites. This research extends this analysis to heterogeneous rocks to determine nucleation and growth rates, and test the assumption of rock-wide equilibrium for some major elements, among a set of compositionally distinct domains evolving in mm- to cm-scale proximity under identical P-T conditions.

Keywords: Garnet, Porphyroblast, Electron Probe Micro-Analysis, X-ray Tomography, crystallization mechanisms

SHP
U

Using Detrital Zircon U-Pb Geochronology to Quantify the Disrupted Flow of Sediment Down the Colorado River by Texas Hill Country Dams

Laura Dafov
Dafov, L., Jackson School of Geosciences, University of Texas at Austin, Austin, TX
Mohrig, D., Jackson School of Geosciences, University of Texas at Austin, Austin, TX
Stockli, D., Jackson School of Geosciences, University of Texas at Austin, Austin, TX

The Colorado River in Texas is home to 6 dams. Upstream from Austin, Texas, in the Texas Hill Country, the Colorado River has 6 lakes formed by the 6 aforementioned dams. The Pedernales River and the Llano River merge into the Colorado River in the interval of interest which contains the 6 dams. Within the interval, the Colorado River is characterized as a meandering river, but lacks any point bars and is saturated by residential industrialization along the riverbanks. Downstream from Austin, in the flatlands of Texas, the Colorado River is characterized as a single meandering channel with no additional input from other rivers that, on the other hand, exhibits an abundant number of significant sandy point bars.
Dams trap sediment upstream, but how is this affecting sedimentation downstream? As observed in this river, dams may not hinder sedimentation downstream, because clearly there is significant sedimentation in the form of point bars downstream from the Colorado River dams. Here we combine geomorphology and morphometrics with deep-time detrital zircon U-Pb geochronology as a tracer to figure out the anthropogenic effect of dams on sand generation, with the Colorado River as a case study. To do this, we collected 16 samples; 7 modern river sediment samples from the bed of the river upstream and downstream from the dams, 1 modern delta sample, 3 point bar samples, and 5 Wilcox bedrock samples. Then we applied U-Pb geochronology methods to analyze the age signatures of the samples.
Furthest upstream, the river cuts through the Llano uplift. Following the dams and lakes, the river cuts through the Wilcox bedrock. We can geomorphically assess the different signals in our samples using the known unique U-Pb age signatures of the Llano point source and Wilcox bedrock versus erosion of alluvium and terraces of the river. With these results we can see which signals disappear and which can be traced all the way through the system. Furthermore, we will combine these results with interpretations of aerial photographs of the river and confirm our analysis with field observations. This will help elucidate on the lag time of modern river sediment. Ultimately, by applying U-Pb geochronology methods coupled with on these samples we hope to 1) elucidate on the exact boundaries between sub-units of the Wilcox formation which is still poorly constrained 2) elucidate on the anthropogenic effect on sedimentation rate and lag time observed in the system.

Keywords: Geochronology, Sedimentology, Geomorphology, Colorado River

U-9

SHP
U

Rates and Mechanisms of Erosion Generating a Wave-Cut Platform at Sargent Beach, Texas, USA

Rose Palermo
Palermo, R., The University of Texas at Austin, Austin, TX
Mohrig, D., The University of Texas at Austin, Austin, TX
Piliouras, A., The University of Texas at Austin, Austin, TX
Swanson, T., Shell; The University of Texas at Austin, Austin, TX

Beaches with the highest rates of coastline retreat in Texas are characterized by a wave-cut platform and bluff morphology. At Sargent Beach, this shoreline topography is being cut into a substrate of weak, Holocene mudstone, composed of centimeter to decimeter thick horizontal beds and associated with the nearby coastal river. Its compressive strength ranges from immeasurably small when submerged and water saturated, to 206 kPa when moist, and 412 kPa when dry. Retreat rates for the face of the 1.5-m-high bluff are estimated using repeat aerial images collected from 2010 – 2014; these rates are 9.39 m/yr, 4.63 m/yr, and 3.73 m/yr. Retreat rates are also measured monthly using erosion pins. Monthly rates are 0.009 m/month and 0.053 m/month. Extrapolated over one year these rates equal 0.114 m/yr and 0.644 m/yr. The platform has a characteristic basinward dip between 1 and 1.5 degrees. Depending on the location, the platform may include centimeter – decimeter steps associated with discrete beds of varying strength in the mudstone or slope-parallel runnels with 0.05 – 0.10 m spacing and 0.03 – 0.05 m relief. All of these morphologies are produced by shell hash and concretion tools that abrade the mudstone within the zone of swash and backwash. Focused abrasion by shell and sediment tools leads to undercutting and ultimately failure of the bluff, produces the runnels, and grinds small potholes. These erosional processes are shut off when sections of the beach become covered with a layer of sand of sufficient thickness; its aerial coverage varies from month to month. We will examine how the widely variable rates of shoreline retreat and mudstone erosion are jointly controlled by changes in sand coverage and wave intensity associated with storms and cold fronts.

Keywords: coast, shoreline change, retreat rate

U-10

SHP
U

Depositional Environment and Provenance of a Boulder-Rich Diamictite, Witmarsum, Paraná State, Brazil

Emily Pease
Pease, E., Undergraduate Student, The University of Texas at Austin, Austin, TX
Anderson-Folnagy, H., University of Montana Western, Dillon, MT
Jennings, C., Department of Earth Sciences, University of Minnesota, Minneapolis, Minneapolis, MN
Rocha-Campos, A., Instituto des Geosciencias, Universidade des Sao Paulo, Sao Paulo, Brazil
Cotter, J., University of Minnesota, Morris, Morris, MN

A previously undescribed, massive, boulder-rich diamictite with large, sub-angular to sub-rounded clasts occurs in a newly discovered outcrop of the Carboniferous Itararé Subgroup in Witmarsum, Paraná State, Brazil. These appear to be glaciogenic diamictites deposited during one of the many advance-retreat phases of the Paraná lobe of the Gondwanan Ice Sheet. The goal of this study is to determine the depositional environment and provenance of this diamictite unit. Images of the outcrop were analyzed to determine the apparent orientation of the boulders with a 3:2 size ratio in order to determine mode of transport (flow). Sediment analysis of inter-clast diamictite samples from the outcrop was conducted to determine sand grain lithology and provenance, grain size, roundness, and sphericity. Results of this research were compared to the results of the analysis of a nearby, presumably correlative, unit (4 m away). Analysis of boulders (greater than 0.2 m in diameter) in this outcrop showed the same orientation as that of the nearby exposure. However, differences were observed. Although the clasts of all sizes in the outcrop studied show no apparent preferred orientation, clasts of all sizes in the nearby exposure do exhibit a preferred orientation that indicates flow. Additionally, sediment analyses show differences in both grain size distribution and provenance between the two exposures. Thus, correlation of the boulder rich unit between the two exposures is tentative. However, if this unit is the result of a subaqueous debris flow, variations in sedimentary characteristics over a small distance would be expected.Research for this study was funded by a grant from the N.S.F.-R.E.U Program (NSF-EAR-1262945).

Keywords: sedimentology, glacial, depositional environment, Brazil